EFFECTS ON THE FETAL CHOLINERGIC BASAL FOREBRAIN FOLLOWING MATERNAL IMMUNE ACTIVATION

by

Lorelei Pratt

A Dissertation submitted to the
Graduate School-Newark
Rutgers, The State University of New Jersey
in partial fulfillment of the requirements
for the degree of
Doctor of Philosophy
Graduate Program in Biological Sciences
written under the direction of
Dr. G. Miller Jonakait
and approved by

____

____

____

____

____

Newark, New Jersey

January, 2013

©2013

Lorelei Pratt

ALL RIGHTS RESERVED

ABSTRACT OF THE DISSERTATION

Effects on the Fetal Cholinergic Basal Forebrain Following Maternal Immune Activation

By Lorelei Pratt

Dissertation Director:

Dr. G. Miller Jonakait

Neurodevelopmental disorders such as autism and schizophrenia may result in part from maternal immune activation (MIA) during pregnancy. However, the mechanisms in the embryonic brain leading to these disorders in offspring remain unclear. Data suggest that interleukin-6 (IL-6) may be a key factor affecting fetal development following MIA.

Abnormalities in the cholinergic basal forebrain (BF) are associated with neurodevelopmental disorders. Previous in vitro studies have shown that factors produced by activated microglia promote the cholinergic differentiation of precursors in the BF. It has not been demonstrated whether fetal microglia become activated *in vivo* following MIA or whether such activation results in increased numbers of BF cholinergic neurons.

To test this, pregnant wild-type and IL-6 knock-out mice were injected with a viral mimic. Fetal/perinatal BFs of offspring were assayed for choline acetyltransferase (ChAT) activity and compared to offspring of saline-injected mice. The number of cholinergic neurons in BFs was quantified using stereological techniques. To determine fetal microglial activation status, lysates from enriched populations of microglial cells were analyzed for cytokine/chemokine protein production using LUMINEX® assays. Studies were performed in culture to determine whether certain elevated chemokines affect BF cholinergic development.

Results show that following MIA, ChAT activity increases in the BF at embryonic days 16.5 (E16.5), E18.5 and postnatal day 1 (P1). Cholinergic cell number also increases. Fetal microglia produce higher levels of several cytokines and chemokines. Unexpectedly, ChAT activity is higher in control IL-6 KO BFs at E16.5 than in wild-types and MIA does not increase ChAT activity further. Non-microglial fetal brain cells also produce cytokines and chemokines. Non-microglial cells from control IL-6 KOs express increased levels of cytokines and chemokines compared to wild-types and MIA does not increase these levels. Culture studies suggest that a C-C chemokine receptor 5 (CCR5) ligand may be a factor affecting BF cell survival.

These data reveal changes following MIA that could potentially affect neural development. The fetal microglial cytokine/chemokine profile is altered. Perinatal increases in ChAT activity may have long-lasting consequences. Results also suggest a role for IL-6 in regulating proper cytokine and chemokine balance during normal brain development.

ACKNOWLEDGMENTS

I am truly thankful for my advisor, Dr. Jonakait. She has encouraged and guided me throughout my research and through the writing of this dissertation. I am sure my project would not have been completed without her. Dr. Jonakait has always been an example to me as a professional educator, as a dedicated lab director and as a sincere, caring friend. I am so thankful to her.

I would also like to thank my committee members, Dr. Joan Morrell, Dr. Wilma Friedman, Dr. Nicholas Ponzio and Dr. Emanuel DiCicco-Bloom. They have all given of their time to attend meetings, provide insight and offer suggestions helpful to the progress of this research. I sincerely appreciate their input. I also thank them for carefully reading and evaluating this dissertation.

I would like to express my gratitude to Dr. Robert Donnelly and Juan Crosby at the NJ Medical School of the University of Medicine and Dentistry of New Jersey. They performed the LUMINEX assays for this research project at their facility at UMDNJ.

I am extremely grateful to Dr. Elizabeth Abercrombie and the members of her lab for the use of their microscope and stereology software. I spent many hours in their lab and the work completed there became an integral part of my thesis. I am also thankful to Dr. Benji Altinbilek. She graciously assisted me in learning how to perform stereological analysis.

I would also like to thank Dr. Gareth Russell for offering his time and statistical expertise. His assistance was invaluable for the analysis of the massive amounts of data generated from the Luminex® assays.

I cannot offer enough thanks to Dr. Li Ni. “Ni” taught me everything I know about lab procedures and it was through his patient instruction that I learned fetal mouse basal forebrain and hippocampus dissections. It has been a pleasure to work with him and to know him.

I also need to thank my co-workers in the lab, Giselles and NK. We have gone through this process together and I am grateful for their friendship. They have both helped to make our lab a positive place to be and work.

I would like to express my thanks to all the staff of the Rutgers-Newark Animal Facility for their help and advice in caring for my mice.

My research project would not have been possible without the funding received from the Governor’s Council on Autism of the New Jersey Department of Health and Senior Services and from Autism Speaks to GMJ. A separate grant from Autism Speaks to Dr. Nicholas Ponzio provided funds for this project as well. I am very grateful for this support.

DEDICATION

I dedicate this dissertation to my family—to my husband, Randy—to my daughters, Charissa, Amy, Ruthi and April—and to my son, Andrew. They have all willingly allowed me to pursue my “other life” in research even when it was inconvenient for them and when it meant I was not available to be there for them. I love you all so much.

TABLE OF CONTENTS

Abstract ii
Acknowledgments iv
Dedication vi
List of Tables ix
List of Figures x

I. Introduction and Background

- 1.1 Introduction 1
  - 1.1.1 Autism Spectrum Disorders 2
  - 1.1.2 Schizophrenia 4
  - 1.1.3 Common findings in neurodevelopmental disorders 6
  - 1.1.4 Animal models support an association between MIA and neurodevelopmental disorders 7
  - 1.1.5 Fetal brain development following MIA 9
- 1.2 The fetal cholinergic basal forebrain 10
- 1.3 Fetal microglia 17
- 1.4 Chemokines 23
- 1.5 Interleukin-6 (IL-6) 29

II. Rationale and Specific Aims 34

III. Materials and Methods 37

IV. Results 51
- 4.1 Specific Aim 1
  - 4.1.1 Poly(I:C) treatment affects behavior and weight gain of dams 51
  - 4.1.2 Poly(I:C) treatment results in an increase in ChAT activity in the BF 52
  - 4.1.3 Poly(I:C) treatment results in an increased number of cholinergic neurons in the BF 53
  - 4.1.4 Poly(I:C) treatment affects GAD mRNA expression in the BF 54
  - 4.1.5 Poly(I:C) treatment has negligible effects on the hippocampus 55
  - Conclusions for Specific Aim 1 58
- 4.2 Specific Aim 2
  - 4.2.1 IL-6 mRNA is increased in the fetal brain following MIA 58
  - 4.2.2 MIA results in changes in fetal brain cytokines and chemokines 60
  - 4.2.3 Numbers of fetal microglia do not change following MIA 62
  - Conclusions for Specific Aim 2 63
- 4.3 Specific Aim 3
  - 4.3.1 Do chemokines regulate cholinergic development? 64
  - 4.3.2 CCR2 inhibition has a biphasic effect on ChAT activity 65
  - 4.3.3 Inhibition of CCR5 66
  - Conclusions for Specific Aim 3 67

4.4 Specific Aim 4

4.4.1 IL-6 in microglial conditioned medium plays a role in cholinergic cell survival 68
4.4.2 Cytokine and chemokine elevations seen in WT fetal microglia are absent in IL-6 knockouts 69
4.4.3 The absence of IL-6 promotes a pro-inflammatory fetal brain environment 70
4.4.4 The increase in ChAT activity in vivo following poly(I:C) treatment is eliminated in the absence of IL-6 71
Conclusions for Specific Aim 4 73

V. Discussion 74
5.1 Increased cholinergic expression following MIA 74
5.2 Potential changes in the hippocampus 75
5.3 Microglial response to MIA 77
5.4 Non-microglial cells respond to MIA 80
5.5 Chemokines in brain development 81
5.6 The role of IL-6 83
5.7 How are immune disorders and brain disorders linked? 86
5.8 How does MIA get translated into developmental disorders? 88

VI. Conclusions 91

VII. References 92

VIII. Tables 113

IX. Figures 118

X. List of Abbreviations 135

XI. Appendices 139
Appendix A: Supplementary Tables 139
Appendix B: Supplementary Figure 157

XII. Curriculum Vitae 158

LIST OF TABLES

Table 1. Primers used for qRT-PCR 43
Table 2. Comparison of maternal weight gain/loss following injection 113
Table 3. Assessment of sickness behavior 114
Table 4. Crown to rump lengths 115
Tables 5A and 5B Summary of cytokines and chemokines in E16.5 fetal brain CD11b$^+$ and CD11b$^-$ fractions (caption) 116
Table 5A. Comparison of cytokine/chemokine levels in CD11b$^+$ control and poly(I:C) treatment groups from wild type and IL-6 KO mice 116
Table 5B. Comparison of cytokine/chemokine levels in CD11b$^-$ control and poly(I:C) treatment groups from wild type and IL-6 KO mice 117

LIST OF SUPPLEMENTARY TABLES

Supplementary Table 1. Raw cycle threshold (Ct) values for chloride transporters from P1 to P9 139
Supplementary Table 2. Similar message expression of chloride transporters between control and poly (I:C) groups 139
Supplementary Tables 3A-10B Comparisons of cytokine and chemokine levels in fetal brain of WT and IL-6 KO mice from control and poly(I:C) treatment groups (caption) 140
Supp. Table 3A. Cytokines: CD11b$^+$ WT CT vs. WT poly(I:C) 141
Supp. Table 3B. Chemokines: CD11b$^+$ WT CT vs. WT poly(I:C) 142
Supp. Table 4A. Cytokines: CD11b$^-$ WT CT vs. WT poly(I:C) 143
Supp. Table 4B. Chemokines: CD11b$^-$ WT CT vs. WT poly(I:C) 144
Supp. Table 5A. Cytokines: CD11b$^+$ IL-6 KO CT vs. IL-6 KO poly(I:C) 145
Supp. Table 5B. Chemokines: CD11b$^+$ IL-6 KO CT vs. IL-6 KO poly(I:C) 146
Supp. Table 6A. Cytokines: CD11b$^-$ IL-6 KO CT vs. IL-6 KO poly(I:C) 147
Supp. Table 6B. Chemokines: CD11b$^-$ IL-6 KO CT vs. IL-6 KO poly(I:C) 148
Supp. Table 7A. Cytokines: CD11b$^+$ WT CT vs. IL-6 KO CT 149
Supp. Table 7B. Chemokines: CD11b$^+$ WT CT vs. IL-6 KO CT 150
Supp. Table 8A. Cytokines: CD11b$^-$ WT CT vs. IL-6 KO CT 151
Supp. Table 8B. Chemokines: CD11b$^-$ WT CT vs. IL-6 KO CT 152
Supp. Table 9A. Cytokines: CD11b$^+$ WT Poly(I:C) vs. IL-6 KO poly(I:C) 153
Supp. Table 9B. Chemokines: CD11b$^+$ WT Poly(I:C) vs. IL-6 KO poly(I:C) 154
Supp. Table 10A. Cytokines: CD11b$^-$ WT Poly(I:C) vs. IL-6 KO poly(I:C) 155
Supp. Table 10B. Chemokines: CD11b$^-$ WT Poly(I:C) vs. IL-6 KO poly(I:C) 156

LIST OF FIGURES

Figure 1. ChAT activity in the fetal basal forebrain increases following maternal poly(I:C) injection 118
Figure 2. The number of cholinergic neurons in the fetal basal forebrain increases following maternal immune activation........ 119
Figure 3. The effect of maternal immune activation on BF ChAT activity is transient 120
Figure 4. GAD65 mRNA decreases in the E16.5 fetal BF following poly(I:C) injection........ 121
Figure 5. α7nAChR, NKCC1 and KCC2 mRNA levels in the postnatal hippocampus following MIA 122
Figure 6. mRNA expression of NRG1, NMDAR and Shank3 in the postnatal hippocampus following MIA 123
Figure 7. Postnatal ChAT protein expression in hippocampus of offspring following MIA 124
Figure 8. Fetal microglia produce increased levels of IL-6 mRNA following maternal immune challenge........ 125
Figure 9. Non-microglial cells produce cytokines........ 126
Figure 10. The number of microglia in the fetal BF does not change following MIA 127
Figure 11. Inhibition of chemokine receptors CCR1, CCR3, CXCR2 and CXCR4 does not reduce ChAT activity in BF cultures........ 128
Figure 12. Inhibition of chemokine receptor CCR2 and addition of exogenous MCP-1 129
Figure 13. Inhibition of CCR5 results in decreased ChAT activity and reduction of cell number in E15 rat BF cultures........ 130
Figure 14. Inhibition of CCR5 reduces cell survival 131
Figure 15. IL-6 is a survival factor for BF cells in culture 132
Figure 16. ChAT activity in the IL-6 KO fetal BF does not change following maternal poly(I:C) injection........ 133
Figure 17. Higher ChAT activity and lower message levels of GAD65 in E16.5 IL-6 KO basal forebrains 134

SUPPLEMENTARY FIGURE

Supplementary Figure 1. Systematic Random Sampling: Grid and Counting frame........ 157

I. Introduction and Background

1.1 Introduction

Prenatal maternal insults can result in infant birth defects. Extensive data show that environmental factors including exposure to drugs or infections contribute to diverse consequences in children. For example, in the past, thalidomide was administered to ease nausea and vomiting during pregnancy. However, this drug resulted in major malformations in the infants born to the women who took it (Lancaster, 2011). Antiepileptic drugs such as valproic acid produce a dose- dependent risk for malformations in children (Tomson et al., 2011). Children exposed prenatally to alcohol are often hyperactive and have decreased IQ along with other behavioral, language and attention deficits (Jones, 2011). Cigarette smoking by pregnant women results in low infant birth weight (Kendrick and Merritt, 1996). A deficit of folic acid can cause neural tube defects, so supplements of this vitamin are routinely given to women as a preventative measure (Taruscio et al., 2011; Czeizel, 2000). Maternal bacterial or viral immune challenges also detrimentally affect fetal outcome. Rubella contracted during the first trimester of pregnancy can cause fetal death and miscarriage or result in various birth defects including deafness, eye abnormalities, congenital heart disease, low birth weight or even mental retardation (2010; Lancaster, 2011).

Although these outcomes are commonly accepted consequences of specific prenatal assaults, there is somewhat more controversy as to the involvement of prenatal environmental factors in the etiology of neurodevelopmental diseases such as schizophrenia (SZ) and autism spectrum disorders (ASD). Nevertheless, accumulating evidence suggests that maternal immune activation plays a contributing role in these disorders as well.

1.1.1 Autism Spectrum Disorders

ASD comprises a spectrum of developmental disorders (including Aspberger and Rett Syndromes) with symptoms that can range from mild to severe. Usually these symptoms appear before age 3. As categorized by the American Psychiatric Association Diagnostic and Statistical Manual of Psychiatric Disorders, all affected individuals display abnormalities in social interaction, communication and behavior (American Psychiatric Association, 2001). Children may be unable to interpret or use non-verbal cues, and they fail to develop peer relationships. They have some language impairment, display restricted, stereotyped or repetitive patterns of behaviors, activities and interests and they may be unable to engage in symbolic or imaginative play (American Psychiatric Association, 2001). Recent data show excessive brain growth in the first years of life in ASD children, though brain volumes do not differ from typically- developing children by age 4 (Courchesne and Pierce, 2005; DiCicco-Bloom et al., 2006). There is no cure for autism. (Bauman, 2005) However, early diagnosis can improve prognosis (LeBlanc and Fagiolini, 2011). According to the most recent study from the Center for Disease Control, an autism spectrum disorder affects 1 in 88 children in the United States (2012; Weintraub, 2011).

Autism is highly heritable (Casey et al., 2011; Holt and Monaco, 2011). Studies show a greater concordance among monozygotic than among dizygotic twins (Holt and Monaco, 2011). However, except in the case of one subset of ASD where a mutation in methyl-CpG binding protein 2 (MeCP2) causes Rett syndrome (Nan and Bird, 2001), no single gene has been found to be responsible for autism. Current consensus points to a heterogeneous genetic origin for the disorder with several gene loci interacting in combination to produce susceptibility (Geschwind, 2008; Muhle et al., 2004). Initial linkage studies implicated the involvement of large regions of several chromosomes, and over a hundred candidate genes for ASD have been identified each showing at least minimal association with the disorder (Holt and Monaco, 2011). Among these candidate genes are those encoding neuropeptides and their transporters (Holt and Monaco, 2011), cell adhesion molecules (Holt and Monaco, 2011), proteins involved in synapse formation and function (Walsh et al., 2008), protein translation (Kelleher, III and Bear, 2008), developmental patterning genes (DiCicco-Bloom et al., 2006) and several of the gamma-aminobutyric acid (GABA) system genes (Di Cristo, 2007). Copy number variations, single nucleotide polymorphisms, genome wide association studies, promoter and control regions of genes all point to a complex genetic etiology underlying ASD. The collected data suggest an altered network or impaired circuit wiring in ASD where brain function as a whole that supports language, social communication and behavior is disrupted owing to the malfunction of any one of the hundreds of individual pieces that make up the system (Geschwind, 2008).

Despite the strong genetic component, environmental factors likely modify phenotypic expression in the disorder (Muhle et al., 2004). There is a greater concordance of ASD among dizygotic twins than there is among non-twin siblings (Hallmayer et al., 2011). This fact implicates a role for the gestational environment (Hallmayer et al., 2011). The increased risk of autism that is found in children exposed prenatally to thalidomide, misoprostol, valproic acid, rubella or the insecticide chlorpyrifos also suggests that prenatal environmental factors contribute to ASD etiology (Pessah et al., 2008; Landrigan, 2010). Though not universally recognized, maternal infection also presents a risk for developing autism (Patterson, 2011b). Epidemiological cohort studies have shown significant correlation between prenatal exposure to viral agents and ASD in offspring (Parker-Athill and Tan, 2010).

1.1.2 Schizophrenia

Schizophrenia is a disorder characterized by delusions, hallucinations, disorganized speech and/or grossly disorganized or catatonic behavior along with other negative symptoms.(American Psychiatric Association, 2001) The age of onset is typically adolescence to adulthood (Gejman et al., 2011). Symptoms include a range of cognitive and emotional dysfunctions. Therefore, diagnosis involves the recognition of a multitude of signs and symptoms associated with impaired perception, inferential thinking, language and communication, behavioral monitoring, affect, fluency and productivity of thought and speech, volition, drive and attention (American Psychiatric Association, 2001). Other symptoms include inappropriate facial expression or mood, sleep disturbance, depersonalization, phobias, odd mannerisms, ritualized or stereotyped behaviors and suicide (American Psychiatric Association, 2001). The enlargement of lateral ventricles in the brain is also characteristic of SZ individuals (American Psychiatric Association, 2001) .

Like autism, schizophrenia is a highly heritable disorder (Gejman et al., 2011). Concordance rates of SZ for monozygotic twins have been found to be approximately 40%–50% compared with 6%–10% in dizygotic twins (Gejman et al., 2011). Family studies of SZ show that a sibling or child of an individual with SZ has a ten-fold elevation in risk for developing SZ themselves over that seen in the general population (Gejman et al., 2011). Genome wide association (GWA) and copy number variation (CNV) studies for SZ reveal a combination of rare and common genetic variants and like autism, polygenic interplay is implicated in its origin (Kim et al., 2011; Gejman et al., 2011). A few of the variants (i.e., especially large chromosomal deletions at 22q11.21) allow for more accurate predictions of risk (Gejman et al., 2011). Neuregulin 1 (NRG1) is a leading schizophrenia susceptibility gene (Coyle et al., 2010; Harrison and Law, 2006), as is Disrupted in Schizophrenia 1 (DISC-1), the N-methyl-D-aspartic acid (NMDA) receptor and dysbindin (Coyle et al., 2010). Other genes associated with SZ include the major histocompatibility complex (MHC) (Gejman et al., 2011; Kim et al., 2011), transcription factor 4 (TCF4), a neuronal transcriptional factor essential for brain development (Kim et al., 2011; Gejman et al., 2011), genetic variation near the gene encoding the microRNA miR-137 (Kim et al., 2011) and neugrin (NGRN) (Gejman et al., 2011; Kim et al., 2011). As in ASD it is hypothesized that the complex disorder of SZ results from the abnormal combinatorial functioning of a molecular network or system (Schadt, 2009; Gejman et al., 2011).

Though the genetic component in SZ is strong, epigenetic mechanisms that contribute to the transmission of SZ are also being actively explored (Gejman et al., 2011). An increased risk of SZ has been found in association with several prenatal and childhood environmental factors though the contribution of each may be relatively modest (McGrath et al., 2008; Gejman et al., 2011; American Psychiatric Association, 2001). These factors include birth complications (Mittal et al., 2008; Mittal et al., 2009; Byrne et al., 2007), urban birth (McGrath et al., 2008), gestational famine (St Clair et al., 2005; McGrath et al., 2008), migrant status (McGrath et al., 2008) and advanced paternal age (Torrey et al., 2009; El Saadi et al., 2004; Gejman et al., 2011). Epidemiological evidence strongly supports an association between maternal immune activation and the subsequent development of SZ in offspring (Brown and Derkits, 2010; Patterson, 2011b; Parker-Athill and Tan, 2010). A nested cohort study found a three-fold to seven-fold increase in the risk of SZ for individuals exposed prenatally to influenza virus during the first half of pregnancy (Brown et al., 2004; Brown and Derkits, 2010).

1.1.3 Common findings in neurodevelopmental disorders

There is considerable genetic overlap between SZ, ASD and other psychiatric disorders (Gejman et al., 2011). These commonalities point to the possibility of a common epigenetic source during development with the specific effects due to the timing of the insult and the stage of brain development at that time. An imbalance of excitatory versus inhibitory transmission is reported to be disturbed in several neurodevelopmental disorders including SZ and ASD (Gogolla et al., 2009), and abnormalities in gamma-aminobutyric acid (GABA) signaling in the GABAergic system are consistently found in neurodevelopmental disorders (Di Cristo, 2007; DiCicco-Bloom et al., 2006; Pessah et al., 2008; Muhle et al., 2004). Postmortem SZ and ASD brains show evidence of changes in both pre- and post-synaptic sites along with lower GABA concentrations, less GABA release and lower production of GAD67 mRNA (Muhle et al., 2004; Nyffeler et al., 2006; Coyle et al., 2010). In these brains, the expression of several $GABA_A$ receptor subunits is also altered (Coyle et al., 2010; Muhle et al., 2004; Pessah et al., 2008). The region of chromosome 15q11-q13 where the genes for 3 of these subunits is located is strongly implicated in autism (Muhle et al., 2004). It has been suggested that the abnormalities observed in GABA signaling in autistic patients may be compensatory for hyper-cholinergic signaling during development (Lippiello, 2006).

1.1.4 Animal models support an association between maternal immune activation (MIA) and neurodevelopmental disorders

Work with rodents provides additional support for an association between prenatal maternal infection and neurodevelopmental disorders such as ASD and SZ. Following maternal influenza administration adult mice offspring exhibit deficits in prepulse inhibition, deficient exploratory behavior and impaired social interaction (Shi et al., 2003) as well as cerebellar pathology (Shi et al., 2009). Additionally, the adult offspring of pregnant mice injected with a human influenza virus show regions of brain atrophy, a thinning of the corpus callosum and altered expression of neural genes (Fatemi et al., 2008). Behavioral deficits depend on the timing of the immune challenge (Meyer et al., 2006a; Meyer et al., 2006b; Meyer et al., 2008c) and distinct patterns of altered neuronal gene expression depend on the time of injection as well (Meyer et al., 2008c). Prenatal immune challenge by a viral mimic, polyinosinic-polycitidylic acid (poly (I:C)) illicits the same behavioral abnormalities as does the virus itself (Shi et al., 2003; Shi et al., 2005) with similar deficits in exploratory behavior, prepulse inhibition and social interaction in the adult offspring when the pregnant dam is injected with poly(I:C) at midgestation (Smith et al., 2007; Meyer et al., 2006b). In rats when poly(I:C) is administered prenatally, latent inhibition is affected in the adult offspring but not in juvenile pre-puberty rats (Zuckerman and Weiner, 2003). A disruption of hippocampal morphology is also reported in these rats (Zuckerman and Weiner, 2003). Following prenatal maternal immune challenge cytokine levels are affected in the adult (Urakubo et al., 2001; Ashdown et al., 2006; Meyer et al., 2006b; Meyer et al., 2006a; Meyer et al., 2008b), including alterations in tumor necrosis factor α (TNFα) (Gilmore et al., 2003; Gilmore et al., 2005), and the expression of $GABA_A$ receptors is also reported to be altered (Nyffeler et al., 2006).

These findings in rodents where a prenatal insult results in the later appearance of behavioral and structural abnormalities in adult offspring parallels neurodevelopmental diseases in humans such as ASD where symptoms first appear in early childhood and schizophrenia where the age of onset of symptoms is adolescence to adulthood.

1.1.5 Fetal brain development following MIA

Epidemiological data associates maternal infection during pregnancy with neurodevelopmental disorders in humans, and experiments using animal models show that maternal infection during gestation can result in aberrant behavior, altered gene expression and brain anomalies in adult offspring. However, little work has focused on the mechanisms and events occurring in the fetal brain as a direct result of MIA. Examination of the fetal brain to uncover the changes occurring there as a result of MIA is needed. An investigation into the mechanisms at play in the embryonic brain could shed light on developmental alterations that become manifest later in life. One such animal study has begun this process. In this investigation maternal inflammation was induced in pregnant mice using poly(I:C) injection and subsequently the mRNA expression levels of several molecules known to be involved in dopaminergic development were evaluated. These molecules included the dopaminergic markers tyrosine hydroxylase, a dopamine transporter, sonic hedgehog, fibroblast growth factor 8, and the 2 transcription factors nuclear receptor related 1 protein (Nurr1) and pituitary homeobox 3 (Pitx3) (Meyer et al., 2008a). All these molecules are altered as a result of mid-gestation administration of poly (I:C) (Meyer et al., 2008a). An increase in the number of dopaminergic neurons in the fetal brain was also observed (Meyer et al., 2008a). Further investigation into aberrant *embryonic* neural development as a result of maternal immune challenge is essential in order to establish a link between the maternal immune response and the resultant behavioral and brain abnormalities seen in adult offspring.

1.2 The fetal cholinergic basal forebrain

One of the fetal brain regions deserving of particular focus when considering the effects of a prenatal maternal insult is the basal forebrain (BF). Abnormalities in the cholinergic basal forebrain are associated with several neurodevelopmental disorders including ASD (Perry et al., 2001; Bauman, 2005; Deutsch et al., 2010; Ni et al., 2007) and SZ (Perry et al., 2001; Brooks et al., 2011; Kristensen et al., 2007; Thomsen et al., 2008; Thomsen et al., 2010). The number of BF neurons is decreased (Johnston et al., 1995; Wenk and Hauss-Wegrzyniak, 1999; Berger-Sweeney, 2003) accompanied by alterations in synaptic morphology in the cortex in both Rett syndrome and Down syndrome (Johnston et al., 2001; Berger-Sweeney, 2003; Johnston et al., 1995). Autopsy of adult brains also reveals reduced expression of nicotinic acetylcholine receptors (nAChRs), although this may reflect compensatory changes rather than developmental etiology (Deutsch et al., 2010; Perry et al., 2001). The presence of cholinergic abnormalities and involvement of elements of the cholinergic system in both ASD and SZ have prompted the use of related therapeutic drug interventions in patients with these disorders (Coyle et al., 2010; Deutsch et al., 2010). Several α7nAChR agonists or modulators have been developed that improve cognitive functions including recall, spatial working memory and speed of performance (Kitagawa et al., 2003; Coyle et al., 2010). The α7nAChR is a logical target for pharmacological intervention since signaling through this receptor is vital to processes of attention and cognition (Deutsch et al., 2010). In a functional MRI study when cholinergic transmission is enhanced in control subjects using physostigmine, a reversible cholinesterase inhibitor, the activity in regions of the brain processing human facial emotion are stimulated (Bentley et al., 2003; Deutsch et al., 2010). The study suggested that excess cholinergic signaling could result in anxiety and that the outcome of diminished or unbalanced cholinergic signaling could be improper processing of social and/or emotional cues (Bentley et al., 2003; Deutsch et al., 2010).

In comparison with unaffected counterparts, the post mortem brains of younger autistic individuals contain cholinergic neurons in the basal forebrain that are increased in size and number whereas the opposite is true in affected adults (Deutsch et al., 2010; Bauman, 2005). Studies have shown that cholinergic neurons in the BFs of children with autism are uncharacteristically large and especially abundant (Deutsch et al., 2010; Lippiello, 2006). Neurons from the same area in autistic *adults* are abnormally small and pale (Deutsch et al., 2010), and they are fewer in number (Bauman, 2005). A recent voxel-based morphometry study found that the volume of gray matter was reduced in the BF and connected brain areas of ASD children who also have other developmental disabilities (Riva et al., 2011).

Based on these data, a further investigation into the *embryonic* BF and changes that occur following maternal immune challenge is warranted. Moreover, data from culture studies in the Jonakait lab indicate that the fate of precursor cells within the embryonic BF can be altered towards a cholinergic one when treated with medium from activated microglia containing pro-inflammatory factors (Jonakait et al., 1996; Jonakait, 2007; Ni et al., 2007). A preferential cholinergic differentiation at the expense of GABAergic differentiation (Ni et al., 2007) may produce hyper-cholinergic signaling during development possibly resulting in the imbalance observed in GABA signaling in neurodevelopmental disorders (Lippiello, 2006).

The BF comprises a group of structures located in the rostral, ventral part of the brain and includes the nucleus basalis, diagonal band of Broca, substantia innominata, and medial septal nuclei. The modulatory neurotransmitter, acetylcholine, that is produced here is dispensed throughout the cortex, hippocampus and thalamus (Berger-Sweeney, 2003; Bauman, 2005). This cholinergic system has been extensively studied in adult animals because of its role in cognitive functions such as attention and memory (Berger-Sweeney, 2003; Bauman, 2005). Less is known about its role in development. However, this period is important for establishing its later function in the adult (Berger-Sweeney, 2003). Acetylcholine signaling in the early brain has a role in setting up circuits (Bauman, 2005) and formation of synapses (Berger-Sweeney, 2003; Berger-Sweeney and Hohmann, 1997; Berger-Sweeney, 1998; Bauman, 2005), and alterations can result in changes in cortical structure and impaired cognitive function (Arters et al., 1998; Bachman et al., 1994; Berger-Sweeney, 2003; Hohmann and Berger-Sweeney, 1998b).

Changes in perinatal cholinergic signaling can result in permanent behavioral and cognitive consequences in the adult, and evidence suggests that proper timing of cholinergic innervation to the cortex is critical for normal cognitive development (Berger-Sweeney, 2003). Cholinergic lesions can be produced by using 192 IgG saporin, a ribosome inactivating protein linked to 192 IgG which targets the toxin specifically to cholinergic cells. In rats when lesions are made using intraventricular injection of 192 IgG saporin at postnatal day 1 (P1) or P3, it results in reduced thickness of cortical layers and changes in dendritic morphology in layer V (Robertson et al., 1998; Ricceri et al., 2002; Bachman et al., 1994; Pappas and Sherren, 2003; Berger-Sweeney, 1998). Behavioral consequences of these lesions include reduced novel object exploration in a spacial open field test as adults and a deficit in passive avoidance (as measured in a 2-compartment light/dark chamber with foot shock) at P15-16 that was especially pronounced in females (Ricceri et al., 2002). While depletion of acetylcholine signaling impairs these functions, perinatal choline (a precursor for acetylcholine) supplementation in rats results in enhanced memory and attention as adults (Williams et al., 1998). Offspring of rats receiving choline supplement during embryonic day 12 (E12) to E17 of gestation have cholinergic cells with larger cell bodies in the medial septum and vertical diagonal band (Williams et al., 1998).

In other experiments in rats where manipulation of the cholinergic system during this critical neonatal period was performed, the organization of mesolimbic-basal forebrain cortical circuitry was permanently impacted and cholinergic transmission as adults was disrupted (Brooks et al., 2011). These adult rats also mirrored several cognitive symptoms of SZ (Brooks et al., 2011).

Lesions made at later time points did not result in the same outcomes or produced more subtle effects, also suggesting a critical window during innervation and synapse formation sensitive to environmental influences (Berger-Sweeney, 2003).

In rodents the critical times most sensitive to BF cholinergic manipulations are during the period of cholinergic BF neurogenesis and during a period of differentiation and synaptogenesis in the cortex as the BF projections provide signals to their targets (Abreu-Villaca et al., 2011; Berger-Sweeney, 2003; Meck and Williams, 2003; Meck et al., 2007). The innervation of the cortex in rodents occurs during the first week after birth. In humans the timing of these two periods is different. Neurogenesis in the BF takes place during the third trimester of pregnancy and the afferent projections from the BF innervate their targets from 7 to 18 months (Bauman, 2005; Berger-Sweeney, 2003; Johnston et al., 2001).

Alterations in embryonic cholinergic signaling could affect the excitatory to inhibitory balance in the brain. Early postnatal endogenous signaling through α7nAChRs plays a role in promoting the development of glutamatergic synapses and pathways in the brain (measured in the CA1 region of the hippocampus) (Lozada et al., 2012). Transgenic mice lacking this receptor do not form as many synapses (Lozada et al., 2012) and exposure to nicotine in culture increases the number of glutamatergic synapses formed (Lozada et al., 2012).

Because acetylcholine produced in the BF is widely distributed throughout the brain, changes in cholinergic signaling should result in downstream effects in innervated target areas. One of the major targets of BF cholinergic fibers from the medial septal BF and diagonal band is the hippocampus. Throughout the hippocampus cholinergic fibers form synapses on granule cells, pyramidal cells, interneurons, and neurons of the hilus (Coyle et al., 2010). This occurs during early postnatal life in the rodent (Berger-Sweeney, 2003.) nAChRs are expressed widely in the hippocampus, though they are located more densely on GABAergic interneurons than on glutamatergic cells (Coyle et al., 2010).

Acetylcholine signaling plays a role in the switch from excitatory to inhibitory GABAergic signaling in the brain (Liu et al., 2006). This switch involves a change in chloride transporter expression from the embryonic sodium potassium chloride co-transporter (NKCC1) to the potassium chloride co-transporter (KCC2), the mature form (Liu et al., 2006). Whereas NKCC1 imports chloride along with sodium, KCC2 transporters export chloride ions from the cell establishing the chloride gradient. As a result, GABA signaling becomes hyperpolarizing as chloride ions flow into the cell. In the hippocampus, calcium influx through α7-nAChRs promotes a change in transcription and conversion from NKCC1 to KCC2 (Le Magueresse et al., 2006; Liu et al., 2006). Alterations in the level of BF cholinergic activity or in the timing of innervation could, therefore, affect the timing of this switch. In the absence of functional α7nAChRs, hippocampal neurons in transgenic mice retain an excitatory response to GABA for an extended time period (Liu et al., 2006). KCC2 also has been shown to have a function in dendritic spine development independent of its transporter activity (Le Magueresse et al., 2006; Li et al., 2007a). and premature expression of KCC2, and an early switch to inhibitory GABA signaling results in decreased length and branch number of neurites on cortical rat neurons in vivo (Cancedda et al., 2007).

Other molecules involved in synapse formation and development in the hippocampus could be affected by alterations in acetylcholine signaling. These include the NMDA receptor (NMDAR), neuregulin-1 (NRG1) and SH3 and multiple ANKyrin repeat domains 3 (Shank3).

NRG1 regulates expression of α7nAChRs in the hippocampus (Liu et al., 2001). In hippocampal cultures addition of NRG1 increases the amplitude of post synaptic currents from GABAergic interneurons and also increases the number of GABAergic interneurons expressing the α7nAChR (Liu et al., 2001). Localization of these receptors on projection neurons in the ventral hippocampus is regulated by NRG1 as well (Zhong et al., 2008). Altered levels of the α7nAChR have been reported in both SZ and ASD (Lippiello, 2006; Graham et al., 2002; Coyle et al., 2010). Post mortem hippocampi of SZ patients contain higher levels of type I NRG1 and lower levels of type III NRG1 than normal subjects (Harrison and Law, 2006; Coyle et al., 2010). Type 1 NRG-1 has also been shown to modulate NMDAR activity (Coyle et al., 2010; Hahn et al., 2006).

The NMDAR is an ionotropic glutamate receptor that is both ligand- and voltage-gated, and it plays a role in synaptic plasticity. Both glutamate and glycine are ligands. NMDA receptor hypofunction is a shared feature of both ASD and SZ (Coyle et al., 2010). The potential of α7nAChR activity to alter NMDAR function has been demonstrated in the rat auditory cortex where α7nAChRs stimulated by chronic nicotine exposure during the second week of life produced enhanced NMDA excitatory post synaptic currents and altered the development of glutamate synapses with lasting effects (Aramakis et al., 2000). Gestational nicotine exposure in mice heightened the expression of several NMDAR subunits including NR1 (Wang et al., 2011).

Shank 3 is an adaptor scaffolding protein in the postsynaptic density. It functions to connect ion channels and neurotransmitter receptors to the actin cytoskeleton. It is an autism-associated gene (Uchino and Waga, 2012; Bozdagi et al., 2010) whose expression is regulated by DNA methylation (Uchino and Waga, 2012). Mutations in scaffolding proteins contribute to ASD and SZ (Lennertz et al., 2012). Haploinsufficiency of the Shank3 gene in mice results in specific deficits in synaptic function and reduced social interaction that model some of the manifestations seen in ASD patients who have the loss of a functional copy of this gene (Bozdagi et al., 2010).

1.3 Fetal microglia

In 2005 Vargas et al. reported the persistent activation of microglia in the brains of autistic patients (Vargas et al., 2005). These studies placed a new spotlight on the possible role played by these cells in the etiology of autism. More recent data using post mortem brains of both children and adults demonstrated a pronounced increase in the expression of the transcription factor nuclear factor kappa B p65 (NF-κB p65) in microglia in the tissue from ASD individuals relative to controls (Young et al., 2011). When microglia become activated, NF-κB p65 is phosphorylated and translocates to the nucleus where it binds to DNA and begins transcription. In this study the expression of phosphorylated NF-κB in the cell nuclei was directly measured (Young et al., 2011).

Altered cytokine production as a result of maternal immune challenge has been implicated in SZ and ASD (Ashdown et al., 2006; Pessah et al., 2008). Microglia produce cytokines. Moreover, these cells are present in the fetal BF and studies from our lab have demonstrated that conditioned medium from activated microglia promotes the cholinergic differentiation of neural precursors from the BF in culture (Jonakait et al., 1996; Jonakait et al., 2000; Mazzoni and Kenigsberg, 1997; Ni et al., 2007), making them prime suspects for altering cholinergic development there.

Microglia are found throughout the central nervous system (CNS). Adult microglia normally manifest a highly ramified morphology with numerous processes extending fifty or more microns in all directions continually sampling their environment (Nimmerjahn et al., 2005). They are capable of rapid motility even in a ramified state (Rezaie et al., 2002b). In response to trauma microglia become activated, retract cellular processes (Chan et al., 2007), become more amoeboid in shape and migrate to the area of trauma (Chan et al., 2007). They also produce a myriad of cytokines and chemokines as well as reactive oxygen species (Chan et al., 2007). They express cell surface markers typical of macrophages, become phagocytic and can present antigen to Tcells in the context of class II MHC surface molecules (Chan et al., 2007). Adult microglia can be activated by and can secrete both cytokines and growth factors (Elkabes et al., 1996; Benveniste, 1992; Hanisch, 2002; Neumann, 2001; Banati et al., 1993; Butovsky et al., 2006; Gehrmann et al., 1995), and their effects can result in neuronal cell damage and death or can promote neuroprotection (Elkabes et al., 1996; Chan et al., 2007).

Microglia are derived from monocyte precursors that populate the nervous system during embryonic development (Chan et al., 2007). During embryonic development, microglial precursors migrate into the brain from the hematopoietic tissue of the liver beginning at mid-gestation in the rodent (Bilbo and Schwarz, 2009; Jonakait, 2007; Kaur et al., 2001). They become ramified throughout the brain parenchyma (Jonakait, 2007; Bilbo and Schwarz, 2009), and are particularly abundant in certain locations of the fetal brain including the developing BF (Jonakait, 2007). It has not been reported whether fetal microglia in vivo become activated in response to maternal immune challenge (Jonakait, 2007). However, when isolated from embryonic brains, fetal microglia do produce cytokines and chemokines (Jonakait et al., 2012). Moreover, those from embryos of poly(I:C)-treated dams produce an altered cytokine/chemokine profile as compared with controls (Jonakait et al., 2012). Should fetal microglia become activated and secrete cytokines and/or chemokines in high local concentrations in the fetal brain, such activation could have significant effects on neurogenesis.

Others have also suggested prenatal microglial involvement in neurodevelopmental disorders (Kannan et al., 2007; Roumier et al., 2008). Roumier et al. used mice with a loss of function mutation in DAP12. DAP12 is a signaling protein that regulates microglial activation and is normally expressed in microglia transiently, only during a perinatal time period. Since DAP12 quashes microglial activation, these mice overexpress inflammatory genes specifically before and around the time of birth (Roumier et al., 2008). As adults, these mice display an increased contribution of AMPA receptors relative to NMDA receptors in the glutamatergic response in their hippocampi (Roumier et al., 2008). The investigators also used lipopolysaccharide (LPS) to prenatally inflame wild-type pregnant mice. At birth hippocampal neurons from offspring of LPS-treated mice were cultured without microglia for 20 days to allow synapse formation. Neurons from the maternally inflamed condition exhibited an increase in AMPA to NMDA ratio when compared with wild-type control (saline-treated) counterparts (Roumier et al., 2008) similar to that observed in the genetically altered mice. These authors concluded that *prenatal* microglial activation was sufficient to affect developing neurons and have an impact on synaptic function (Roumier et al., 2008).

Neurogenesis of adult rodent olfactory bulb neurons is also affected by activation of microglia located there (Lazarini et al., 2012). After selective lesions of sensory afferents to the olfactory bulb are made, microglia are activated and proliferate, and the survival of newborn, newly-arrived neurons decreases (Lazarini et al., 2012). When the antibiotic minocycline was used to prevent microglial activation in response to deafferentation, microglial cell proliferation decreased and expression of their activation markers was reduced. At the same time the numbers of surviving neurons no longer decreased although there were still no longer sensory afferents (Lazarini et al., 2012). These experiments showed that the reduced survival of neurons was due to the activation of microglia and not to the lack of sensory afferents.

The means by which maternal inflammation could generate fetal microglial activation is not clear. Most researchers would propose that placental cytokines could reach the fetal brain and either directly affect neurogenesis or activate fetal microglia. An abundance of cytokines and growth factors are produced in the normal placenta (Helliwell et al., 2006; Keelan et al., 1999; Marvin et al., 2002; Sato et al., 2001; Sato et al., 2003; Shen et al., 2008), and these levels change following maternal infection or poly(I:C) administration (Ashdown et al., 2006; Benveniste, 1992; Gilmore et al., 2005; Meyer et al., 2006a; Meyer et al., 2008b; Urakubo et al., 2001; Fatemi et al., 2008; Meyer et al., 2006b; Shen et al., 2008). Notable among those with increased levels are the pro-inflammatory cytokines interleukin-1β (IL-1β), TNFα and IL-6 (Ashdown et al., 2006; Parker-Athill and Tan, 2010; Sato et al., 2001; Smith et al., 2007; Urakubo et al., 2001), and each of these has been shown to affect the survival and/or differentiation of neuronal precursor cells in culture (Ben Hur et al., 2003; Islam et al., 2009; Cacci et al., 2008; Li et al., 2007b; Ajmone-Cat et al., 2010). While it is suggested that cytokines cross the placental barrier and detrimentally affect development in the fetal brain, it is not entirely clear which cytokines, if any, are able to do so (Dahlgren et al., 2006; Gilmore et al., 2005; Zaretsky et al., 2004; Jonakait, 2007). In an ex vivo human placental perfusion model it has been shown that there is very minimal transfer of IL-1α and TNFα across the placental barrier (Zaretsky et al., 2004). On the other hand, in that same model IL-6 did transfer to the fetal circulation (Zaretsky et al., 2004). In rats maternal IL-6 has been shown to cross the placenta during mid-gestation (Dahlgren et al., 2006) although it is not clear whether IL-6 becomes elevated in the fetal brain as a result (Bilbo and Schwarz, 2009; Smith et al., 2007).

However, other connections between microglia and the placenta have recently come to light allowing an alternative speculation. Microglia are derived from myeloid precursors during embryonic development (Kaur et al., 2001; Chan et al., 2007). These, in turn, are generated from hematopoietic stem cells (HSCs) arising in the vasculature of the placenta as well as in sites of the fetal yolk sac and the aorta-gonad-mesonephros region (AGM) (Gekas et al., 2005). The peak of production in the placenta occurs from E12 to E14 in the mouse (Gekas et al., 2005), the time at which poly(I:C) is administered to pregnant dams in many animal studies. The placenta provides a place for the HSCs to expand prior to their seeding of the liver, the main site for HSC expansion and differentiation in the fetus (Rhodes et al., 2008; Gekas et al., 2005; Mikkola et al., 2005). Inflammatory cytokines produced in the placenta as a result of the maternal immune response could skew the differentiation and/or the timing of differentiation of these HSCs. Such skewed differentiation could have consequences for developing microglia. IL-6 is one of the cytokines elevated in the inflamed placenta at mid-gestation and notably the IL-6 family of cytokines can regulate HSC differentiation and proliferation (Seita et al., 2008). While there is scant data to confirm this, changes in the placental environment leading to changes in the HSC differentiation pathway offer an intriguing alternative for direct activation of fetal microglia.

Regardless of the source of their activation, should fetal microglia become activated, they could potentially produce large amounts of inflammatory cytokines affecting neuronal precursor differentiation and fetal brain development.

1.4 Chemokines

Recent research has uncovered previously unrecognized functions for chemokines in normal brain development. Over fifty chemokines have been identified and they are grouped according to structural criteria relating to the cysteines near their amino terminus (Tran and Miller, 2003b). The α chemokines (CXCL) have 1 amino acid separating two cysteines. In β chemokines (CCL) the cysteines follow each other, in γ chemokines (XCR), there is a single cysteine and in δ chemokines (CX_3CR1) three amino acids separate the cysteines (Tran and Miller, 2003b). The effects of chemokines are transduced by G-protein-coupled receptors and these receptors are also categorized as α, β, γ, and δ based on the class of chemokines they bind (Tran and Miller, 2003b). Most chemokines can bind to several receptors, and, conversely, chemokine receptors usually bind several different chemokines. Chemokines are known to function in the regulation of chemotaxis of leukocytes and other cells both in response to inflammation and in normal cell migration (Tran and Miller, 2003b; Rezaie et al., 2002a). Recent findings reveal that during embryonic development chemokine signaling is also involved in directing organogenesis, angiogenesis and the development of secondary lymphoid tissue as well as regulating the proliferation, differentiation and migration of different types of stem cells (Rezaie et al., 2002a; Tran and Miller, 2003b). Their role in brain development is only recently beginning to be investigated (Tran and Miller, 2003b). In the brain neurons, astrocytes and microglia all express receptors for chemokines and all are capable of producing chemokines as well (Tran and Miller, 2003b). Constitutive expression of macrophage inflammatory protein 1 alpha (MIP-1α) and the chemokine receptors CCR2 and CXCR4 along with induced expression of monocyte chemotactic protein 1 (MCP-1) is reported in primary microglia and astrocyte co-cultures derived from the human fetal CNS (Tran et al., 2007; Rezaie et al., 2002a; Conductier et al., 2010). Chemokines participate in the development of the cerebellum and hippocampus (Tran and Miller, 2003b), regulate oligodendrocyte maturation and mylenation (Jakovcevski et al., 2009; Tran and Miller, 2003b) and can influence axonal growth and neuronal survival (Locatelli et al., 2012; Tran and Miller, 2003b). In mouse embryos CXCR4 is expressed by neural crest cells migrating from the dorsal neural tube and is also observed in the dorsal root ganglia (DRG) (Belmadani et al., 2005). Stromal cell-derived factor-1 (SDF-1 or CXCL12), the single agonist for CXCR4, is expressed along the path taken by crest cells to the DRGs, suggesting that SDF-1/CXCR4 signaling is needed for their migration. CXCR4 null mice exhibit small and malformed DRGs (Belmadani et al., 2005).

Chemokines and their receptors are involved in the proliferation and migration of progenitor cells. SDF-1/ CXCR4 is the pair most studied in respect to development (Belmadani et al., 2005; Tran and Miller, 2003b; Tran and Miller, 2003a). In lymphocyte development SDF-1 is expressed by cells in the secondary lymphoid organs to attract and maintain precursor cells. In knockouts, stem cells are not distributed correctly (Ma et al., 1998; Tran and Miller, 2003b). Knockouts of either SDF-1 or its receptor usually die perinatally and they show defects in organogenesis and brain development (Ma et al., 1998; Tran and Miller, 2003b).

Both SDF-1 and its receptor are expressed at varying levels throughout embryonic development and are highly expressed in the developing nervous system (Tran and Miller, 2003b). In the cerebellum during early postnatal development, precursor granule neurons proliferate in the external granule layer (EGL) before migrating. SDF-1 is expressed in the meningeal cells and CXCR4 is expressed by the dividing progenitor cells (Klein et al., 2001; Ma et al., 1998; Tran and Miller, 2003b). SDF-1 attracts these progenitor cells to maintain them in the EGL and cooperates with sonic hedgehog (Shh) to enhance their proliferation (Klein et al., 2001; Tran and Miller, 2003a; Tran and Miller, 2003b). Later, at the proper time to migrate in, the cells downregulate CXCR4 (Tran and Miller, 2003b), and begin to migrate in response to BDNF (Tran and Miller, 2003b).

SDF-1/CXCR4 signaling is also involved in hippocampal development. In the hippocampus of CXCR4 knockout mice, the dentate gyrus does not develop correctly (Bagri et al., 2002; Tran and Miller, 2003b). In this case there are fewer cells with markers for granule neurons and they are ectopically located (Tran and Miller, 2003a; Tran and Miller, 2003b; Bagri et al., 2002), implying that SDF-1 might normally have effects on proliferation and/or migration (Bagri et al., 2002;

Tran and Miller, 2003a; Tran and Miller, 2003b). These examples point to the importance of chemokines for proliferation of precursor populations and their migration to the proper locale (Tran and Miller, 2003b).

It is suggested that MIP-1α and one of its receptors, CCR1, are involved in the maturation of neurites and synapse formation (Cowell and Silverstein, 2003; Tran and Miller, 2003a). CCR1 is transiently expressed by all cells in the cerebellum including granule cells, Purkinje cells, Golgi cells, Bergmann glia, astrocytes and microglia, but receptor expression occurs at different times for each cell type (Cowell and Silverstein, 2003; Tran and Miller, 2003a; Tran and Miller, 2003b). Each type of cell interacts with Purkinje cells when their expression of CCR1 is highest (Cowell and Silverstein, 2003; Tran and Miller, 2003a; Tran and Miller, 2003b). In addition to microglial cells in the white matter, Purkinje cells also produce MIP-1α (Cowell and Silverstein, 2003; Tran and Miller, 2003a; Tran and Miller, 2003a). Taken together, these observations imply an interaction between MIP-1α and CCR1in the process of neurite extension and synapse formation (Cowell and Silverstein, 2003; Tran and Miller, 2003a; Tran and Miller, 2003b). SDF-1 also plays a role in neurite extension as it can attract or repel growth cones in response to either a high or low cyclic guanosine monophosphate (cGMP) concentration (Xiang et al., 2002; Tran and Miller, 2003b).

Chemokines also play a role in oligodendrocyte development. Growth related oncogene-alpha (Gro-α, KC or CXCL1), one of the ligands for CXCR2, is synthesized by astrocytes in the ventral spinal cord where oligodendrocyte precursor cells (OPCs) are developing in the ventricular zone. The chemokine's effect is to inhibit OPC migration by enhancing interactions with the extracellular matrix. At the same time, in concert with platelet-derived growth factor (PDGF), Gro-α enhances the proliferation of OPCs (Jakovcevski et al., 2009; Tran and Miller, 2003b).

Chemokines might also be involved in the process of myelination in the peripheral nervous system (PNS). In response to injury when Schwann cells are proliferating, they downregulate the transcription factor mammalian achaete scute homolog 2 (Mash2), a negative regulator of proliferation. Downstream of Mash2, interferon gamma-induced protein 10 (IP-10, CXCL10) is produced as well as the SDF-1 receptor CXCR4 (Kury et al., 2002; Tran and Miller, 2003b). Since mature Schwann cells express Mash2, CXCR4 and SDF-1, it is likely that these chemokines contribute to Schwann cell development (Kury et al., 2002; Tran and Miller, 2003b).

In neurosphere cultures of progenitor cells isolated from germinal zones of embryonic mice CXCR4 expression is present as early as embryonic day 10.5 (E10.5) and increases until E17 (Tran et al., 2004). These progenitor cells migrate towards an SDF-1 gradient in culture, and AMD3100, a CXCR4 receptor antagonist, blocks this migration (Tran et al., 2004).

Chemokines have also been found to function as differentiation factors in culture. CCL2 and CCL7 are expressed and developmentally regulated in rodent ventral midbrain cultures (Edman et al., 2008a). When mRNA in these cultures was measured at E10.5 and subsequent days, message for these chemokines as well as for their receptors, CCR1 and CCR2, increased (Edman et al., 2008a). CCL2 or CCL7 treatment of E14.5 ventral midbrain precursor cultures (midbrain dopaminergic precursors) results in an increased number of tyrosine hydroxylase positive (TH+) cells as well as an increase in the percentage of Nurr+ (a marker for dopaminergic neurons) cells (Edman et al., 2008a). CCL2 and CCL7 do not promote the proliferation or survival of precursor/progenitor cells, but both CCL2 and CCL7 increase the neurite length two-fold.(Edman et al., 2008a) The α-chemokines are also developmentally expressed (Edman et al., 2008b) and of them CXCL1, CXCL6, and CXCL8 increase the number of dopaminergic neurons in ventral midbrain precursor and neurosphere cultures.(Edman et al., 2008b)

Chemokine receptors are found on neural progenitor cells not only in culture, but in vivo on progenitor cells in the adult mouse brain as well (Tran et al., 2007). The receptors CCR1, CCR2, CCR5, CXCR3 and CXCR4 were all shown by in situ hybridization to be present on cells located in the subventricular zone, the olfactory bulb and the dentate gyrus. These receptors also colocalize with the neural progenitor markers nestin and TLX and with Ki67, a marker for dividing cells.(Tran et al., 2007)

Glial cell production of chemokines has been suggested as a means by which they may modulate neuronal signaling (Puma et al., 2001). Adult rat cholinergic septal neurons express either one or both of the chemokine receptors CXCR1 and CXCR2 (Puma et al., 2001). IL-8 (CXCL8), a ligand for these receptors, is produced by glia and reduces calcium currents in these neurons in a concentration-dependent manner (Puma et al., 2001). These results in culture suggest that IL-8 release by glia in vivo may modulate neuronal excitability (Puma et al., 2001).

The upregulation of chemokine responses in diseased brains points to a role for them in neuroinflammatory disease (Tran et al., 2004). Chemokines are upregulated in the fetal mouse brain in response to MIA (Arrode-Bruses and Bruses, 2012), and microglia isolated from embryonic brains following maternal inflammation produce a variety of cytokines and chemokines (Jonakait et al., 2012). Whether altered chemokines in the fetal brain result in changes in the differentiation, proliferation or survival of precursor cells and whether this occurs in the basal forebrain is not known.

1.5 Interleukin-6 (IL-6)

It has been suggested that IL-6 mediates the effects of maternal immune activation resulting in these behavioral anomalies (Parker-Athill and Tan, 2010; Smith et al., 2007). Viral infection, poly(I:C) injection and recombinant IL-6 injection all lead to autistic-like behavioral abnormalities in mice (Fatemi et al., 2008; Meyer et al., 2006b; Meyer et al., 2006a; Meyer et al., 2008b; Meyer et al., 2008c; Shi et al., 2003; Shi et al., 2005; Parker-Athill and Tan, 2010; Smith et al., 2007). Fetal exposure to IL-6 has produced abnormalities in the adult rat hippocampal structure as well as decreased learning during adulthood (Samuelsson et al., 2006). Administering an antibody to IL-6 at the same time as poly(I:C) injection nullifies the adverse adult behavioral effects and poly(I:C) injection of IL-6 KO mice does result in adult behavioral or cognitive deficits(Smith et al., 2007). Both point to a role for IL-6 in mediating MIA (Smith et al., 2007). IL-6 is one of the cytokines that peaks in the placenta following maternal inflammation (Urakubo et al., 2001; Ashdown et al., 2006; Pessah et al., 2008; Smith et al., 2007), and some studies have shown an increase in IL-6 mRNA in the fetal brain following maternal infection as well (Liverman et al., 2006). Moreover, in culture an antibody against IL-6 blocks the action of microglial conditioned medium in promoting cholinergic differentiation in basal forebrain cultures (Jonakait et al., 2012). Because these studies suggest a role for IL-6 in mediating maternal immune activation, this thesis investigates its potential involvement in alterations in fetal basal forebrain cholinergic development.

Though usually considered pro-inflammatory, interleukin-6 (IL-6) is a pleiotropic cytokine with both pro-inflammatory and anti-inflammatory influences. IL-6 belongs to a family of cytokines which includes IL-11, IL-27, IL-31, leukemia inhibitory factor (LIF), oncostatin (OSM), cardiotrophin-1 (CT-1), ciliary neurotrophic factor (CNTF) and neuropoietin (NPN). All of these molecules share a common signal-transducing receptor, glycoprotein 130 (gp130). Binding to their own individualized receptor (which is also signal-transducing for all except IL-6 and IL-11) causes dimerization with gp130. When IL-6 binds to its non-signaling IL-6 receptor α (IL-6Rα), it induces the homodimerization of gp130. Consequently, Janus kinases (JAK-1 and JAK-2) are activated and phosphorylate specific tyrosines in the cytoplasmic tails of gp130. Signal transducer and activator of transcription molecules (STATs) are recruited to these sites where they are also phosphorylated by JAKs, subsequently dimerize, translocate to the nucleus and affect transcription. IL-6 signaling in the CNS uses STAT3 in the JAK-STAT pathway (Spooren et al., 2011; Sanz et al., 2008). IL-6 can also signal through the mitogen-activated protein kinase (MAPK) pathway. In this case SH2-domain-containing tyrosine phosphatase (SHP2) is recruited to a phosphorylated residue of gp130 and subsequently interacts with the growth factor-receptor-bound protein2/Son of Sevenless (grb2-SOS) complex. This allows Ras activation, leading to the activation of the Ras-Raf-MAPK pathway (Heinrich et al., 2003).

IL-6 can also signal to cells lacking the specific IL-6Rα by means of a soluble IL-6 receptor (sIL-6R) that is produced either by alternative mRNA splicing or by membrane receptor shedding (Jones et al., 2001; Spooren et al., 2011). In this *trans*signaling, IL-6 bound to its soluble receptor signals through gp130, making all cells responsive to IL-6 since gp130 is expressed ubiquitously. This type of signaling is of importance in the CNS and in disease (Spooren et al., 2011; Jones et al., 2001).

A mechanism of IL-6 self-regulation exists. IL-6 signaling induces the expression of suppressor of cytokine signaling 3 (SOCS 3). SOCS3 in turn prevents phosphorylation of tyrosine 759 on the gp130 receptor thereby desensitizing the receptor for further signaling though levels of both IL-6R and gp130 on the surface remain constant (Fischer et al., 2004).

IL-6 is involved in neuroinflammation. Mice overexpressing IL-6 exhibit astrogliosis (Chiang et al., 1994; Campbell et al., 1993), a condition of increased volume and number of astrocytes concomitant with changes in morphology, protein expression and microgliosis as well (Tilgner et al., 2001; Chiang et al., 1994). IL-6 results in microglial proliferation in vitro (Streit et al., 2000) and in their increased phagocytic activity (Shafer et al., 2002). In response to IL-6 microglia can exert either neuroprotective or neurotoxic effects (Krady et al., 2008; Eskes et al., 2002; Eskes et al., 2003). IL-6 knock-out mice have reduced gliosis following injury (Klein et al., 1997) and astrogliosis induced by LPS can be inhibited by injection of an antibody to IL-6 (Pang et al., 2006). It should be noted, however, that in STAT3 -/- mice, although gliosis is attenuated, it is accompanied by an enhanced inflammation state. This includes increased lesion size, disrupted scar formation and reduced behavioral recovery after injury (Herrmann et al., 2008). Therefore, gliosis has positive as well as negative effects.

IL-6 regulates the inflammatory state of the brain. As a result of IL-6 signaling, astrocytes and microglia produce cytokines, chemokines, prostaglandins and other inflammatory molecules (Quintana et al., 2008; Chikuma et al., 2009). In concordance with its pleiotropic characteristics, IL-6 has also been shown to induce growth factors such as neurotrophic growth factor (NGF), neurotrophin-3 (NT-3) and NT-4/5 (Marz et al., 1999).

IL-6 has been shown to enhance neuronal differentiation in culture (Zhang et al., 2007; Cao et al., 2006; Kunz et al., 2009) synergizing with NGF (Kunz et al., 2009). It has been shown to promote the survival of many kinds of neurons including cholinergic neurons (Hama et al., 1991; Hama et al., 1989) and acetylcholinesterase-positive neurons in primary cultures (Kushima and Hatanaka, 1992).

The above studies have demonstrated that IL-6 participates in normal brain development and in neuroinflammation. Since it has also been suggested that IL-6 is a key player in mediating maternal immune activation, this thesis investigates its potential role in altering fetal BF cholinergic development following a prenatal maternal immune challenge.

II. Rationale and Specific Aims

Increasing evidence suggests that neurodevelopmental disorders like autism and schizophrenia may result in part from maternal immune responses during pregnancy following pro-inflammatory stimuli. The mechanism(s) that yield neurodevelopmental disorders in offspring following maternal inflammatory events remain unclear. The data suggest that interleukin-6 (IL-6) may be one of the immune-related cytokines that affects fetal brain development.

In previous studies from our laboratory, it has been shown in vitro that the development of cholinergic neurons from the fetal BF is profoundly affected by soluble factor(s) arising from activated microglia. Conditioned medium from pro-inflammatory microglia promotes the differentiation of undifferentiated precursors in the BF to become cholinergic neurons, possibly at the expense of GABAergic differentiation (Jonakait et al., 1996; Ni et al., 2007). However, the identification of this factor or factors has remained elusive. Moreover, whether fetal microglia become activated in vivo following maternal inflammation has not been directly demonstrated, nor has it been shown that such activation results in increased numbers of cholinergic neurons. In order to address these issues, 4 specific aims were proposed:

1) To determine whether a maternal inflammatory challenge results in increased cholinergic cell number in vivo in the fetal basal forebrain. For these studies, pregnant dams were injected with a viral mimic and the BFs of their fetuses assayed at different ages for choline acetyltransferase (ChAT) activity, the hallmark of cholinergic development. In addition, stereological measurements of cholinergic cell number were done using transgenic mice in which EGFP is expressed under the control of the ChAT promoter allowing for direct visualization of cholinergic neurons.

2) To determine whether fetal microglia become activated following a maternal immune event. This was accomplished using two strategies. Initial data came from PCR studies examining mRNA levels of specific pro-inflammatory cytokines as well as the anti-inflammatory cytokine IL-10 in fetal brain tissue following a maternal inflammatory challenge. Further studies examined the cytokine/chemokine profile of fetal brain tissue following maternal inflammatory challenge using a Luminex® multi-plex assay. Protein expression of thirty-two separate molecules were determined by this assay in both microglial enriched populations ($CD11b^+$) and other brain tissue ($CD11b^-$). Finally, the possibility of microglial proliferation was assessed by stereology within the fetal basal forebrain.

3) To examine a possible role for several chemokines in mediating changes in cholinergic differentiation. These studies were performed in vitro examining bi-potential precursors in the fetal BF to determine the effect of chemokines on proliferation, survival and/or differentiation.

4) To determine a possible role for IL-6 in mediating possible changes in cholinergic differentiation. Studies were done both in vivo and in vitro. For in vivo studies, IL-6 knockout mice were examined for cholinergic development following MIA and compared with wild-type controls. In vitro, antibodies against IL-6 were included with conditioned medium in cultured rat BF to determine any effects of IL-6 in mediating possible alterations in cholinergic differentiation known to occur in the in-vitro situation.

III. Materials and Methods

Animals

Wild type mice (C57BL/6J stock #664) and transgenic strains were purchased from The Jackson Laboratory (Bar Harbor, ME). Homozygous B6.129P-Cx3cr1$^{tm/Litt}$/J (stock #5582) (Cx3cr1-GFP) mice express enhanced green fluorescent protein (EGFP) under the control of the promoter for the fractalkine receptor (CX3CR1). In these mice EGFP is expressed in place of the receptor and monocytes, dendritic cells, NK cells and microglia fluoresce green. In the brain microglia are the only cells that appear green. B6.Cg-Tg (RP23-268L19-eGFP)2Mik/J (stock # 7902) (ChAT^{BAC}-EGFP) mice express EGFP along with the endogenous choline acetyltransferase (ChAT) protein. In B6.129S2-Il6^{tm1Kopf}/J (stock # 2650) IL-6 knockout mice, the IL-6 gene is disrupted and no endogenous IL-6 is expressed in these mice.

Mice were mated overnight and the presence of a vaginal plug considered embryonic day 0.5 (E0.5) Pregnant mice were given intraperitoneal (i.p.) injections of 20 mg/kg poly(I:C) (potassium salt; Sigma-Aldrich, St. Louis, MO) freshly dissolved in 200 µl 0.9 % sterile saline. This dosage has previously been found effective with i.p. delivery(Shi et al., 2003; Smith et al., 2007). Control mice were given injections of 200 µl sterile saline.

Sprague-Dawley rats were purchased from Charles River Laboratories International, Inc. (Wilmington, MA). All animals were housed in the Rutgers/Newark AAALAC-approved animal facility.

Assessment of Sickness Behavior

Sickness behavior of saline-injected and poly (I:C)-injected mice was assessed at 4 hrs and 24 hrs following injection. Mice were evaluated to distinguish between normal and “sickness” behavior according to a rubric based on mouse physical examination guidelines (Crawley, 2007). Pregnant females were placed in a novel environment (new cage) and observed for 2 min. They were given scores in 5 categories as follows: (1) Home cage: Normal is a well-groomed mouse with a well prepared nest. A sick mouse is ungroomed and leaves the bedding square untouched. (2) Cage exploration: In a novel environment normal mice explore, stretch, cross the cage several times, rise up on hind feet and move around the entire cage. Sick mice stay in one place. (3) General behavior: Normal mice sniff, scratch and exhibit normal posture. Sick mice exhibit a hunched posture, remain still, shiver and/or shake. (4) Locomotion: Normal mice run quickly. Sick mice stay in one position or wobble with an impaired gait. (5) Reactivity: Mice were touched with a pencil. The normal mouse quickly responds and runs. The sick mouse lacks response and remains in one spot, resistant to being moved. Mice were scored from 0 to 4 in each of the 5 behavior areas. A score of 4 indicates normal behavior and a score of 0 indicates sickness behavior (no normal behavior in that category). Intermediate scores of 1 for 1 occurrence of normal behavior, 2 for 2-3 occurrences and 3 for 4-5 occurrences of normal behavior in a category were given. A “normal” mouse would score 4 in each behavior category for a total score of 20.

Preparation of microglial conditioned medium

Mixed glial cultures were prepared from the cortices of neonatal mouse pups as previously described.(Jonakait et al., 1994; Jonakait et al., 1996; Jonakait et al., 1998; Ni et al., 2007) Cortices were cleared of meninges, minced, triturated with a fire-polished Pasteur pipette and plated into poly-lysine-coated 75 cm^2 flasks in medium (SCM) containing D-MEM/F12 (1:1), penicillin (25 U/ml), streptomycin (25 µg/ml), D-glucose (0.6%), and 10% heat-inactivated fetal bovine serum (Cell Generation, Ft. Collins, CO). Medium was replaced on day 3 and half the medium exchanged every 3 days thereafter. Microglia were shaken off 12-14-day old mixed glial cultures on an orbital shaker (350 RPM X 40 min), floating cells were collected and plated onto uncoated 75mm^2 flasks in 1:1 SCM/N2. After 24 hours medium was replaced with N2 and treated with lipopolysaccharide (LPS 50 ng/ml, Sigma-Aldrich, St. Louis, MO). 24 hours after LPS treatment supernatant was removed, filtered and the microglial conditioned medium (CM) used to treat basal forebrain cultures.

Basal forebrain cultures

Basal forebrains were removed from an entire litter of E15 rat embryos, pooled and minced in SCM. After transfer to a 50 ml tube and removal of SCM, the pieces were triturated in N2 to a single cell suspension. Cells were counted and plated in 35 mm petri dishes (pre-coated 24 hours with poly-D-lysine) at 1 x 10^6 cells per dish in N2 or LPS-microglial conditioned medium (CM) in a final 2% serum concentration and incubated at 37℃ for 2-5 d ays depending on the assay requirements.

Choline Acetyltransferase (ChAT) Assay

To assay rat basal forebrain cultures, the BF cultures were harvested after 5 days. Cells were washed with PBS, scraped, collected in 1.5 ml centrifuge tubes and centrifuged 20 min at 12,000 rpm at 4℃. Supernatant was discarded and 15 µl EDTA (10 mM) containing 0.5% (v/v) Triton X-100 was added to lyse cells. Cells were homogenized on ice, centrifuged 15 min at 12,000 rpm at 4℃ to pellet. Supernatant was transferred to a new tube to be used for the ChAT assay and for determination of protein concentration (Bio-Rad, Bio-Rad Laboratories, Hercules, CA). For the ChAT Assay reaction 2.5 µl supernatant was placed in a 0.5 microcentrifuge tube. To that 5 µl incubation mixture was added. For each sample the incubation mixture contains 0.5 µl EDTA (240 mM), 0.5 µl sodium phosphate buffer (700 mM), 0.5 µl sodium chloride (4.2 M), 0.5 µl choline bromide (112 mM), 0.5 µl unlabeled acetyl CoA (0.2 mM), 0.5 µl eserine (1.4 mM) and 2.0 µl ^{14}C acetyl CoA. Reaction tubes were incubated in a 37℃ shaker water bath for 60 min. For each sample 10 mg tetraphenylboron was dissolved in 2 ml acetonitrile and placed in a scintillation vial. After incubation the reaction was stopped by addition of 5 ml sodium phosphate buffer (10 mM) to the reaction tube in the scintillation vial containing the tetraphenylboron/acetonitrile. 10 ml EcoscintO (National Diagnostics, Yorkshire, UK; Atlanta, Georgia, USA) was added and vials were inverted gently to mix. Samples were counted on a β-counter 3 minutes each ≥ 2 times.

To perform the ChAT assay on basal forebrain tissue samples, lysis buffer (EDTA (10 mM) containing 0.5% (v/v) Triton X-100) was added directly to the tissue in 1.5 ml microcentrifuge tubes, homogenized on ice, centrifuged and the supernatant transferred to a new tube. The ChAT assay proceeded as above with the following modifications. Volume of lysis buffer added to the tissue depended on the age of embryo/pup from which the BF sample was taken (E16.5: 10 µl; E18.5: 15 µl; P1: 15 µl; P9: 20 µl; P18: 20 µl). Volume of sample supernatant added to the reaction tube was 3.0 µl for E16.5, E18.5 and P1 samples and 2.5 µl for P9 and P18 samples.

Stereological Analysis

E16.5 and P1 brains from CX3CR1-EGFP and ChAT-EGFP mice were fixed in 4% paraformaldehyde/0.1 M PBS, rinsed thoroughly in 0.1 M PBS, cryoprotected in 7% then 15 % sucrose solutions and sliced in 60 µm coronal sections. Mounted sections were rinsed 3X 10 min. in 0.01 M PBS, coverslipped using Vectashield® Hard Set (Vector Laboratories, Inc,, Burlingame, CA) and sealed.

Sections were examined with an Olympus Bx51 microscope which was equipped with an *x–y–z* motorized stage and RetigaTM 200R digital camera (QImaging®. Surrey, BC, Canada). Section outlines and basal forebrain contours were drawn using the Optical Fractionator probe of StereoInvestigator® software (MicroBrightField (MBF), Williston, VT, USA) using brightfield and a 4x objective. Counts were performed using a 40x objective and filter for GFP detection. Cells were randomly sampled and counted to obtain unbiased estimates of cell numbers using the Optical Fractionator probe of StereoInvestigator® software. The grid size was set at 300 µm x 325 µm and the counting frame size was set at

150 µm × 150 µm. This size counting frame and grid allowed for sufficient total number of cells to be counted to obtain a reliable estimate of total population size. Guard zones were 2 µm at the top and bottom of the section and counting was performed in a 20 µm z-depth region. A cell was only counted if the top of the soma was entirely within the counting frame or in contact with the inclusion borders. It was not counted if it was touching the exclusion borders (see Supplementary Figure 1). Section thickness was measured at each site and the cell population estimates reported here are weighted by section thickness. Cells were counted within the basal forebrain (BF) contour in 10 sections from each E16.5 brain and 12 sections from P1 brains beginning rostrally at the first appearance of the medial septal region. Population estimates thus represent a 600 µm and 720 µm section of the BF respectively. The coefficient of error was <0.10. (Some later estimates were based on counting every other section from the same brain region, i.e. 5 sections from E16.5 brains and 6 sections from P1 brains).

Quantitative real-time PCR (qRT-PCR)

Total RNA was extracted using TRIzol® Reagent (Ambion by Life Technologies, Carlsbad, CA) according to the manufacturer's instructions. cDNA was produced from 0.5 µg of RNA by using random hexamers and MMLV reverse transcriptase (Promega, Madison, WI) according to the manufacturer's instructions. For qRT-PCR, cDNA was amplified using SYBR® Green PCR Master Mix (Applied Biosystems, Foster City, or CA) or RT² SYBR® Green/ROX™ qPCR Mastermix (SA Biosciences®, Qiagen Sciences, Inc., Germantown, MD) according to the manufacturer’s instructions. The primers used for amplification were obtained from Integrated DNA Technologies, Inc. (IDT, Coralville, IA) and were designed using Primer Express® (Applied Biosystems, Foster City, CA) or Primer-Blast (www.ncbi.nlm.nih.gov). Primers are listed in Table 1. RT-PCR was performed using the ABI Prism 7900HT Sequence Detection System (Applied Biosystems, Foster City, CA). PCR conditions were 2 minutes at 50℃, 10 minutes at 95 °C, followed by 40 amplification cycles of 15 seconds at 95°C and 1 minute at 60°C. An additional dissociation stage of 15 seconds at 95°C was run. Serially diluted standards were prepared from sample cDNA for each primer to calculate relative concentration of target message. Relative concentration of target message was normalized to the relative concentration of glyceraldehyde 3-phosphate dehydrogenase (GAPDH) in each sample.

Table 1. Primers used for qRT-PCR

	Primers	
Name	Forward (5' - 3')	Reverse (5' - 3')
α7nAChR	TGCACGTGTCCCTGCAAGGC	TGAGCGGCTGCGAGTCGTTG
GABA receptor subunit α1	ATCCGGTTTGCGCTGGGACG	TCTGCGTGCTCCTGCACTGG
GAD 65	CCTATGAGATCGCCCCTGTA	GCATGGCATACATGTTGGAG
GAD 67	CACAAACTCAGCGGCATAGA	CTGGAAGAGGTAGCCTGCAC
GAPDH	GGAGCGAGACCCCACTAACA	ACATACTCAGCACCGGCCTC
IL-1β	AAATACCTGTGGCCTTGGGC	CTTGGGATCCACACTCTCCAG
IL-6	TTCCATCCAGTTGCCTTCTTGG	TTCTCATTTCCACGATTTCCCAG
IL-10	TGACTGGCATGAGGATCAGC	ACTCCGCAGCTCTAGGAGCA
KCC2	TGGCGGCCGAGAGGTCATCA	CCAGGGCATGGGCAACTGGG
NKCC1	GGCCAAGGGCAGCGAGGAAG	GTCCCCGCCGTTCTGGAAGC
NMDA receptor subunit NR1	ACAAGCGACACAAGGATGCCCG	GGTCGGGCTCTGCTCTACCACT
Shank3	GCCTGCGTCTGGACCCAACC	ATCCAGGAACTTGCCGGCGC
TNFα	CGTGGAACTGGCAGAAGAGG	CTGCCACAAGCAGGAATGAG
type I Neuregulin1	GAGCCCAGCATTGCCTCCCAG	CCTACGGTTCAGCTCATTCCCG
type III Neuregulin1	TCTCTCGATGGGCTTCCGGC	GAGACGCTCCGCTTCCAGGC

GFP ELISA

Protein was extracted from hippocampal tissue samples using Tissue Extraction Reagent I (FNN0071; Invitrogen, Life Technologies^{TM} Grand Island, NY) and proteinase inhibitor cocktail (Sigma-Aldrich, St. Louis, MO). A GFP ELISA kit (Cell BioLabs, Inc, San Diego, CA) was used to quantify GFP in hippocampal tissue samples according to the manufacturer's instructions. Briefly, 70 µg protein from each sample in 100 µl total volume assay diluent was added to wells of a 96 well anti-GFP antibody coated plate. Serially diluted recombinant GFP standards were included in each assay. Plates were incubated overnight at 4℃. Samples and standards were assayed in duplicate. Wells were washed 3X with wash buffer,100 µl biotinylated anti-GFP antibody added and the plate was incubated 2 hours at room temperature on an orbital shaker. Wells were washed 3X, 100 µl streptavidin-enzyme conjugate added and the plate was incubated 1 hour at room temperature on an orbital shaker. Wells were washed 3X and substrate solution added. 100 µl stop solution was added to stop the reaction and absorbance at 450 nm was read using a Fusion^{TM} Universal Microplate Analyzer (Packard BioScience Company, Packard Instrument Co., Meriden, CT). Data are reported as pg GFP/mL/µg protein.

Enriched populations of fetal microglia

A protocol was adapted to obtain an enriched population of fetal microglia from the brains of embryos. A similar protocol is used to isolate microglia from adult mouse brains (Nikodemova and Watters, 2012). Brains from all embryos of a litter were pooled, minced and transferred to a gentleMACS C tube. Excess liquid was removed and 3.5 ml of enzyme mixture containing 0.05% trypsin, 2 mM EDTA and 20 µg/ml Deoxyribonuclease I (DNASE) (all purchased from Sigma-Aldrich, St. Louis, MO) in 1X PBS was added. Tubes containing the mixture were run through 2 programs of mechanical dissociation using the gentleMACS dissociator (Miltenyi Biotec Inc., Auburn, CA) separated by a 10 incubation at 37℃, To stop the reaction, 10 ml SCM containing 0.5 mg/ml soybean trypsin inhibitor (Sigma-Aldrich, St. Louis, MO) and 40 µg/ml DNASE was added followed by two additional 10 min. incubation periods at 37℃ and an additional mechanical dissociation step. The cell suspension was filtered through a 40 µm cell strainer (BD Falcon, Franklin Lakes, NJ), centrifuged (10 min, 8℃, 800 rpm) and the supernatant aspirated completely. Cells were resuspended in 10 ml rinsing buffer (1X PBS/2 mM EDTA) and centrifuged. Pellet was resuspended in 90 µl running buffer (1X PBS/2 mM EDTA/0.5% BSA) per 10^7 total cells and 10 µl anti-CD11b magnetic beads (Miltenyi Biotec Inc., Auburn, CA) per 10^7 total cells were added and mixed. Cells were incubated with beads 15 min at 4℃ after which they were washed and centrifuged. The supernatant was removed completely, 500 µl running buffer was added and the cell suspension was separated using an autoMACS magnetic cell sorter (Miltenyi Biotec Inc., Auburn, CA). Both positive and negative fractions were maintained on ice for protein or RNA extraction.

LUMINEX® Assays

Protein was extracted from cells of the CD11b$^+$ and CD11b$^-$ fractions using Tissue Extraction Reagent I (FNN0071; Invitrogen, Life Technologies™

Grand Island, NY) and proteinase inhibitor cocktail (Sigma-Aldrich, St. Louis, MO). The Mouse 32-plex Cytokine/Chemokine LUMINEX® assays (EMD Millipore, Billerica, MA) were performed by Robert Donnelly (The New Jersey Medical School, UMDNJ). Only 25 µl sample is required to run the panel of 32 cytokines and chemokines in a single well. The principle of the assay is summed as follows. Proprietary dyes are used to internally code microbeads. In this assay beads with 32 different internal codes would be used. The beads are coated with an antibody so that beads binding a particular cytokine or chemokine share a unique internal code. A biotinylated secondary antibody is used and a streptavidin-PE reporter. For detection, microbeads pass through 2 lasers. One excites the internal dyes and the other excites PE. A digital-signal processing system identifies the spheres and quantifies results. Samples and standards were run in duplicate. Results were normalized to protein concentration of samples and are reported as pg/mg protein.

Flow Cytometry

Flow cytometry was used to determine the percentage of microglia in cell suspensions from whole fetal brains using CX3CR1-GFP mice. In the suspensions of brain cells from these embryos only microglia would express GFP protein. Brains from the same number of embryos of saline- and poly(I:C)-injected females were pooled, minced, enzymatically and mechanically dissociated as above, filtered, rinsed and centrifuged. This single cell suspension from whole fetal brains was then washed, pelleted, and resuspended in FACSbuffer (Becton Dickinson, Mountainview, CA). GFP detection in cells was performed using a FACScan™ flow cytometer (Becton Dickinson, Mountainview, CA) and data was analyzed using CellQuest® software (Becton Dickinson, Mountainview, CA).

Chemokines, chemokine receptor inhibitors, cytokines and antibodies

Pharmacological inhibitors of chemokine receptors used were J113863 (CCR1 inhibitor), BMS CCR2 22 (CCR2 inhibitor), SB328437 (CCR3 inhibitor), DAPTA (CCR5 inhibitor), SB265610 (CXCR2 inhibitor) and AMD3100 (CXCR4 inhibitor). All were purchased from Tocris Bioscience (R & D Systems®, Minneapolis, MN). Chemokine receptor inhibitors were added to cells for 10 minutes before the addition of CM or N2. Recombinant rat MIP-1α, MIP-1β, MCP-1 and RANTES were all purchased from Peprotech (Rocky Hill, NJ). Recombinant rat IL-6 and rabbit antibodies to IL-6, were purchased from MBL® Int'l (Woburn, MA) and from R & D Systems,® (Minneapolis, MN). Control rabbit IgGs were purchased from R & D Systems.® Cytokine, chemokine and antibody treatments were added to the CM or N2 immediately before adding medium to cells.

CellTiter 96® AQ$_{ueous}$ One Solution Cell Proliferation Assay

Single suspensions of E15 rat basal forebrain cells were prepared for culture as above in N2 or conditioned medium (CM) with or without recombinant rat IL-6 (20 ng/ml), αIL-6 (2 µg/ml, 1 µg/ml, 0.5 µg/ml or 0.1 µg/ml), MIP-1β (200 ng/ml), and/or DAPTA (20 µM). Cells were seeded at 25,000 cells per well in 100 µl in 96 well plates. After 2 days in culture 20 µl CellTiter 96® AQ$_{ueous}$ One Solution reagent (Promega, Madison, WI) was added to each well and plates were returned to 37℃. Living cells convert the MTS tetrazolium reagent to a colored formazan product with the amount of product directly proportional to the number of living cells. After 2-4 hours absorbance at 450 nm was measured by a Fusion^{TM} Universal Microplate Analyzer (Packard BioScience Company, Packard Instrument Co., Meriden, CT). The plates contained wells with N2 and reagent only (no cells) as background controls. The average of readings from these wells served as the blank and this value was subtracted from the experimental values.

Live/Dead® Assays

Single suspensions of E15 rat basal forebrain cells were prepared for culture as above in N2 or conditioned medium with or without recombinant rat IL-6 (20 ng/ml), αIL-6 (2 µg/ml, 1 µg/ml, 0.5 µg/ml or 0.1 µg/ml), MIP-1β (1 µg/ml, 200 ng.ml) and/or DAPTA (20 µM) and plated at 1 x 10^6 cells on sterile glass coverslips in 35 mm petri dishes and incubated at 37℃ for 2-3 days. To determine cell viability a LIVE/DEAD® Viability/Cytotoxicity Kit, for mammalian cells (Molecular Probes^{TM}, Life Technologies, Grand Island, NY) was used according to the manufacturer's instructions. Following incubation cells were washed with PBS. A reagent solution of 4 µM Ethidium homodimer-1 (EthD-1) and 2 µM calcein AM was prepared and 200 µl added to each coverslip for 30 min. Calcein AM permeates cell membranes and in live cells is enzymatically converted from non-fluorescent to a green fluorescent calcein that then remains inside live cells. EthD-1 only enters cells with damaged membranes and when it binds to nucleic acids its fluorescence is magnified making dead cells appear bright red. After incubation with reagent, coverslips were mounted. Live and dead cells in 10 fields of view were counted. The ten fields of view were systematically selected in 3 columns: 3 in the first column, 4 in the middle column and 3 in the third column. A Zeiss Axiovert 200M fluorescence microscope with 20x objective and AxioVision Release 4.8.2 software was used to visualize cells.

BrDU Cell Proliferation Assay

A colorimetric BrdU Cell Proliferation Assay Kit (Cell Signaling Technologies, Inc, Danvers. MA) was used according to the manufacturer's instructions to detect BrDU incorporation, Briefly, single cell suspensions of E15 rat basal forebrain cells were prepared for culture as above in N2 or conditioned medium (CM) with or without recombinant rat MIP-1β (200 ng.ml) and/or DAPTA (20 µM) and plated at 70,000 cells per well in 96 well plates in 180 µl medium with 20 µl 10X BrDU labeling solution and incubated for 5 hours or 24 hours at 37℃. Following incubation medium was removed and c ells were fixed, denatured and detection antibody, HRP-conjugated secondary, TMB substrate and stop solution steps were sequentially performed with appropriate washes in between. Absorbance at 450 nm was read with a Fusion^{TM} Universal Microplate Analyzer (Packard BioScience Company, Packard Instrument Co., Meriden, CT).

Statistical Analysis

Statistical Analyses were performed using Sigma Stat® 2.03, XLSTAT 2012, Primer of Biostatistics and VassarStats. Data reported are the mean ± SEM. A Student's t-test was used to compare 2 groups (a non-parametric Mann-Whitney test was also used to compare 2 groups when appropriate). Data for multiple groups were compared using a one- or two-way ANOVA or an ANCOVA and were followed by a Tukey post hoc test to determine statistical differences between groups. Statistical analyses of data obtained from the LUMINEX® assays were performed after logarithmic transformation of the data. A one sample, one-tailed t-test was used to compare the log-transformed values. Relevant tests used are noted in figure legends. A p value <0.05 was considered significant throughout the analysis.

IV. Results

4.1 Specific Aim 1. *To determine whether a maternal inflammatory challenge results in increased cholinergic cell number in vivo in the fetal basal forebrain.*

Culture studies have demonstrated that factors produced by activated microglia promote cholinergic differentiation of undifferentiated embryonic basal forebrain precursor cells (Jonakait et al., 1994; Jonakait et al., 1996; Jonakait et al., 2000; Ni et al., 2007). Whether maternal immune activation results in increased numbers of cholinergic neurons in the fetal BF in vivo has not been investigated. In order to address this question, pregnant mice at E12.5 were injected with poly(I:C) (20 mg/kg) or sterile saline and the basal forebrain of their embryos/offspring assayed for choline acetyltransferase (ChAT) activity and numbers of ChAT+ neurons.

4.1.1 Poly(I:C) treatment affects behavior and weight gain of dams

In order to verify that the poly(I:C) injection was effective, maternal weight and behavior were monitored. Dams were weighed on the day of mating as a baseline. They were also weighed on the day of injection (E12.5) and one day after injection. Control females injected with saline gained weight from E12.5 to E13.5, showing an average gain of +0.64 ± 0.08 grams (n= 51). By contrast, poly(I:C)-injected females lost weight, -0.91 ± 0.12 grams (n= 66), showing a statistically significant difference between the 2 groups ($p < 0.001$, Table 2).

In addition to weight loss, sickness behavior was assessed (see *Materials and Methods*). Four hrs after injection, saline-injected animals received a total score of 19.3 ± 0.19 indicating normal behavior (Table 3). The lower score in the home cage behavior category of some control mice was due to an incompletely made nest. All were active, exploring and responsive in the novel environment. On the other hand, pregnant females injected with poly(I:C) were lethargic and unresponsive 4 hrs post injection. Their scores were significantly lower than controls in all categories with a total score of only 6.03 ± 0.75 (Table 3; Control: n= 41, Poly(I:C): n= 54; $p < 0.0001$). The loss of weight and the behavioral assessments indicate that poly(I:C) injection causes a robust but transient response to the drug. However, after 24 hrs. all females exhibited normal behavior (Table 3).

Poly(I:C) administration did not affect the length of gestation, number of pups or size of embryos. The duration of pregnancy was 20.5 days for both poly(I:C)-injected and saline-injected females and litter sizes for both groups averaged 6-7 pups per litter. The crown-to-rump lengths of their embryos did not differ significantly between poly(I:C)-treated dams and controls at equivalent days of gestation (Table 4).

4.1.2 Poly(I:C) treatment results in an increase in ChAT activity in the BF

Having confirmed the effectiveness of the poly(I:C) treatment, experiments were performed to compare basal forebrain ChAT activity and number of cholinergic neurons between the offspring of both groups.

In order to determine whether there is more ChAT activity in the fetal BF following a maternal immune challenge, BFs were dissected from E16.5 and E18.5 embryos and P1 pups. Protein extracted from these samples was analyzed using a ChAT assay in which the synthesis of ^{14}C-acetylcholine is measured (see *Materials and Methods*).

ChAT activity was significantly higher following poly (I:C) treatment at these early time points (CPM/µg protein for control at E16.5: 92.66 ± 1.71, E18.5: 117.73 ± 9.08, P1: 215.66 ± 18.74; CPM/µg protein for poly(I:C) at E16.5:112.08 ± 2.63, E18.5: 160.42 ± 7.44, P1: 279.60 ± 14.32, $p<0.001$ Figure 1A). An analysis of covariance (ANCOVA) with a post-hoc Tukey test using all individual basal forebrain samples as separate data points also revealed a significant difference between the two groups over this time period ($p< 0.0001$ Figure 1B). These data clearly demonstrate that cholinergic activity increases in the fetal basal forebrain following maternal immune activation.

4.1.3 Poly(I:C) treatment results in an increased number of cholinergic neurons in the BF

To determine whether the number of cholinergic neurons found in the fetal BF also increases in vivo following maternal immune activation, transgenic mice were used that express EGFP under the control of the ChAT promoter while also expressing a fully functional ChAT protein. At E12.5 pregnant mice were injected with either saline or poly(I:C) (20 mg/kg). Stereo Investigator® software was used to quantify the number of EGFP+ cells and obtain an estimate of the number of cholinergic neurons in a 600 µm portion of each E16.5 BF and a 720 µm portion of each P1 BF (see *Materials and Methods*).

Results show that the number of cholinergic neurons is significantly higher at E16.5 and at P1 in the poly(I:C) group as compared to controls (Figure 2). At

E16.5 the average estimated number of ChAT+ neurons increases from 1869 ± 111 in the control samples to 3336 ± 451 in the poly(I:C) samples, a 78% increase. At P1 there is also an increase in the estimated population of ChAT+ neurons from 10,354 ± 497 in the control basal forebrain to 17,770 ± 616 in the poly(I:C) group, an increase of approximately 70%. These findings are not only consistent with the increase in ChAT activity observed in early BF development, but the increase in ChAT+ cell number due to poly(I:C) administration is of even greater magnitude. Maternal immune activation has a marked effect on cholinergic development in the fetal BF.

The effect on ChAT activity is, however, transient. By P9, levels have returned to that of saline-injected controls (Figure 3). Even though the effect on cholinergic development was transient, we investigated the possibility that even a transient increase in cholinergic cell number at a sensitive developmental window could have significant consequences. We chose to investigate a number of these including potential changes within the BF itself and one of its downstream targets, the hippocampus.

4.1.4 Poly(I:C) treatment affects glutamic acid decarboxylase mRNA expression in the BF

In BF cultures an increase in ChAT activity and cholinergic cell number is accompanied by a decrease in message for glutamic acid decarboxylase 65 (GAD65) (Ni et al., 2007). To determine whether a parallel situation occurs in vivo, RNA was extracted from E16.5 and P1 BFs of offspring of both saline-injected and poly(I:C)-injected pregnant mice. This RNA was then reverse transcribed and the message levels for GAD65 and the related molecules GAD67 and the gamma-aminobutyric acid receptor α-subunit 1 (GABARα1) were quantified by RT-PCR. Message for GAD65 was significantly lower in the E16.5 basal forebrains of embryos of poly(I:C)-treated dams with message levels at only half the levels found in controls (Figure 4). A significant difference was not found in expression levels of GAD67 or GABARα1 between the two groups at this time point. At P1 none of the molecules was significantly different from control suggesting that by birth GAD65 levels had recovered.

4.1.5 Poly(I:C) treatment has negligible effects on the hippocampus

Because septal BF cholinergic neurons begin to extend processes through the fimbria to the hippocampus during this perinatal period, we reasoned that downstream effects of increased BF cholinergic activity would be reflected there. The hippocampus contains abundant acetylcholine receptors. Calcium influx through these receptors--particularly those with the α7 subunit (α7nAChRs) (Le Magueresse et al., 2006; Liu et al., 2006)--promotes a conversion from excitatory GABAergic signaling to inhibitory by increasing the transcription of KCC2, the mature form of the chloride transporter (Liu et al., 2006). Liu et al. found that this shift in chloride transporter molecules from the immature form (NKCC1) to the mature form occurs between P6 and P13 in the rodent (Liu et al., 2006). In the absence of functional α7nAChRs hippocampal neurons retained an excitatory response to GABA (Liu et al., 2006). We wanted to determine whether an increased cholinergic cell number in the BF might alter the timing of this conversion and produce a premature switch in chloride transporter expression.

We first verified by RT-PCR that message for the α7nAChR was present in early postnatal mouse hippocampi from both saline- and poly(I:C)-treated offspring (Figure 5A). Moreover, expression levels were the same over time in both treatment groups.

Having confirmed the presence of the receptor, we asked whether increased cholinergic expression in the BF might affect mRNA levels of chloride transporter forms. RNA was extracted from the hippocampi of pups of saline- and poly(I:C)-injected mice at P1, P2, P3, and P9, reverse transcribed and assayed by RT-PCR (Figure 5B and 5C). Like Liu et al., we detected a shift in transporter profile with NKCC1 giving way to the mature form of the transporter, KCC2. However, poly(I:C) treatment did not affect the timing of this transition even though there were more cholinergic neurons in the developing BF (Figure 5B and 5C and Supplementary Tables 1 and 2).

mRNA levels for three other molecules involved in synapse formation and function were assessed. These were typeI and type III neuregulin1 (NRG1), the NMDA receptor subunit NR1 (NMDAR) and SH3 and multiple ankyrin repeat domains 3 (Shank 3). Type III NRG1 regulates α7nAChRs on hippocampal interneurons (Liu et al., 2001) as well as on projection neurons in the ventral hippocampus (Zhong et al., 2008). Hippocampi of schizophrenia patients contain higher levels of type I NRG1 and lower levels of type III NRG1 than normal subjects, (Harrison and Law, 2006; Coyle et al., 2010) and altered levels of the α7nAChR have been reported in both schizophrenia and autism (Lippiello, 2006; Graham et al., 2002; Coyle et al., 2010). Because gestational nicotine exposure in mice heightens the expression of several NMDAR subunits including NR1 (Wang et al., 2011), we hypothesized that excessive cholinergic activity from the BF might have a similar action in raising levels of the NMDAR. Shank 3 is an adaptor protein that has a function in the postsynaptic density to connect ion channels and neurotransmitter receptors to the cytoskeleton. It is an autism-associated gene (Bozdagi et al., 2010). Note that genetic alterations or levels of expression and function of all of these molecules have been implicated in autism and/or schizophrenia (see Introduction and Background).

No significant differences in message levels between the control and poly(I:C) groups were found for type I NRG1, type III NRG1 or the NR1 subunit of NMDAR (Figure 6A, 6B and 6C). However, Shank3 levels were significantly increased at both P3 (Control = 0.374 ± 0.066; poly(I:C) = 0.498 ± 0.061; $p<0.05$) and P9 (Control = 0.615 ± 0.023; poly(I:C) = 0.843 ± 0.053; $p<0.05$), more than a 30% increase at both time points (Figure 6D). These data are consistent with recent studies by Burton, et al. showing a similar increase in perinatal rat hippocampal Shank3 mRNA levels following maternal infection with *mycoplasma pulmonis* (Burton et al., 2012).

While the alteration in Shank3 message levels in the hippocampus was apparent, it was not clear whether increased cholinergic innervation in the hippocampus was the cause. In order to gain an estimate of cholinergic innervation, ChAT levels were determined in the hippocampus of offspring from both saline- and poly(I:C)-injected ChAT-EGFP mice at P1, P3, P7 and P14. In this instance GFP was assayed as an indicator of the quantity of ChAT using a

GFP ELISA kit (Cell BioLabs, San Diego, CA). No significant difference was found in the amount of GFP protein when controls were compared to poly(I:C) samples (Figure 7). Therefore, it is unlikely that cholinergic signaling from the BF can account for the increase in Shank3 message expression seen there.

Conclusions for Specific Aim 1

Following maternal immune challenge:

- ChAT activity is transiently increased in the fetal BF;
- The number of ChAT+ neurons increases in the fetal BF;
- Message levels for GAD65 in the fetal BF are transiently lower;
- Message levels for Shank3 are increased in the first post-natal week in the hippocampus;
- Postnatal effects of transient cholinergic increases do not affect the following hippocampal molecules:
  - ✓ Chloride channel transporters
  - ✓ Type 1 and type III NRG1
  - ✓ The NR1 subunit of the NMDA receptor
  - ✓ ChAT protein

4.2 Specific Aim 2. *To determine whether fetal microglia become activated following a maternal immune event.*

4.2.1 IL-6 mRNA is increased in fetal brains following MIA

Previous studies have shown that microglial conditioned medium (CM) enhances cholinergic differentiation in the BF in culture (Jonakait et al., 1996; Ni et al., 2007). We have now found an increase in cholinergic cell number in the fetal BF following MIA. This prompts the question of whether activated fetal microglia are responsible for the cholinergic increase in vivo.

Although indirect evidence suggests that fetal microglia are activated following MIA (Kannan et al., 2007; Roumier et al., 2008), direct demonstration is lacking. In order to re-open this investigation, pregnant mice at E12.5 were injected with poly(I:C) (20 mg/kg) or sterile saline. At E 15.5 and E16.5 fetal brains were prepared either for RT-PCR analysis or a Luminex® assay for the determination of message and protein levels of various cytokines and chemokines.

To assure that our assays measured primarily microglial products, we obtained an enriched population of microglia from fetal brains of CX3CR1-GFP transgenic mice. These mice express EGFP under control of the fractalkine receptor (CX3CR1) promoter. Because microglia are the only cells in the brain that express this receptor, only microglia are fluorescent. Brains were pooled from a single litter, minced, trypsinized and mechanically dissociated using the GentleMACS® (Miltenyi Biotec, Inc.) cell dissociator (see *Materials and Methods*). This single-cell suspension was separated using magnetic CD11b$^+$ beads and a magnetic cell sorter (autoMACS®, Miltenyi). Approximately 2.20 ± 0.33 x 10^6 cells were recovered using this method of which 1.02 ± 0.19 x 10^6 were GFP+ indicating that approximately 50% of the recovered cells were microglia. These were prepared for RT-PCR analysis of pro-inflammatory cytokines interleukin 1β (IL-1β), IL-6 and tumor necrosis factor-alpha (TNFα) and the anti-inflammatory cytokine interleukin IL-10 (see *Materials and Methods*). Of the cytokines measured, only IL-6 showed a significant increase in mRNA expression following maternal treatment with poly(I:C) (Figure 8).

4.2.2 MIA results in changes in fetal brain cytokines and chemokines

While mRNA levels were instructive, we wanted to determine whether microglia in vivo were producing cytokine or chemokine proteins after maternal immune challenge. Initial studies utilized fetal slice cultures from CX3CR1-GFP transgenic mice. 300 µm slice cultures were established from E16.5 and E17.5 mouse brain cortices with the planned objective of treating these cultures with inflammatory stimuli in future experiments to evaluate the microglial cytokine/chemokine response. Following 3 days in culture, histochemical analysis revealed that activated microglia had proliferated profusely throughout the culture and overwhelmed the entire slice (data not shown). Clearly fetal microglia were capable of becoming activated. Presumably the act of cutting the fetal brain was in itself a sufficient stimulus. However, it was clear that these cultures could not be used as an experimental system to determine an in vivo fetal microglial response to inflammatory stimuli.

Therefore, in order to assess the production in vivo of microglial cytokines or chemokines a 32-plex Mouse Cytokine/Chemokine Luminex® assay was used (conducted by Robert Donnelly at NJ Medical School, UMDNJ). For this assay an enriched population of E16.5 CD11b$^+$ fetal microglia was obtained from wild type mice as above by pooling all embryonic brains from a single litter, preparing a single cell suspension from these brains and separating out the microglia using anti-CD11b magnetic beads (see *Materials and Methods*). Cells were then lysed and protein extracted. Because Luminex® requires only a 25 µl sample to assay the entire panel of cytokines/chemokines, at E16.5 sufficient protein could be obtained from CD11b$^+$ fraction lysates. Moreover, preliminary data from mRNA studies had used this time point (see above). In order to determine whether cells other than microglia produced these molecules as well, the CD11b$^-$ fraction was also assayed.

Consistent with mRNA data, neither TNFα nor IL-β showed an increase following maternal challenge (Supplementary Table 3A). While the mRNA for IL-6 showed an increase, the IL-6 protein levels failed to reach statistical significance in the Luminex® assay, though the trend was upward. IL-1α, a classic pro-inflammatory cytokine, along with GM-CSF, M-CSF, IL-4 and IL-9 also showed significant elevations (Table 5A and Supplementary Table 3A).

Unexpectedly, a number of chemokines also showed statistically significant increases (Table 5A and Supplementary Table 3B). These included Eotaxin (CCL11), MIP-1β (CCL4), LIX (CXCL5) and RANTES (CCL5). Levels of MCP-1 (CCL2), while not reaching significance, also trended upwards (Supplementary Table 3B).

While our focus was on CD11b$^+$ (i.e., microglial) fractions, the negative fractions also produced significant quantities of cytokines, often in much larger quantities than in the CD11b$^+$ fraction (Figure 9). Data from microglial fractions and those from non-microglial fractions were pooled disregarding treatments. Observing the data this way revealed that cytokines are present in the normal developing brain in non-microglial compartments. Unlike the dramatic elevation in levels of several cytokines and chemokines that occurs with poly(I:C) treatment in the CD11b$^+$ fractions, little change is seen in the levels of these molecules in the CD11b$^-$ fractions between treatment groups (Table 5B and Supplementary Tables 4A and 4B). Notably, however, lower levels of the anti-inflammatory cytokine IL-10 and the chemokine MCP-1 are found in the CD11b$^-$ fractions from the poly(I:C) treatment group (Table 5B and Supplementary Tables 4A and 4B).

4.2.3 Numbers of fetal microglia do not change with maternal immune challenge

To determine whether fetal microglial populations change in vivo as a result of MIA, two strategies were used. In the first, single cell suspensions were prepared from brains in E16.5 litters from both control and poly (I:C) groups using CX3CR1-GFP mice and these were assessed by flow cytometry. Under both conditions GFP+ cells (microglia) made up approximately 1% of the total cell number (0.940 % ± 0.007 vs. 0.955 % ± 0.035 *p*=0.605, n=4 experiments) suggesting that there was no dramatic change in microglial numbers.

In order to determine definitively whether maternal immune challenge resulted in an increased population of microglia in the fetal basal forebrain, microglia were assessed by stereology in the basal forebrains of embryos of both saline-injected and poly(I:C)-injected mice. CX3CR1-GFP mice were used for these investigations.

Since CX3CR1-GFP mice lack a functional fractalkine receptor it would hypothetically be possible a downregulation of the receptor would mean that some microglia might go undetected. To determine whether all the microglial cells were being detected in these mice, brain sections from CX3CR1-GFP mice were stained with ionized calcium binding adaptor molecule 1 (Iba-1), a calcium binding protein that is a marker for microglial cells. Examination by fluorescent microscopy revealed 100% co-localization. Because all cells stained with Iba-1 were also EGFP positive, we could be confident that use of the CX3CR1-GFP mice yielded accurate counts (data not shown).

Using these mice, Stereo Investigator® software provided a microglial population estimate for a 600 µm basal forebrain section at E16.5 and a 720 µm section at P1 (see *Materials and Methods*). There was no significant difference in population estimates between control and poly (I:C) groups. Average microglial population estimates are 3888 ± 353 for the controls and 3800 ± 479 for the poly(I:C) group at E16.5 and 9,156 ± 933 and 9381 ± 719 at P1 for the same groups respectively (Figure 10).

Conclusions for Specific Aim 2:

Following maternal immune challenge:

- Fetal microglia upregulate IL-6 mRNA but not TNFα or IL-1β mRNA;
- Fetal microglia upregulate cytokines GM-CSF, M-CSF, IL-1α, IL-4, and IL-9 as well as chemokines Eotaxin, MIP-1β, LIX and RANTES;
- Fetal non-microglial brain cells downregulate IL-10 and MCP-1; and
- There is no significant increase in the number of fetal microglia.

These data taken together suggest that alterations in fetal brain chemistry following maternal immune challenge from both microglial and non-microglial sources have the potential to affect neural development.

Specific Aim 3. *To examine a possible role for several chemokines in mediating changes cholinergic differentiation.*

4.3.1 Do chemokines regulate cholinergic development?

Because of the unexpected finding of large amounts of chemokines in both the microglial and non-microglial lysates in the developing brain, we questioned whether these molecules play a role in altering cholinergic development in the basal forebrain following maternal inflammation. Chemokines have been associated with proliferation, differentiation and migration of neural stem cells (Edman et al., 2008b; Edman et al., 2008a; Tran and Miller, 2003b; Tran et al., 2004). Moreover, studies from our lab using E14 rat cortical neurospheres indicate that inhibition of the C-C chemokine receptor 5 (CCR5) significantly reduces total numbers of Tuj-1 cells (a marker for mature neurons) while modestly lowering the number of DAPI+ cells after 3 days in culture (Li Ni, personal communication). We have also seen a modest but consistent inhibition of neurosphere cell proliferation (Li Ni, personal communication). These data led us to hypothesize that chemokines in general and CCR5 agonists in particular may affect basal forebrain precursors or their descendents similarly.

Since we were unable to obtain sufficient numbers of basal forebrain cells for cultures from mouse embryos, E15 rat basal forebrain cultures were used to determine the effect of chemokines on BF precursor cells with the understanding that rats are not identical to mice. Because chemokines and their receptors do not have exclusive binding partners, chemokine signaling was blocked using pharmacological inhibitors of the receptors. The cultures were assessed using a

ChAT assay. Inhibiting the receptor of a chemokine involved in cholinergic differentiation would be expected to decrease the amount of ChAT activity measured. These results would then need to be followed up by parsing the effect of individual ligands for that receptor.

E15 rat basal forebrain cells were cultured for 5 days in microglial conditioned medium with or without J113863 (a CCR1 inhibitor), BMS CCR2 22 (a CCR2 inhibitor), SB328437 (a CCR3 inhibitor), DAPTA (a CCR5 inhibitor), SB265610 (a CXCR2 inhibitor) or AMD3100 (a CXCR4 inhibitor) (Figures 11-13). Of these only BMS CCR2 22 (CCR2 inhibitor, Figure 12A) and DAPTA (CCR5 inhibitor, Figure 13A) significantly decreased the amount of ChAT activity.

4.3.2 CCR2 inhibition has a biphasic effect on ChAT activity

The CCR2 receptor was of interest because one of its ligands, MCP-1, was found by the Luminex® assay to be present in both the non-microglial fractions as well as in the microglial fractions where it was elevated by poly(I:C) treatment. Moreover, MCP-1 has been the focus of several studies on ASD. Its elevation in the amniotic fluid mothers of ASD children (Abdallah et al., 2012), the serum of ASD children (Ashwood et al., 2011b) and the cerebral spinal fluid of ASD patients (Vargas et al., 2005), have pointed to a potential role in maintaining the elevated pro-inflammatory immune status that characterizes many autistic patients (Onore et al., 2012). To determine a possible effect on cholinergic development, the CCR2 receptor inhibitor was added together with microglial CM (Figure 12A). Increasing concentrations of the inhibitor produced a bi-phasic dose-response curve with 5 nM being the only concentration at which ChAT activity was significantly lower than the CM. The addition of MCP-1 (the CCR2 ligand with the highest affinity for the receptor) together with the inhibitor (at 5 nM) actually lowered ChAT activity further (Figure 12B). Despite its presence in the poly(I:C)-treated fetal brains, MCP-1 is unlikely to be responsible for the observed increase in the number of cholinergic neurons. Moreover, these data suggest a complex interaction between the CCR2 receptor and its various ligands, which will be discussed further below.

4.3.3 Inhibition of CCR5

Inhibiting CCR5, a receptor for MIP-1β, MIP-1α and RANTES, with increasing doses of the pharmacological inhibitor D-Ala-Ser-Thr-Thr-Thr-Asn-Tyr-Thr-NH_2 (DAPTA) produced a consistent and statistically significant decrease in ChAT activity at 20 µM when compared to that of microglial CM (Figure 13A). This suggests that one or more of these chemokines might be active factors in the CM. Because MIP-1β was significantly increased in the poly(I:C)-treated microglial fractions in the Luminex® assay (Table 5A), and because, unlike other chemokines, CCR5 is its sole receptor, we focused on this molecule. However, MIP-1β at 200 ng/ml could not reverse the DAPTA-induced decline in ChAT activity (Figure 13B).

DAPTA-treated cultures not only had decreased amounts of ChAT activity, but a CellTiter96® AQ_{ueous} One Solution assay that measures total cell number confirmed that DAPTA-treated cultures had fewer live cells than those treated with microglial CM alone. MIP-1β even at 1 µg/ml was unable to reverse the loss of cells (Figure 13C).

The smaller number of cells could have been due to the inhibition of proliferation and/or survival. To determine whether DAPTA inhibited proliferation, BrdU was added to BF cultures at the time of plating. After 24 hrs in culture BrdU was incorporated into all cultures. However, there was no significant difference in BrdU incorporation between untreated controls, DAPTA-treated and MIP-1β-treated cells (Figure 13D).

To test whether DAPTA affected survival, a Live/Dead® assay was performed. In this assay calcein AM and ethidium homodimer-1 (EthD-1) are added to cells. When non-fluorescent calcein AM enters living cells it is enzymatically converted to a fluorescent green. EthD-1 is excluded by intact cell membranes but enters dead ones and upon binding to nucleic acids fluoresces red. Live cells (green) and dead cells (red) are then counted using fluorescence microscopy (see *Materials and Methods*). Data show that the addition of DAPTA results in fewer live cells in a dose-dependent manner (Figure 14A), suggesting an effect on survival.

The fact that MIP-1β did not overcome the DAPTA-induced decline in ChAT activity or in the CellTiter96® AQ$_{\text{ueous}}$ One Solution survival assay suggests that another CCR5 ligand (RANTES or MIP-1α) may have been responsible. We conservatively conclude, however, that a CCR5 ligand in the microglial CM may play a role in BF precursor and/or cholinergic cell survival.

Conclusions for Specific Aim 3:

In BF cultures:

- CCR2 inhibition exerts a biphasic effect on ChAT activity

- MCP-1, a CCR2 antagonist, lowers ChAT activity beyond that seen with CCR2 inhibition
- CCR5 inhibition lowers ChAT activity, primarily through an effect on cell survival

Specific Aim 4. *To determine a possible role for IL-6 in mediating changes in cholinergic differentiation.*

4.4.1 IL-6 in microglial conditioned medium plays a role in cholinergic cell survival

IL-6 has been shown by several studies to be an important player during brain development. Importantly for autism studies, IL-6 may mediate alterations in specific behaviors that result from maternal immune activation with poly(I:C) (Smith et al., 2007). In these studies administration of IL-6 to pregnant dams mimics the effects of poly(I:C) and administration of an antibody to IL-6 neutralizes them (Parker-Athill and Tan, 2010; Smith et al., 2007). Because of these studies, we focused some attention on IL-6 as a possible mediator of the observed effects on cholinergic expression in the basal forebrain.

IL-6 is a major constituent of the conditioned medium (CM) that we have used to treat embryonic basal forebrains. IL-6 concentrations assayed by ELISA in microglial CM revealed high concentrations of the cytokine (2l.8 ± 2.9 ng/ml, n=10). Moreover, the addition of neutralizing antibodies to IL-6 together with CM decreased ChAT activity in a dose-dependent manner (Figure 15A). A control rabbit IgG had no such inhibiting effect, suggesting that the decline was due specifically to the neutralization of IL-6.

Two commercial assays -- Live/Dead® assays (Invitrogen Life Technologies) and CellTiter96® AQ$_{ueous}$ One Solution assays (Promega) -- were used to determine the effect of the neutralizing antibody on cell survival. Results from both assays show fewer viable cells after 48 hours in culture with IL-6 antibody added to CM. (Figure 15B and C). A control rat IgG had no effect. Adding exogenous recombinant rat IL-6 (20 ng/ml) along with the antibody to IL-6 did not reverse the loss of cell viability (Figure 15C), nor did the addition of IL-6 to cultures in N2 alone result in an increase in the number of viable cells (Figure 15D). These data suggest that IL-6 may be necessary but not sufficient for basal forebrain cell survival.

4.4.2 Cytokine and chemokine elevations seen in WT fetal microglia are absent in IL-6 knockouts

To determine whether IL-6 plays a role in altering cholinergic expression in vivo, we used transgenic IL-6 knockout mice. In these mice the IL-6 gene is interrupted so that they do not produce message or protein for IL-6. To determine whether the absence of IL-6 affects the fetal brain cytokine/chemokine environment, we analyzed CD11b$^+$ and CD11b$^-$ fractions from E16.5 embryonic brains of both wild type and IL-6 knockout mice using LUMINEX® assays (performed by Robert Donnelly, UMDNJ).

Cytokine and chemokine production was first evaluated in enriched CD11b$^+$ fractions from saline-treated dams. When CD11b$^+$ samples from WT embryos are compared directly to IL-6 KOs, there are no detectable significant differences (Table 5A, Column 3; Supplementary Tables 7A and 7B). However, consideration of the poly(I:C)-treated samples reveals a major change. In the WT animals in the CD11b$^+$ fraction, poly(I:C) treatment elevates IL-1α, IL-4, IL-9, GM-CSF, M-CSF, Eotaxin (CCL11), MIP-1β (CCL4), LIX (CXCL5) and RANTES (CCL5) (see above and Table 5A Column 1). However, in the KO animals, these statistically significant increases do not occur (Table 5A, Column 2). Instead levels of IL-10 decrease. These data suggest a possible role for IL-6 in regulating microglial output of cytokines and chemokines, both in normal development as well as in response to inflammation. For complete IL-6 knockout data, see Supplementary Tables 5A and 5B.

While the increase between the saline-treated and the poly(I:C)-treated animals is eliminated in the KOs, there is only one cytokine that differs significantly between the poly(I:C)-treated WT and the poly(I:C)-treated KO *in the CD11b$^+$ fraction*, IL-15. Therefore, the microglial output (CD11b$^+$ fractions) from the WT and the KO appear to be quite similar (Table 5A, Column 4; Supplementary Tables 9A and 9B).

4.4.3 The absence of IL-6 promotes a pro-inflammatory fetal brain environment

CD11b$^-$ fractions behave differently. Comparisons between the saline-treated WT and the poly(I:C) WT CD11b$^-$ fractions (Table 5B, Column 1) show that IL-10 and MCP-1 levels decline following poly(I:C) treatment. In the saline-treated KO vs. the poly(I:C)-treated KO, only MIP-2 levels decline with poly(I:C) (Table 5B, Column 2; Supplementary Tables 6A and 6B). Comparisons between WT poly(I:C)-treated and KO poly(I:C)-treated animals reveal no significant differences (Table 5B, Column 4; Supplementary Tables 10A and 10B). Major differences, however, are detected when saline-treated WTs are compared with saline-treated KOs (Table 5B, Column 3; Supplementary Tables 8A and 8B). IFNγ, IL-9, IL-10, IL12p70, IL-13, MCP-1, MIP-1α, MIG and RANTES are all significantly elevated in the KOs. Thus, data from the CD11b$^-$ fractions indicate an altered fetal brain environment at E16.5 that is not associated with maternal poly(I:C) injection, but due to the absence of IL-6. It appears, therefore, that the absence of IL-6 alters the fetal brain environment towards a more inflammatory phenotype. This is somewhat counterintuitive, but may point to a role for IL-6 in maintaining immunological homeostasis. Because the brain environment is already inflamed, a maternal poly(I:C) injection may not be as effective in elevating levels further. This is consistent with the data of Lasala et al. who have suggested that a pre-existing inflammatory environment may suppress a subsequent response to inflammation (Lasala and Zhou, 2007).

4.4.4 The increase in ChAT activity in vivo following poly(I:C) treatment is eliminated in the absence of IL-6

Having found that the absence of IL-6 tends to create a more inflamed fetal brain environment, we sought to determine whether the absence of IL-6 would affect the poly(I:C)-induced increase in ChAT activity in the fetal BF in vivo. BFs were dissected from E16.5 and E18.5 embryos and P1 pups of WT and IL-6 KO females injected with poly(I:C) or saline. Protein extracted from these samples was analyzed using a ChAT assay in which the synthesis of ^{14}C-acetylcholine is measured (see *Materials and Methods*). Unlike the WT (see above, Figure 1), there was no significant difference in ChAT activity between saline-treated and poly(I:C)-treated KOs (CPM/µg protein for IL-6 KO control at E16.5: 130.56 ± 12.17, E18.5: 134.25 ± 22.59, P1: 246.64 ± 36;37; CPM/µg protein for IL-6 KO poly(I:C) at E16.5: 133.20 ± 7.65, E18.5: 140.17 ± 17.82, P1: 232.14 ± 21.02, Figure 16A). An ANCOVA reveals that the data points from both groups can be represented by a single line where counts per minute (CPM) per µg protein is expressed as a function of time. There is no significant difference due to the treatment groups (Figure 16B). This is unlike WT where the data are best represented as two separate linear relationships both dependent on time, but with the poly(I:C) group producing more ^{14}C-acetylcholine (CPM/µg protein) at every point along the time interval (Figure 16C). Note that the variation in the range of values for both saline-treated and poly(I:C)-treated KO samples is much greater at each time point than for WT (Figure 16B and C).

Although there is no difference between the saline-treated and poly(I:C)-treated KOs, there is a difference between the levels of ChAT in the saline-treated KOs when compared to the saline-treated WT animals at E16.5 (Figure 17A). The increase in ChAT is accompanied by a decrease in GAD65 mRNA (Figure 17B). This is consistent with our previous data showing that at E16.5 when ChAT levels increase, GAD65 levels decline (see above, Figure 4). There was no significant difference in GAD65 levels between IL-6 KO controls and IL-6 KO poly(I:C) groups, and both groups were similar to WT poly(I:C) samples (Figure 17B).

These data are consistent with findings from the Luminex® assay that suggest that the absence of IL-6 results in an inflammatory fetal brain environment.

Conclusions for Specific Aim 4.

- IL-6 may be a survival factor for cholinergic neurons differentiating in culture.
- The absence of IL-6 in vivo results in an inflammatory fetal brain environment.
- IL-6 may be required to maintain proper cytokine/chemokine balance during brain development.

V. Discussion

5.1 Increased cholinergic expression following maternal immune activation

Original studies from the Jonakait lab indicated that activated microglia produce a factor or a cocktail of factors that promotes cholinergic differentiation of undifferentiated precursors in the cultured embryonic rat basal forebrain (Jonakait et al., 1994; Jonakait et al., 1996; Ni et al., 2007). Our findings now show an increase in both the number of cholinergic neurons and ChAT activity in the fetal/perinatal basal forebrain in vivo following MIA. Similar to findings in culture, GAD65 levels in the BF declined as ChAT levels increased. The transient decrease in GAD65 expression could reflect a delay or a skewing in the differentiation of GABAergic interneurons. Because of the variety of GABAergic interneurons that are derived from temporally separated progenitor pools, the normal differentiation and/or distribution of these pools may be affected. In the cortex, this has important ramifications since GABAergic interneurons regulate development at the level of proliferation, migration and differentiation, as well as in refining local circuits and in generating synchrony in networks of glutamatergic neurons (see review by Di Cristo, 2007).

While the effect on both cholinergic cell number and GAD expression is transient, dysregulation of cholinergic development in this brain region could have permanent cognitive and behavioral alterations in the adult (Berger-Sweeney, 1998; Berger-Sweeney, 2003). The consequences of increased cholinergic activity in the BF will warrant future studies. So, e.g., BF afferents are widely distributed throughout the cortex. In particular, pyramidal neurons in layer

VI in the early postnatal prefrontal cortex express several different nicotinic ACh receptor forms (Bruel-Jungerman et al., 2011; Kassam et al., 2008), and are, as a result, excited by nicotine. Because corticothalamic neurons from this layer play a critical role in attention, perinatal exposure to nicotine impairs cognitive function in adults (Hohmann and Berger-Sweeney, 1998a; Bruel-Jungerman et al., 2011). Thus, excessive cholinergic signaling from the BF during this perinatal time window could have a lasting effect on these and similar areas of the brain that deal with attention, learning and memory.

5.2 Potential changes in the hippocampus

We investigated several specific changes in the hippocampus that were likely to result from increased cholinergic activity in the BF. One of them was the transition of chloride transporters in the hippocampus from an embryonic form (NKCC1) to a mature (KCC2) form. Levels of these transporters are reportedly controlled by endogenous acetylcholine (ACh) signaling through α7nAChRs (Liu et al., 2006). Although we observed the same transition from NKCC1 to KCC2 observed by others, the timing of that switch was not affected by the increase in BF ChAT activity. We also investigated hippocampal levels of neuregulin 1 (NRG1) which regulates the localization of a7nAChRs (Liu et al., 2001), and NMDA receptors, which are affected by both cholinergic input and NRG1 activity (Wang et al., 2011; Zhong et al., 2008). However, expression of these did not change either. Even though there is an increase in cholinergic cell number in the BF, ChAT levels in the hippocampus did not change significantly. It is perhaps the case that even in light of increased cholinergic cell number in the BF, this did not translate into increased axonal outgrowth into the hippocampus. The extent of axonal outgrowth is worth future study.

The increased expression of Shank3 in the hippocampus following MIA is intriguing. Shank3 haploinsufficiency mice are used to model some of the symptoms of autism as a loss of function of this gene results in some autistic-like symptoms (Bozdagi et al., 2010). If MIA indeed leads to autistic-like symptoms, we would expect levels of this molecule to decline following MIA. However, here we see levels increase. Our results are in agreement with others who have measured Shank3 levels following maternal infection. In these studies fetal brains from embryos of pregnant rats injected at E14 with *Mycoplasma pulmonis* had increased Shank3 mRNA at E21 (Burton et al., 2012). Shank 3, a scaffolding protein known for its function in recruiting several receptors to the post synaptic density (Bozdagi et al., 2010), was recently found to be up-regulated following cerebral ischemia. It was considered to be part of a feedback mechanism designed to stimulate the innate immune response in order to activate nerve regeneration (Datta et al., 2011). Thus, one might speculate that Shank3, induced following an immune challenge, is upregulated as part of a protective mechanism to counteract inflammatory damage. It has been suggested that overexpression of Shank3 may also result in symptoms of ASD as Asperger syndrome has been reported in an individual with 3 copies of this gene (Bozdagi et al., 2010). Also, addition of Shank3 to aspiny cerebellar neurons in culture results in spine development and synapses with functional glutamate receptors (Bozdagi et al., 2010). Further investigation is necessary to clarify its role.

5.3 Microglial response to MIA

Results from our studies provide insight as to how the maternal immune response can affect the fetal brain. Several clear patterns emerge from the LUMINEX® assays. While the results from the three assays were somewhat variable, certain findings are, nevertheless, reproducible. Consistent elevations are seen in specific cytokines and chemokines when the $CD11b^+$ (i.e., migroglial) fractions from the poly(I:C)-treated group are compared with those from the saline-treated (control) group. These results show that the profile of cytokines and chemokines in microglia, the primary immune responders of the brain, is altered following MIA. The cytokines IL-1α, IL-4, IL-9, chemokines MIP-1β, RANTES, Eotaxin, and LIX along with GM-CSFand M-CSF, are all expressed at higher levels in the poly(I:C)-treated $CD11b^+$ fractions than in controls. This points to a role for microglia in mediating the effects of MIA in the fetal brain. Other researchers have also found evidence for the involvement of fetal microglia in mediating the effects of prenatal infection (Roumier et al., 2008; Kannan et al., 2007).

Certain limitations are inherent in the LUMINEX® assay. In order to obtain sufficient numbers of cells for the assay, enriched microglial samples were extracted from the whole fetal brain. Therefore, our results are a picture of the fetal brain as a whole and do not reflect regional differences that may occur. Indeed, Garay et al. have provided evidence for differences in cytokine/chemokine expression by region in *postnatal* brain tissue analysis following MIA (Garay et al., 2012). These postnatal differences may be indicative of prenatal variation by region as well. Microglia in these different areas of the brain are likely to respond to their particular microenvironment, secreting what is appropriate in their area. Note also that our results are taken from lysates of microglia and are not a measurement of the secreted cytokines. Also, since the assay was performed at E16.5, four days after maternal injection, they may not reflect acute inflammatory cytokine levels.

Nevertheless, changes were detected, and these may affect brain development. These cytokine effects have been studied primarily in cultured cells where products of microglial activation have been shown to affect cholinergic differentiation (Jonakait et al., 1996; Jonakait et al., 2000; Ni et al., 2007), as well as survival of immature mesencephalic neurons (Nagata et al., 1993). Some inflammatory cytokines, however, will inhibit survival of fully differentiated dopaminergic and serotonergic neurons (Jarskog et al., 1997). IL-1β, TNFα and IL-6 have all been shown to affect the survival and/or differentiation of neuronal precursor cells in culture (Jarskog et al., 1997; Ben Hur et al., 2003; Islam et al., 2009; Cacci et al., 2008; Li et al., 2007b; Ajmone-Cat et al., 2010). Recent studies have found chemokines to be involved in the survival (Locatelli et al., 2012), differentiation (Edman et al., 2008a), proliferation (Edman et al., 2008b) and migration (Bagri et al., 2002; Belmadani et al., 2005; Klein et al., 2001) of neurons in the developing brain as well as in axon growth and the maturation of neurites (Locatelli et al., 2012), synapse formation (Cowell and Silverstein, 2003) and in myelination (Jakovcevski et al., 2009; Kury et al., 2002). Chemokines will be discussed in more detail below.

While elevations of specific cytokines and chemokines in the microglial profile are apparent following MIA, other canonical indications of microglial activation do not occur. Microglia often proliferate when activated (Gehrmann et al., 1995), yet we detected no increase in the number of fetal microglia following MIA. After trauma or brain lesion, adult microglia respond by retracting their processes which then appear “stubby” or short and microglia migrate to the source of injury (Gehrmann et al., 1995). Thus, most studies use immunohistochemistry to distinguish “activated” microglia from “resting” ones by their morphology. That is, an assessment of morphology is taken as an indicator of their activation status. A seminal study in the autism literature has suggested that post-mortem brains from both children and adult autistic patients contain activated microglia, and have based their findings heavily on morphological characterization (Vargas et al., 2005). By contrast, our examination of the fetal microglia in mouse brain tissue from the offspring of poly(I:C)- and saline-treated mice does not reveal any obvious morphological distinction between the two groups. Both contain highly ramified microglia, microglia with short, stubby processes as well as amoeboid microglia. When tissues were stained with an antibody to IL-6 (a cytokine expressed by activated microglia) or an antibody to phosphorylated p38 (a transcription factor phosphorylated during the microglial production of cytokines), we detected positive expression in neither control nor poly(I:C)-treated samples (data not shown). While a few isolated microglia appeared to be positive, it was not clear whether the microglial cell expressed the antigen or whether the microglia was phagocytosing another cell expressing the antigen.

While we did not detect morphological changes in microglia, the Luminex$^{®}$ data confirm that they responded to MIA. Consequently, a better way to view microglia, even fetal microglia, is to see them as continually sampling and reacting to their immediate environment instead of being in one of two states, either “activated” or “resting.” Images of adult microglia in vivo show that these “resting” microglia are highly active, constantly surveying their area and sampling the environment. They are poised to react when something is out of balance in that specific area (Nimmerjahn et al., 2005). The role of microglia both in the adult and in the fetal brain, therefore, may be primarily one of maintaining homeostasis. When something is out of order they can respond specifically, directly and quickly to that specific event in that one particular space.

5.4 Non-microglial cells respond to MIA

Microglia are not the only cells in the fetal brain that produce cytokines and chemokines. Data from the $CD11b^{-}$ fraction of the LUMINEX$^{®}$ assay show that cells other than microglia in the fetal brain produce large quantities of these molecules including IL-1β, IL-9, IL-13 and the anti-inflammatory cytokine IL-10 (See Supplementary Table 4A). Note that adult astrocytes and neurons also produce these molecules and respond to them as well (Garay and McAllister, 2010). While astrocytes are not present in the rodent brain until the perinatal period, they are present earlier (15 weeks) in human brain development (Roessmann and Gambetti, 1986). The fact that these molecules are found in the saline-treated fetal brains points to a role for cytokines in normal brain development. Higher levels of IL-10 in the non-microglial fraction could play a protective role in the developing brain and serve to inhibit over-production of inflammatory cytokines (Meyer et al., 2008b; Sredni-Kenigsbuch, 2002). Meyer et al. hypothesize that during prenatal life, proper brain and behavioral development require an appropriate cytokine balance. A shift in either direction towards excess pro-inflammatory molecules or towards excess anti-inflammatory ones results in adult brain and behavior abnormalities (Meyer et al., 2008b; Meyer et al., 2009).

5.5 Chemokines in brain development

The substantial quantities of chemokines found in both the positive and negative fractions in the LUMINEX® assay indicate an under-reported role for chemokines in the developing brain. It is now becoming evident that these molecules have a distinct role in the developing brain apart from their canonical role as chemoattractants for hematopoietic cells to sites of injury (Tran and Miller, 2003b; Tran and Miller, 2003a; Tran et al., 2004; Tran et al., 2007; Turbic et al., 2011). Alterations in the levels of these chemokines following MIA are observed in the LUMINEX® assay and point to possible alterations in brain development. While RANTES, MIP-1α and MCP-1 are spatially and temporally expressed in the normal developing brain (Geppert, 2003), MIA resulted in significant microglial elevations in MIP-1β, RANTES, Eotaxin and LIX.

The elevations of chemokines in the microglial fraction as well as data indicating a broader role for chemokines led us to examine the possibility that chemokines were active constituents in the microglial CM that promoted cholinergic differentiation. Our studies in BF cultures with CM show that inhibition of CCR2 has a biphasic effect on ChAT activity, lowering activity, but only at one concentration, 5 nM. Addition of the ligand MCP-1 together with the inhibitor lowered ChAT activity even further. CCR2 is coupled to a G-protein of the $G\alpha_i$ class. Thus the primary signal transduction pathway of CCR2 is the inhibition of adenylate cyclase and a resultant decrease in intracellular cAMP (Old and Malcangio, 2012). Moreover, because ChAT is regulated in part by cAMP (Blusztajn et al., 1992), we would expect activation of CCR2 to lower ChAT and that blockade of the receptor in the presence of other cAMP-generating ligands would allow ChAT activity to remain intact. This is largely what we saw. It is not clear, therefore, why one single concentration of the inhibitor resulted in lower activity. It may reflect a complicated interaction among the multiple CCR2 agonists and/or other cAMP-inducing molecules in the CM that would require additional study.

Inhibition of CCR5 in BF cultures also resulted in lower ChAT activity primarily due to its effect on cell survival. We conclude that of the CCR5 ligands, RANTES and/or MIP-1α may play a role in BF precursor and/or cholinergic cell survival in culture. A similar role for these chemokines in vivo is yet to be investigated.

Clearly the effect of chemokines on brain development is complicated. Further study is needed to determine the role of particular chemokines in specific brain regions. Looking at chemokines in a region-specific manner could elucidate the part chemokines play in both normal and aberrant brain development.

Investigating these roles could also lead to an understanding of some mechanisms that could mediate MIA to abnormalities in the fetal brain.

5.6 The role of IL-6

IL-6 has assumed particular significance in the autism literature as a mediator of MIA. This is due to recent reports that IL-6 mediates the process by which deficits in cognition and behavior are produced in the adult offspring of poly(I:C)-injected pregnant mice (Parker-Athill and Tan, 2010; Smith et al., 2007). In these studies direct maternal injection of IL-6 mimics the pre-pulse inhibition (PPI) and latent inhibition (LI) deficits in the adult offspring seen with poly(I:C) injection. Administration of anti-IL-6 antibody at the same time as poly(I:C) injection prevents these deficits and neutralizes the MIA-induced deficits in open-field exploration and social interaction as well. Poly(I:C) injection in IL-6 KO mice does not result in some of the behavioral changes seen in wild-type mice (Smith et al., 2007). These data are in agreement with other studies showing behavioral and cognitive abnormalities in adult mice following perinatal injection of hyper-IL-6, a fusion protein made up of IL-6 and the soluble IL-6 receptor (Jones et al., 2001; Spooren et al., 2011). The site of IL-6 production has not been clarified. A maternal immune response would include the production of IL-6, and its possible crossing of the placenta into the fetus. IL-6 is also produced in the fetal side of the placenta (Mandal et al., 2010; Mandal et al., 2011) and production in the placenta is greatly increased following MIA (Ashdown et al., 2006; Pessah et al., 2008; Smith et al., 2007; Urakubo et al., 2001). Though our findings of increased mRNA production in the fetal brain are in agreement with those that have been reported by others (Liverman et al., 2006), we were somewhat surprised that the LUMINEX® assay did not reveal significant fetal brain elevations in IL-6 protein following poly(I:C) injections. However, this measurement represents a snapshot of IL-6 intracellular protein concentration at just one time point. Because the assay was performed 4 days after poly(I:C) injection, an acute response including peak IL-6 production may have been missed.

Nevertheless, our findings shed light on additional aspects of IL-6 function in the developing brain. In our experiments offspring of saline-injected IL-6 KO mice have increased amounts of inflammatory cytokines and chemokines in the CD11b$^-$ fractions when compared to offspring of wild-type, saline-injected mice. This suggests that the “control” embryonic brain environment in the KOs is inflamed without ever being exposed to a maternal immune challenge. However, we cannot rule out the possibility that IL-6KO mice are hyper-reactive to the injection itself. Such a maternal reaction might possibly result in an alteration of baseline cytokines and chemokines in the fetal brains. We did not measure cytokine levels in the fetal brains of offspring of uninjected IL-6KO females.

In the wild-type fetal brain, CD11b$^+$ (microglial) cells produce a robust reaction to the poly(I:C) immune challenge. However, no such change is apparent in the IL-6 KO mice. In the KOs no significant difference in cytokine/chemokine production is found between the saline and poly(I:C) treatment groups in either the CD11b$^+$ or the CD11b$^-$ fractions suggesting that the already-inflamed state of the brain is not inflamed further as a result of MIA. This indicates an impaired immune response.

In addition, ChAT activity was measured at E16.5 in the BFs of the IL-6 KO embryos and compared to levels in the wild-type animals. More ChAT activity was measured in the BFs of both control and poly(I:C) groups in the KOs than either the control or poly(I:C) groups in wild-type mice. Furthermore, at this age lower levels of GAD65 mRNA were detected in both control and poly(I:C) IL-6 KOs. Levels were similar to that of the poly(I:C)-treated wild-types and were significantly less than wild-type controls. These data are consistent with the idea that there is a heightened inflammatory state in the IL-6 KO embryonic brains that is accompanied by higher ChAT activity and lower GAD65 expression.

Taken together, these observations suggest a role for IL-6 in the orchestration of cytokine and chemokine expression in the brain. They point to a role for IL-6 in the activation of microglia, specifically in the regulation of their output of cytokines and chemokines in response to inflammation. Also, in the absence of IL-6 an appropriate response to inflammation is impaired. These data imply a normal role for IL-6 as a “shut-off” switch -- a way to turn off excessive pro-inflammatory signaling and regulate the inflammatory environment. This regulation is missing in the IL-6 KO mice.

It is worth noting that in the Smith et al. study, mice treated with an IL-6 antibody or IL-6 KO mice over-reacted to a viral insult. Unlike wild-type mice, these either died or miscarried. This observation correlates with our own insofar as we see both a hyper-inflamed brain environment as well as an impaired response to subsequent immune challenge. These data may show that IL-6 restrains excessive immune responses.

5.7 How are immune disorders and brain disorders linked?

We and others have shown that MIA results in alterations in fetal brain development that are due to an altered immune environment. Similarly, others have shown that MIA affects peripheral immune responses in offspring. It is notable in this regard that SZ and ASD patients have a higher incidence of auto-immune disorders (particularly gastrointestinal problems) than do people in the general population (Brown and Mehl-Madrona, 2011; Steyaert and De la, 2008). Moreover, affected children have higher pro-inflammatory cytokine levels in their serum (Ashwood et al., 2011a), and cerebral spinal fluid (CSF) (Vargas et al., 2005). Animal studies show that MIA results in a greater number of Th17 (pro-autoimmune) cells in spleens of offspring when presented with an immune challenge later in life (Mandal et al., 2010; Mandal et al., 2011).

There is an intimate relationship between the immune and nervous systems. Activity outside the brain affects the activity of neurons within the brain and vice versa. So, e.g., peripheral infections lead to changes in synaptic connections in the brain that last for weeks (Patterson, 2011a), and chronic stress suppresses the immune system increasing susceptibility to disease (Patterson, 2011a). Curiously, autistic children with a fever show improvements in behavioral symptoms (Curran et al., 2007). Several unsatisfactory explanations have been suggested for these results, but the fact remains that the two systems are continually interacting.

This raises the possibility that a single stimulus affects both systems. Some molecules are common to both brain and immune systems. MHC class I, e.g., is known for its function in the adaptive immune response where it presents processed viral peptides on the surface of antigen-presenting cells. MHC class I molecules are also constituents of the developing nervous system where they are displayed on the surface of neurons and are involved in pruning and refining synaptic connections during embryonic development (Huh et al., 2000). Their role continues into adulthood where they facilitate activity-dependent long term depression in the hippocampus (Huh et al., 2000; Boulanger et al., 2001; Boulanger and Shatz, 2004). Thus, one could hypothesize that a mutation in one of the MHC class I genes or an epigenetic change in their expression could have consequences that are manifested in both immune system and brain. Interestingly, some MHC class I genes are located in a region on chromosome 6 that has been associated with an increased risk for SZ and bipolar disorder (Lee et al., 2012; Shirts et al., 2007).

Complement proteins are other immune system-related molecules that function in the CNS. In the immune system they help to destroy invading pathogens, whereas in the developing brain they function in the elimination of synapses.(Boulanger and Shatz, 2004) Some studies have associated a null allele for complement factor C4B with an increased risk for autism (Odell et al., 2005), and decreased C4B protein concentrations have been reported in autistic patients (Warren et al., 1994). Because these proteins function in both the immune system and in the brain, a mutation or alteration in their expression could result in disorders in both.

5.8 How does MIA get translated into developmental brain disorders?

We and others have shown that MIA leads to changes in cytokine/chemokine regulation in the developing brain and results in substantive – if transient – changes there. It remains unclear, however, how it is that MIA produces these changes. Animal models have demonstrated that these are due to the maternal inflammatory response, not the actual virus itself (Shi et al., 2005). Between the initial insult to the mother and the results in the fetal brain lie the maternal circulatory system and the placenta

The placenta is the maternal/fetal interface. It serves to protect the fetus, to transfer nutrients to and wastes away from the fetus, and it provides a favorable growth environment for the developing fetus (Jonakait, 2007). Cytokines and growth factors are produced in the normal placenta, and the levels of several -- including IL-1β, TNFα and IL-6 -- are increased following maternal infection or poly (I:C) injection (Ashdown et al., 2006; Parker-Athill and Tan, 2010; Sato et al., 2001; Smith et al., 2007; Urakubo et al., 2001). Inflammatory cytokines such as these may cross the placental barrier, enter the fetal system and affect the fetal brain directly. However, of these three molecules, only IL-6 has clearly been demonstrated to cross the placenta (Dahlgren et al., 2006; Zaretsky et al., 2004). Studies differ as to which inflammatory cytokines may become elevated in the fetal brain following MIA and whether or not they are derived from the placenta (Meyer et al., 2006b; Meyer et al., 2008b; Urakubo et al., 2001; Bilbo and Schwarz, 2009; Smith et al., 2007).

Hsiao and Patterson suggest an additional mechanism whereby IL-6 acting in the placenta could affect fetal development (Hsiao and Patterson, 2011). They show that IL-6 produced in the maternal compartment of the placenta acts on cells in the spongiotrophoblast layer on fetal side through the JAK-STAT3 pathway to produce changes in the expression of hormones and growth factors. While offering this indirect mechanism of influencing fetal brain development, Hsiao and Patterson did not rule out the direct action of IL-6 on the fetal brain either by crossing the placental barrier or by its production in the fetal brain itself (Hsiao and Patterson, 2011).

We also suggest an alternative speculation. The differentiation of hematopoietic stem cells (HSCs) generated in the vasculature of the placenta in the E12 to E14 mouse (Gekas et al., 2005) may be altered due to inflammatory cytokine signaling or the reduction in placental growth factors. Notably the IL-6 family of cytokines can regulate HSC differentiation and proliferation (Seita et al., 2008). This could have consequences for the developing myeloid cells, precursors to the microglia which populate the fetal brain and produce cytokines and chemokines there.

We and others have shown direct effects of cytokines on brain development. However, not every baby born to a woman that has influenza while she is pregnant goes on to develop ASD or SZ or other neurodevelopmental disorder. This is most likely because these disorders result from an interaction of genetic susceptibility with the prenatal immune challenge during a vulnerable time period. Both are needed. A maternal prenatal insult may not result in the development of the disorder by itself. Likewise, the presence of a particular susceptibility gene will not in itself result in a neurodevelopmental disorder. An example of this is seen in tuberous sclerosis (TSC), a rare genetic disorder. Mutations in the TSC gene cause benign tumors to grow, and approximately 40-50% of individuals with this disorder are also affected with ASD (Ehninger et al., 2012). Mice that are heterozygous for the TSC mutation display a lack of normal social approach behavior (autistic-like behavior) as adults *but only* if they were the offspring of poly(I:C) injected females (Ehninger et al., 2012). In this study neither the poly(I:C) injection nor the mutation alone resulted in a behavioral deficit. An interaction between them was necessary. Findings from an analysis of birthdate information of individuals with ASD and individuals with both ASD and TSC suggested an association between third trimester of gestation and peak flu season only for individuals with both ASD and TSC (Ehninger et al., 2012).

Cytokine/chemokine dysregulation could also effect epigenetic modifications. The principle of early life epigenetic modification or programming by interaction with environmental factors has been demonstrated. E.g., in rats, the handling of neonates (to mimic increased maternal attention and care) up-regulates the expression of IL-10 early in development within the nucleus accumbens. This increased expression of IL-10 occurs by decreased methylation of the IL-10 gene in microglia specifically. The upregulation is maintained as adults (Schwarz et al., 2011).

VI. Conclusions

These results reveal changes in the fetal brain following MIA that could affect neural development. ChAT activity and cholinergic cell number increase in the perinatal BF and there is a transient decrease in the amount of GAD65 mRNA produced. Though transient, these changes may have long-lasting consequences affecting adult cognition and behavior. Following maternal poly(I:C) injection, the fetal microglial cytokine/chemokine profile is altered; they increase production of several of these molecules. This suggests that microglia may participate in mediating the effects of MIA in the fetal brain. Large amounts of chemokines were present in the lysates of both microglial and non-microglial fractions of the LUMINEX® assay implying functions for them in normal brain development. In the absence of IL-6, ChAT activity in the fetal BF increases, message for GAD65 decreases and the fetal brain cytokine/chemokine environment is altered. It does not change further following MIA. These findings suggest a role for IL-6 in maintaining proper cytokine and chemokine balance during normal brain development.

VII. References

(2010). Progress toward control of rubella and prevention of congenital rubella syndrome --- worldwide, 2009. MMWR Morb. Mortal. Wkly. Rep. *59*, 1307-1310.

(2012). Prevalence of autism spectrum disorders--Autism and Developmental Disabilities Monitoring Network, 14 sites, United States, 2008. MMWR Surveill Summ. *61*, 1-19.

Abdallah,M.W., Larsen,N., Grove,J., Norgaard-Pedersen,B., Thorsen,P., Mortensen,E.L., and Hougaard,D.M. (2012). Amniotic fluid chemokines and autism spectrum disorders: an exploratory study utilizing a Danish Historic Birth Cohort. Brain Behav. Immun. *26*, 170-176.

Abreu-Villaca,Y., Filgueiras,C.C., and Manhaes,A.C. (2011). Developmental aspects of the cholinergic system. Behav. Brain Res. *221*, 367-378.

Ajmone-Cat,M.A., Cacci,E., Ragazzoni,Y., Minghetti,L., and Biagioni,S. (2010). Pro-gliogenic effect of IL-1alpha in the differentiation of embryonic neural precursor cells in vitro. J. Neurochem. *113*, 1060-1072.

American Psychiatric Association (2001). Diagnostic and Statistical Manual of Mental Disorders, Fourth Edition. (Washington, DC: American Psychiatric Publishing, Inc).

Aramakis,V.B., Hsieh,C.Y., Leslie,F.M., and Metherate,R. (2000). A critical period for nicotine-induced disruption of synaptic development in rat auditory cortex. J. Neurosci. *20*, 6106-6116.

Arrode-Bruses,G. and Bruses,J.L. (2012). Maternal immune activation by poly(I:C) induces expression of cytokines IL-1beta and IL-13, chemokine MCP-1 and colony stimulating factor VEGF in fetal mouse brain. J. Neuroinflammation. *9*, 83.

Arters,J., Hohmann,C.F., Mills,J., Olaghere,O., and Berger-Sweeney,J. (1998). Sexually dimorphic responses to neonatal basal forebrain lesions in mice: I. Behavior and neurochemistry. J. Neurobiol. *37*, 582-594.

Ashdown,H., Dumont,Y., Ng,M., Poole,S., Boksa,P., and Luheshi,G.N. (2006). The role of cytokines in mediating effects of prenatal infection on the fetus: implications for schizophrenia. Mol. Psychiatry *11*, 47-55.

Ashwood,P., Krakowiak,P., Hertz-Picciotto,I., Hansen,R., Pessah,I., and Van De,W.J. (2011a). Elevated plasma cytokines in autism spectrum disorders provide evidence of immune dysfunction and are associated with impaired behavioral outcome. Brain Behav. Immun. *25*, 40-45.

Ashwood,P., Krakowiak,P., Hertz-Picciotto,I., Hansen,R., Pessah,I.N., and Van De,W.J. (2011b). Associations of impaired behaviors with elevated plasma chemokines in autism spectrum disorders. J. Neuroimmunol. *232*, 196-199.

Bachman,E.S., Berger-Sweeney,J., Coyle,J.T., and Hohmann,C.F. (1994). Developmental regulation of adult cortical morphology and behavior: an animal model for mental retardation. Int. J. Dev. Neurosci. *12*, 239-253.

Bagri,A., Gurney,T., He,X., Zou,Y.R., Littman,D.R., Tessier-Lavigne,M., and Pleasure,S.J. (2002). The chemokine SDF1 regulates migration of dentate granule cells. Development *129*, 4249-4260.

Banati,R.B., Gehrmann,J., Schubert,P., and Kreutzberg,G.W. (1993). Cytotoxicity of microglia. Glia *7*, 111-118.

Bauman,M.L..and Kemper,T.L., ed., (2005). The Neurobiology of Autism. (Baltimore. Maryland The Johns Hopkins University Press).

Belmadani,A., Tran,P.B., Ren,D., Assimacopoulos,S., Grove,E.A., and Miller,R.J. (2005). The chemokine stromal cell-derived factor-1 regulates the migration of sensory neuron progenitors. J. Neurosci. *25*, 3995-4003.

Ben Hur,T., Ben Menachem,O., Furer,V., Einstein,O., Mizrachi-Kol,R., and Grigoriadis,N. (2003). Effects of proinflammatory cytokines on the growth, fate, and motility of multipotential neural precursor cells. Mol. Cell Neurosci. *24*, 623-631.

Bentley,P., Vuilleumier,P., Thiel,C.M., Driver,J., and Dolan,R.J. (2003). Cholinergic enhancement modulates neural correlates of selective attention and emotional processing. Neuroimage. *20*, 58-70.

Benveniste,E.N. (1992). Inflammatory cytokines within the central nervous system: sources, function, and mechanism of action. Am. J. Physiol *263*, C1-16.

Berger-Sweeney,J. (1998). The effects of neonatal basal forebrain lesions on cognition: towards understanding the developmental role of the cholinergic basal forebrain. Int. J. Dev. Neurosci. *16*, 603-612.

Berger-Sweeney,J. (2003). The cholinergic basal forebrain system during development and its influence on cognitive processes: important questions and potential answers. Neurosci. Biobehav. Rev. *27*, 401-411.

Berger-Sweeney,J. and Hohmann,C.F. (1997). Behavioral consequences of abnormal cortical development: insights into developmental disabilities. Behav. Brain Res. *86*, 121-142.

Bilbo,S.D. and Schwarz,J.M. (2009). Early-life programming of later-life brain and behavior: a critical role for the immune system. Front Behav. Neurosci. *3*, 14.

Blusztajn,J.K., Venturini,A., Jackson,D.A., Lee,H.J., and Wainer,B.H. (1992). Acetylcholine synthesis and release is enhanced by dibutyryl cyclic AMP in a neuronal cell line derived from mouse septum. J. Neurosci. *12*, 793-799.

Boulanger,L.M., Huh,G.S., and Shatz,C.J. (2001). Neuronal plasticity and cellular immunity: shared molecular mechanisms. Curr. Opin. Neurobiol. *11*, 568-578.

Boulanger,L.M. and Shatz,C.J. (2004). Immune signalling in neural development, synaptic plasticity and disease. Nat. Rev. Neurosci. *5*, 521-531.

Bozdagi,O., Sakurai,T., Papapetrou,D., Wang,X., Dickstein,D.L., Takahashi,N., Kajiwara,Y., Yang,M., Katz,A.M., Scattoni,M.L., Harris,M.J., Saxena,R., Silverman,J.L., Crawley,J.N., Zhou,Q., Hof,P.R., and Buxbaum,J.D. (2010). Haploinsufficiency of the autism-associated Shank3 gene leads to deficits in synaptic function, social interaction, and social communication. Mol. Autism *1*, 15.

Brooks,J.M., Sarter,M., and Bruno,J.P. (2011). Transient inactivation of the neonatal ventral hippocampus permanently disrupts the mesolimbic regulation of prefrontal cholinergic transmission: implications for schizophrenia. Neuropsychopharmacology *36*, 2477-2487.

Brown,A.C. and Mehl-Madrona,L. (2011). Autoimmune and gastrointestinal dysfunctions: does a subset of children with autism reveal a broader connection? Expert. Rev. Gastroenterol. Hepatol. *5*, 465-477.

Brown,A.S., Begg,M.D., Gravenstein,S., Schaefer,C.A., Wyatt,R.J., Bresnahan,M., Babulas,V.P., and Susser,E.S. (2004). Serologic evidence of prenatal influenza in the etiology of schizophrenia. Arch. Gen. Psychiatry *61*, 774-780.

Brown,A.S. and Derkits,E.J. (2010). Prenatal infection and schizophrenia: a review of epidemiologic and translational studies. Am. J. Psychiatry *167*, 261-280.

Bruel-Jungerman,E., Lucassen,P.J., and Francis,F. (2011). Cholinergic influences on cortical development and adult neurogenesis. Behav. Brain Res. *221*, 379-388.

Burton,A., Kizhner,O., Brown,M.B., and Peltier,M.R. (2012). Effect of experimental genital mycoplasmosis on gene expression in the fetal brain. J. Reprod. Immunol. *93*, 9-16.

Butovsky,O., Ziv,Y., Schwartz,A., Landa,G., Talpalar,A.E., Pluchino,S., Martino,G., and Schwartz,M. (2006). Microglia activated by IL-4 or IFN-gamma differentially induce neurogenesis and oligodendrogenesis from adult stem/progenitor cells. Mol. Cell Neurosci. *31*, 149-160.

Byrne,M., Agerbo,E., Bennedsen,B., Eaton,W.W., and Mortensen,P.B. (2007). Obstetric conditions and risk of first admission with schizophrenia: a Danish national register based study. Schizophr. Res. *97*, 51-59.

Cacci,E., Ajmone-Cat,M.A., Anelli,T., Biagioni,S., and Minghetti,L. (2008). In vitro neuronal and glial differentiation from embryonic or adult neural precursor cells are differently affected by chronic or acute activation of microglia. Glia *56*, 412-425.

Campbell,I.L., Abraham,C.R., Masliah,E., Kemper,P., Inglis,J.D., Oldstone,M.B., and Mucke,L. (1993). Neurologic disease induced in transgenic mice by cerebral overexpression of interleukin 6. Proc. Natl. Acad. Sci. U. S. A *90*, 10061-10065.

Cancedda,L., Fiumelli,H., Chen,K., and Poo,M.M. (2007). Excitatory GABA action is essential for morphological maturation of cortical neurons in vivo. J. Neurosci. *27*, 5224-5235.

Cao,Z., Gao,Y., Bryson,J.B., Hou,J., Chaudhry,N., Siddiq,M., Martinez,J., Spencer,T., Carmel,J., Hart,R.B., and Filbin,M.T. (2006). The cytokine interleukin-6 is sufficient but not necessary to mimic the peripheral conditioning lesion effect on axonal growth. J. Neurosci. *26*, 5565-5573.

Casey,J.P., Magalhaes,T., Conroy,J.M., Regan,R., Shah,N., Anney,R., Shields,D.C., Abrahams,B.S., Almeida,J., Bacchelli,E., Bailey,A.J., Baird,G., Battaglia,A., Berney,T., Bolshakova,N., Bolton,P.F., Bourgeron,T., Brennan,S., Cali,P., Correia,C., Corsello,C., Coutanche,M., Dawson,G., de Jonge,M., Delorme,R., Duketis,E., Duque,F., Estes,A., Farrar,P., Fernandez,B.A., Folstein,S.E., Foley,S., Fombonne,E., Freitag,C.M., Gilbert,J., Gillberg,C., Glessner,J.T., Green,J., Guter,S.J., Hakonarson,H., Holt,R., Hughes,G., Hus,V., Igliozzi,R., Kim,C., Klauck,S.M., Kolevzon,A., Lamb,J.A., Leboyer,M., Le Couteur,A., Leventhal,B.L., Lord,C., Lund,S.C., Maestrini,E., Mantoulan,C., Marshall,C.R., McConachie,H., McDougle,C.J., McGrath,J., McMahon,W.M., Merikangas,A., Miller,J., Minopoli,F., Mirza,G.K., Munson,J., Nelson,S.F., Nygren,G., Oliveira,G., Pagnamenta,A.T., Papanikolaou,K., Parr,J.R., Parrini,B., Pickles,A., Pinto,D., Piven,J., Posey,D.J., Poustka,A., Poustka,F., Ragoussis,J., Roge,B., Rutter,M.L., Sequeira,A.F., Soorya,L., Sousa,I., Sykes,N., Stoppioni,V., Tancredi,R., Tauber,M., Thompson,A.P., Thomson,S., Tsiantis,J., Van Engeland,H., Vincent,J.B., Volkmar,F., Vorstman,J.A., Wallace,S., Wang,K., Wassink,T.H., White,K., Wing,K., Wittemeyer,K., Yaspan,B.L., Zwaigenbaum,L., Betancur,C., Buxbaum,J.D., Cantor,R.M., Cook,E.H., Coon,H., Cuccaro,M.L., Geschwind,D.H., Haines,J.L., Hallmayer,J., Monaco,A.P., Nurnberger,J.I., Jr., Pericak-Vance,M.A., Schellenberg,G.D., Scherer,S.W., Sutcliffe,J.S., Szatmari,P., Vieland,V.J., Wijsman,E.M., Green,A., Gill,M., Gallagher,L., Vicente,A., and Ennis,S. (2011). A novel approach of homozygous haplotype sharing identifies candidate genes in autism spectrum disorder. Hum. Genet.

Chan,W.Y., Kohsaka,S., and Rezaie,P. (2007). The origin and cell lineage of microglia: new concepts. Brain Res. Rev. *53*, 344-354.

Chiang,C.S., Stalder,A., Samimi,A., and Campbell,I.L. (1994). Reactive gliosis as a consequence of interleukin-6 expression in the brain: studies in transgenic mice. Dev. Neurosci. *16*, 212-221.

Chikuma,T., Yoshimoto,T., Ohba,M., Sawada,M., Kato,T., Sakamoto,T., Hiyama,Y., and Hojo,H. (2009). Interleukin-6 induces prostaglandin E(2) synthesis in mouse astrocytes. J. Mol. Neurosci. *39*, 175-184.

Conductier,G., Blondeau,N., Guyon,A., Nahon,J.L., and Rovere,C. (2010). The role of monocyte chemoattractant protein MCP1/CCL2 in neuroinflammatory diseases. J. Neuroimmunol.

Courchesne,E. and Pierce,K. (2005). Brain overgrowth in autism during a critical time in development: implications for frontal pyramidal neuron and interneuron development and connectivity. Int. J. Dev. Neurosci. *23*, 153-170.

Cowell,R.M. and Silverstein,F.S. (2003). Developmental changes in the expression of chemokine receptor CCR1 in the rat cerebellum. J. Comp Neurol. *457*, 7-23.

Coyle,J.T., Balu,D., Benneyworth,M., Basu,A., and Roseman,A. (2010). Beyond the dopamine receptor: novel therapeutic targets for treating schizophrenia. Dialogues. Clin. Neurosci. *12*, 359-382.

Crawley,J. (2007). What's Wrong With My Mouse? (Hoboken, NJ: John Wiley and Sons, Inc.).

Curran,L.K., Newschaffer,C.J., Lee,L.C., Crawford,S.O., Johnston,M.V., and Zimmerman,A.W. (2007). Behaviors associated with fever in children with autism spectrum disorders. Pediatrics *120*, e1386-e1392.

Czeizel,A.E. (2000). Primary prevention of neural-tube defects and some other major congenital abnormalities: recommendations for the appropriate use of folic acid during pregnancy. Paediatr. Drugs *2*, 437-449.

Dahlgren,J., Samuelsson,A.M., Jansson,T., and Holmang,A. (2006). Interleukin-6 in the maternal circulation reaches the rat fetus in mid-gestation. Pediatr. Res. *60*, 147-151.

Datta,A., Jingru,Q., Khor,T.H., Teo,M.T., Heese,K., and Sze,S.K. (2011). Quantitative neuroproteomics of an in vivo rodent model of focal cerebral ischemia/reperfusion injury reveals a temporal regulation of novel pathophysiological molecular markers. J. Proteome. Res. *10*, 5199-5213.

Deutsch,S.I., Urbano,M.R., Neumann,S.A., Burket,J.A., and Katz,E. (2010). Cholinergic Abnormalities in Autism: Is There a Rationale for Selective Nicotinic Agonist Interventions? Clin. Neuropharmacol.

Di Cristo,G. (2007). Development of cortical GABAergic circuits and its implications for neurodevelopmental disorders. Clin. Genet. *72*, 1-8.

DiCicco-Bloom,E., Lord,C., Zwaigenbaum,L., Courchesne,E., Dager,S.R., Schmitz,C., Schultz,R.T., Crawley,J., and Young,L.J. (2006). The developmental neurobiology of autism spectrum disorder. J. Neurosci. *26*, 6897-6906.

Edman,L.C., Mira,H., and Arenas,E. (2008a). The beta-chemokines CCL2 and CCL7 are two novel differentiation factors for midbrain dopaminergic precursors and neurons. Exp. Cell Res. *314*, 2123-2130.

Edman,L.C., Mira,H., Erices,A., Malmersjo,S., Andersson,E., Uhlen,P., and Arenas,E. (2008b). Alpha-chemokines regulate proliferation, neurogenesis, and dopaminergic differentiation of ventral midbrain precursors and neurospheres. Stem Cells *26*, 1891-1900.

Ehninger,D., Sano,Y., de Vries,P.J., Dies,K., Franz,D., Geschwind,D.H., Kaur,M., Lee,Y.S., Li,W., Lowe,J.K., Nakagawa,J.A., Sahin,M., Smith,K., Whittemore,V., and Silva,A.J. (2012). Gestational immune activation and Tsc2 haploinsufficiency cooperate to disrupt fetal survival and may perturb social behavior in adult mice. Mol. Psychiatry *17*, 62-70.

El Saadi,O., Pedersen,C.B., McNeil,T.F., Saha,S., Welham,J., O'Callaghan,E., Cantor-Graae,E., Chant,D., Mortensen,P.B., and McGrath,J. (2004). Paternal and maternal age as risk factors for psychosis: findings from Denmark, Sweden and Australia. Schizophr. Res. *67*, 227-236.

Elkabes,S., DiCicco-Bloom,E.M., and Black,I.B. (1996). Brain microglia/macrophages express neurotrophins that selectively regulate microglial proliferation and function. J. Neurosci. *16*, 2508-2521.

Eskes,C., Honegger,P., Juillerat-Jeanneret,L., and Monnet-Tschudi,F. (2002). Microglial reaction induced by noncytotoxic methylmercury treatment leads to neuroprotection via interactions with astrocytes and IL-6 release. Glia *37*, 43-52.

Eskes,C., Juillerat-Jeanneret,L., Leuba,G., Honegger,P., and Monnet-Tschudi,F. (2003). Involvement of microglia-neuron interactions in the tumor necrosis factor-alpha release, microglial activation, and neurodegeneration induced by trimethyltin. J. Neurosci. Res. *71*, 583-590.

Fatemi,S.H., Reutiman,T.J., Folsom,T.D., Huang,H., Oishi,K., Mori,S., Smee,D.F., Pearce,D.A., Winter,C., Sohr,R., and Juckel,G. (2008). Maternal infection leads to abnormal gene regulation and brain atrophy in mouse offspring: implications for genesis of neurodevelopmental disorders. Schizophr. Res. *99*, 56-70.

Fischer,P., Lehmann,U., Sobota,R.M., Schmitz,J., Niemand,C., Linnemann,S., Haan,S., Behrmann,I., Yoshimura,A., Johnston,J.A., Muller-Newen,G., Heinrich,P.C., and Schaper,F. (2004). The role of the inhibitors of interleukin-6 signal transduction SHP2 and SOCS3 for desensitization of interleukin-6 signalling. Biochem. J. *378*, 449-460.

Garay,P.A., Hsiao,E.Y., Patterson,P.H., and McAllister,A.K. (2012). Maternal immune activation causes age- and region-specific changes in brain cytokines in offspring throughout development. Brain Behav. Immun.

Garay,P.A. and McAllister,A.K. (2010). Novel roles for immune molecules in neural development: implications for neurodevelopmental disorders. Front Synaptic. Neurosci. *2*, 136.

Gehrmann,J., Matsumoto,Y., and Kreutzberg,G.W. (1995). Microglia: intrinsic immuneffector cell of the brain. Brain Res. Brain Res. Rev. *20*, 269-287.

Gejman,P.V., Sanders,A.R., and Kendler,K.S. (2011). Genetics of schizophrenia: new findings and challenges. Annu. Rev. Genomics Hum. Genet. *12*, 121-144.

Gekas,C., Dieterlen-Lievre,F., Orkin,S.H., and Mikkola,H.K. (2005). The placenta is a niche for hematopoietic stem cells. Dev. Cell *8*, 365-375.

Geppert,A.M. (2003). Constitutive patterns of RANTES, MCP-1 and MIP-1 alpha expression at the mRNA and protein level during postnatal development of the rat brain. Folia Neuropathol. *41*, 79-88.

Geschwind,D.H. (2008). Autism: many genes, common pathways? Cell *135*, 391-395.

Gilmore,J.H., Jarskog,L.F., and Vadlamudi,S. (2003). Maternal infection regulates BDNF and NGF expression in fetal and neonatal brain and maternal-fetal unit of the rat. J. Neuroimmunol. *138*, 49-55.

Gilmore,J.H., Jarskog,L.F., and Vadlamudi,S. (2005). Maternal poly I:C exposure during pregnancy regulates TNF alpha, BDNF, and NGF expression in neonatal brain and the maternal-fetal unit of the rat. J. Neuroimmunol. *159*, 106-112.

Gogolla,N., LeBlanc,J.J., Quast,K.B., Sudhof,T.C., Fagiolini,M., and Hensch,T.K. (2009). Common circuit defect of excitatory-inhibitory balance in mouse models of autism. J. Neurodev. Disord. *1*, 172-181.

Graham,A.J., Martin-Ruiz,C.M., Teaktong,T., Ray,M.A., and Court JA (2002). Human brain nicotinic receptors, their distribution and participation in neuropsychiatric disorders. Curr. Drug Targets. CNS. Neurol. Disord. *1*, 387-397.

Hahn,C.G., Wang,H.Y., Cho,D.S., Talbot,K., Gur,R.E., Berrettini,W.H., Bakshi,K., Kamins,J., Borgmann-Winter,K.E., Siegel,S.J., Gallop,R.J., and Arnold,S.E. (2006). Altered neuregulin 1-erbB4 signaling contributes to NMDA receptor hypofunction in schizophrenia. Nat. Med. *12*, 824-828.

Hallmayer,J., Cleveland,S., Torres,A., Phillips,J., Cohen,B., Torigoe,T., Miller,J., Fedele,A., Collins,J., Smith,K., Lotspeich,L., Croen,L.A., Ozonoff,S., Lajonchere,C., Grether,J.K., and Risch,N. (2011). Genetic heritability and shared environmental factors among twin pairs with autism. Arch. Gen. Psychiatry *68*, 1095-1102.

Hama,T., Kushima,Y., Miyamoto,M., Kubota,M., Takei,N., and Hatanaka,H. (1991). Interleukin-6 improves the survival of mesencephalic catecholaminergic and septal cholinergic neurons from postnatal, two-week-old rats in cultures. Neuroscience *40*, 445-452.

Hama,T., Miyamoto,M., Tsukui,H., Nishio,C., and Hatanaka,H. (1989). Interleukin-6 as a neurotrophic factor for promoting the survival of cultured basal forebrain cholinergic neurons from postnatal rats. Neurosci. Lett. *104*, 340-344.

Hanisch,U.K. (2002). Microglia as a source and target of cytokines. Glia *40*, 140-155.

Harrison,P.J. and Law,A.J. (2006). Neuregulin 1 and schizophrenia: genetics, gene expression, and neurobiology. Biol. Psychiatry *60*, 132-140.

Heinrich,P.C., Behrmann,I., Haan,S., Hermanns,H.M., Muller-Newen,G., and Schaper,F. (2003). Principles of interleukin (IL)-6-type cytokine signalling and its regulation. Biochem. J. *374*, 1-20.

Helliwell,R.J., Keelan,J.A., Marvin,K.W., Adams,L., Chang,M.C., Anand,A., Sato,T.A., O'Carroll,S., Chaiworapongsa,T., Romero,R.J., and Mitchell,M.D. (2006). Gestational age-dependent up-regulation of prostaglandin D synthase (PGDS) and production of PGDS-derived antiinflammatory prostaglandins in human placenta. J. Clin. Endocrinol. Metab *91*, 597-606.

Herrmann,J.E., Imura,T., Song,B., Qi,J., Ao,Y., Nguyen,T.K., Korsak,R.A., Takeda,K., Akira,S., and Sofroniew,M.V. (2008). STAT3 is a critical regulator of astrogliosis and scar formation after spinal cord injury. J. Neurosci. *28*, 7231-7243.

Hohmann,C.F. and Berger-Sweeney,J. (1998a). Cholinergic regulation of cortical development and plasticity. New twists to an old story. Perspect. Dev. Neurobiol. *5*, 401-425.

Hohmann,C.F. and Berger-Sweeney,J. (1998b). Sexually dimorphic responses to neonatal basal forebrain lesions in mice: II. Cortical morphology. J. Neurobiol. *37*, 595-606.

Holt,R. and Monaco,A.P. (2011). Links between genetics and pathophysiology in the autism spectrum disorders. EMBO Mol. Med. *3*, 438-450.

Hsiao,E.Y. and Patterson,P.H. (2011). Activation of the maternal immune system induces endocrine changes in the placenta via IL-6. Brain Behav. Immun. *25*, 604-615.

Huh,G.S., Boulanger,L.M., Du,H., Riquelme,P.A., Brotz,T.M., and Shatz,C.J. (2000). Functional requirement for class I MHC in CNS development and plasticity. Science *290*, 2155-2159.

Islam,O., Gong,X., Rose-John,S., and Heese,K. (2009). Interleukin-6 and neural stem cells: more than gliogenesis. Mol. Biol. Cell *20*, 188-199.

Jakovcevski,I., Filipovic,R., Mo,Z., Rakic,S., and Zecevic,N. (2009). Oligodendrocyte development and the onset of myelination in the human fetal brain. Front Neuroanat. *3*, 5.

Jarskog,L.F., Xiao,H., Wilkie,M.B., Lauder,J.M., and Gilmore,J.H. (1997). Cytokine regulation of embryonic rat dopamine and serotonin neuronal survival in vitro. Int. J. Dev. Neurosci. *15*, 711-716.

Johnston,M.V., Hohmann,C., and Blue,M.E. (1995). Neurobiology of Rett syndrome. Neuropediatrics *26*, 119-122.

Johnston,M.V., Jeon,O.H., Pevsner,J., Blue,M.E., and Naidu,S. (2001). Neurobiology of Rett syndrome: a genetic disorder of synapse development. Brain Dev. *23 Suppl 1*, S206-S213.

Jonakait,G.M. (2007). The effects of maternal inflammation on neuronal development: possible mechanisms. Int. J. Dev. Neurosci. *25*, 415-425.

Jonakait,G.M., Luskin,M.B., and Ni,L. (1998). Transforming growth factor-alpha expands progenitor cells of the basal forebrain, but does not promote cholinergic differentiation. J. Neurobiol. *37*, 405-412.

Jonakait,G.M., Luskin,M.B., Wei,R., Tian,X.F., and Ni,L. (1996). Conditioned medium from activated microglia promotes cholinergic differentiation in the basal forebrain in vitro. Dev. Biol. *177*, 85-95.

Jonakait,G.M., Pratt,L., Acevedo,G., and Ni,L. (2012). Microglial regulation of cholinergic differentiation in the basal forebrain. Dev. Neurobiol. *72*, 857-64.

Jonakait,G.M., Wei,R., Sheng,Z.L., Hart,R.P., and Ni,L. (1994). Interferon-gamma promotes cholinergic differentiation of embryonic septal nuclei and adjacent basal forebrain. Neuron *12*, 1149-1159.

Jonakait,G.M., Wen,Y., Wan,Y., and Ni,L. (2000). Macrophage cell-conditioned medium promotes cholinergic differentiation of undifferentiated progenitors and synergizes with nerve growth factor action in the developing basal forebrain. Exp. Neurol. *161*, 285-296.

Jones,K.L. (2011). The effects of alcohol on fetal development. Birth Defects Res. C. Embryo. Today *93*, 3-11.

Jones,S.A., Horiuchi,S., Topley,N., Yamamoto,N., and Fuller,G.M. (2001). The soluble interleukin 6 receptor: mechanisms of production and implications in disease. FASEB J. *15*, 43-58.

Kannan,S., Saadani-Makki,F., Muzik,O., Chakraborty,P., Mangner,T.J., Janisse,J., Romero,R., and Chugani,D.C. (2007). Microglial activation in perinatal rabbit brain induced by intrauterine inflammation: detection with 11C-(R)-PK11195 and small-animal PET. J. Nucl. Med. *48*, 946-954.

Kassam,S.M., Herman,P.M., Goodfellow,N.M., Alves,N.C., and Lambe,E.K. (2008). Developmental excitation of corticothalamic neurons by nicotinic acetylcholine receptors. J. Neurosci. *28*, 8756-8764.

Kaur,C., Hao,A.J., Wu,C.H., and Ling,E.A. (2001). Origin of microglia. Microsc. Res. Tech. *54*, 2-9.

Keelan,J.A., Marvin,K.W., Sato,T.A., Coleman,M., McCowan,L.M., and Mitchell,M.D. (1999). Cytokine abundance in placental tissues: evidence of inflammatory activation in gestational membranes with term and preterm parturition. Am. J. Obstet. Gynecol. *181*, 1530-1536.

Kelleher,R.J., III and Bear,M.F. (2008). The autistic neuron: troubled translation? Cell *135*, 401-406.

Kendrick,J.S. and Merritt,R.K. (1996). Women and smoking: an update for the 1990s. Am. J. Obstet. Gynecol. *175*, 528-535.

Kim,Y., Zerwas,S., Trace,S.E., and Sullivan,P.F. (2011). Schizophrenia genetics: where next? Schizophr. Bull. *37*, 456-463.

Kitagawa,H., Takenouchi,T., Azuma,R., Wesnes,K.A., Kramer,W.G., Clody,D.E., and Burnett,A.L. (2003). Safety, pharmacokinetics, and effects on cognitive function of multiple doses of GTS-21 in healthy, male volunteers. Neuropsychopharmacology *28*, 542-551.

Klein,M.A., Moller,J.C., Jones,L.L., Bluethmann,H., Kreutzberg,G.W., and Raivich,G. (1997). Impaired neuroglial activation in interleukin-6 deficient mice. Glia *19*, 227-233.

Klein,R.S., Rubin,J.B., Gibson,H.D., DeHaan,E.N., Alvarez-Hernandez,X., Segal,R.A., and Luster,A.D. (2001). SDF-1 alpha induces chemotaxis and enhances Sonic hedgehog-induced proliferation of cerebellar granule cells. Development *128*, 1971-1981.

Krady,J.K., Lin,H.W., Liberto,C.M., Basu,A., Kremlev,S.G., and Levison,S.W. (2008). Ciliary neurotrophic factor and interleukin-6 differentially activate microglia. J. Neurosci. Res. *86*, 1538-1547.

Kristensen,S.E., Thomsen,M.S., Hansen,H.H., Timmermann,D.B., Hay-Schmidt,A., and Mikkelsen,J.D. (2007). The alpha7 nicotinic receptor agonist SSR180711 increases activity regulated cytoskeleton protein (Arc) gene expression in the prefrontal cortex of the rat. Neurosci. Lett. *418*, 154-158.

Kunz,D., Walker,G., Bedoucha,M., Certa,U., Marz-Weiss,P., Dimitriades-Schmutz,B., and Otten,U. (2009). Expression profiling and Ingenuity biological function analyses of interleukin-6- versus nerve growth factor-stimulated PC12 cells. BMC. Genomics *10*, 90.

Kury,P., Greiner-Petter,R., Cornely,C., Jurgens,T., and Muller,H.W. (2002). Mammalian achaete scute homolog 2 is expressed in the adult sciatic nerve and regulates the expression of Krox24, Mob-1, CXCR4, and p57kip2 in Schwann cells. J. Neurosci. *22*, 7586-7595.

Kushima,Y. and Hatanaka,H. (1992). Interleukin-6 and leukemia inhibitory factor promote the survival of acetylcholinesterase-positive neurons in culture from embryonic rat spinal cord. Neurosci. Lett. *143*, 110-114.

Lancaster,P.A. (2011). Causes of birth defects: lessons from history. Congenit. Anom. (Kyoto) *51*, 2-5.

Landrigan,P.J. (2010). What causes autism? Exploring the environmental contribution. Curr. Opin. Pediatr. *22*, 219-225.

Lasala,N. and Zhou,H. (2007). Effects of maternal exposure to LPS on the inflammatory response in the offspring. J. Neuroimmunol. *189*, 95-101.

Lazarini,F., Gabellec,M.M., Torquet,N., and Lledo,P.M. (2012). Early activation of microglia triggers long-lasting impairment of adult neurogenesis in the olfactory bulb. J. Neurosci. *32*, 3652-3664.

Le Magueresse,C., Safiulina,V., Changeux,J.P., and Cherubini,E. (2006). Nicotinic modulation of network and synaptic transmission in the immature hippocampus investigated with genetically modified mice. J. Physiol *576*, 533-546.

LeBlanc,J.J. and Fagiolini,M. (2011). Autism: a "critical period" disorder? Neural Plast. *2011*, 921680.

Lee,K.W., Woon,P.S., Teo,Y.Y., and Sim,K. (2012). Genome wide association studies (GWAS) and copy number variation (CNV) studies of the major psychoses: what have we learnt? Neurosci. Biobehav. Rev. *36*, 556-571.

Lennertz,L., Wagner,M., Wolwer,W., Schuhmacher,A., Frommann,I., Berning,J., Schulze-Rauschenbach,S., Landsberg,M.W., Steinbrecher,A., Alexander,M., Franke,P.E., Pukrop,R., Ruhrmann,S., Bechdolf,A., Gaebel,W., Klosterkotter,J., Hafner,H., Maier,W., and Mossner,R. (2012). A promoter variant of SHANK1 affects auditory working memory in schizophrenia patients and in subjects clinically at risk for psychosis. Eur. Arch. Psychiatry Clin. Neurosci. *262*, 117-124.

Li,H., Khirug,S., Cai,C., Ludwig,A., Blaesse,P., Kolikova,J., Afzalov,R., Coleman,S.K., Lauri,S., Airaksinen,M.S., Keinanen,K., Khiroug,L., Saarma,M., Kaila,K., and Rivera,C. (2007a). KCC2 interacts with the dendritic cytoskeleton to promote spine development. Neuron *56*, 1019-1033.

Li,L., Lu,J., Tay,S.S., Moochhala,S.M., and He,B.P. (2007b). The function of microglia, either neuroprotection or neurotoxicity, is determined by the equilibrium among factors released from activated microglia in vitro. Brain Res. *1159*, 8-17.

Lippiello,P.M. (2006). Nicotinic cholinergic antagonists: a novel approach for the treatment of autism. Med. Hypotheses *66*, 985-990.

Liu,Y., Ford,B., Mann,M.A., and Fischbach,G.D. (2001). Neuregulins increase alpha7 nicotinic acetylcholine receptors and enhance excitatory synaptic transmission in GABAergic interneurons of the hippocampus. J. Neurosci. *21*, 5660-5669.

Liu,Z., Neff,R.A., and Berg,D.K. (2006). Sequential interplay of nicotinic and GABAergic signaling guides neuronal development. Science *314*, 1610-1613.

Liverman,C.S., Kaftan,H.A., Cui,L., Hersperger,S.G., Taboada,E., Klein,R.M., and Berman,N.E. (2006). Altered expression of pro-inflammatory and developmental genes in the fetal brain in a mouse model of maternal infection. Neurosci. Lett. *399*, 220-225.

Locatelli,D., Terao,M., Fratelli,M., Zanetti,A., Kurosaki,M., Lupi,M., Barzago,M.M., Uggetti,A., Capra,S., D'Errico,P., Battaglia,G.S., and Garattini,E. (2012). Human axonal survival of motor neuron (a-SMN) protein stimulates axon growth, cell motility, C-C motif ligand 2 (CCL2), and insulin-like growth factor-1 (IGF1) production. J. Biol. Chem. *287*, 25782-25794.

Lozada,A.F., Wang,X., Gounko,N.V., Massey,K.A., Duan,J., Liu,Z., and Berg,D.K. (2012). Glutamatergic synapse formation is promoted by alpha7-containing nicotinic acetylcholine receptors. J. Neurosci. *32*, 7651-7661.

Ma,Q., Jones,D., Borghesani,P.R., Segal,R.A., Nagasawa,T., Kishimoto,T., Bronson,R.T., and Springer,T.A. (1998). Impaired B-lymphopoiesis, myelopoiesis, and derailed cerebellar neuron migration in C. Proc. Natl. Acad. Sci. U. S. A *95*, 9448-9453.

Mandal,M., Marzouk,A.C., Donnelly,R., and Ponzio,N.M. (2010). Preferential development of Th17 cells in offspring of immunostimulated pregnant mice. J. Reprod. Immunol. *87*, 97-100.

Mandal,M., Marzouk,A.C., Donnelly,R., and Ponzio,N.M. (2011). Maternal immune stimulation during pregnancy affects adaptive immunity in offspring to promote development of TH17 cells. Brain Behav. Immun. *25*, 863-871.

Marvin,K.W., Keelan,J.A., Eykholt,R.L., Sato,T.A., and Mitchell,M.D. (2002). Expression of angiogenic and neurotrophic factors in the human amnion and choriodecidua. Am. J. Obstet. Gynecol. *187*, 728-734.

Marz,P., Heese,K., Dimitriades-Schmutz,B., Rose-John,S., and Otten,U. (1999). Role of interleukin-6 and soluble IL-6 receptor in region-specific induction of astrocytic differentiation and neurotrophin expression. Glia *26*, 191-200.

Mazzoni,I.E. and Kenigsberg,R.L. (1997). Microglia from the developing rat medial septal area can affect cholinergic and GABAergic neuronal differentiation in vitro. Neuroscience *76*, 147-157.

McGrath,J., Saha,S., Chant,D., and Welham,J. (2008). Schizophrenia: a concise overview of incidence, prevalence, and mortality. Epidemiol. Rev. *30*, 67-76.

Meck,W.H. and Williams,C.L. (2003). Metabolic imprinting of choline by its availability during gestation: implications for memory and attentional processing across the lifespan. Neurosci. Biobehav. Rev. *27*, 385-399.

Meck,W.H., Williams,C.L., Cermak,J.M., and Blusztajn,J.K. (2007). Developmental periods of choline sensitivity provide an ontogenetic mechanism for regulating memory capacity and age-related dementia. Front Integr. Neurosci. *1*, 7.

Meyer,U., Engler,A., Weber,L., Schedlowski,M., and Feldon,J. (2008a). Preliminary evidence for a modulation of fetal dopaminergic development by maternal immune activation during pregnancy. Neuroscience *154*, 701-709.

Meyer,U., Feldon,J., Schedlowski,M., and Yee,B.K. (2006a). Immunological stress at the maternal-foetal interface: a link between neurodevelopment and adult psychopathology. Brain Behav. Immun. *20*, 378-388.

Meyer,U., Feldon,J., and Yee,B.K. (2009). A review of the fetal brain cytokine imbalance hypothesis of schizophrenia. Schizophr. Bull. *35*, 959-972.

Meyer,U., Murray,P.J., Urwyler,A., Yee,B.K., Schedlowski,M., and Feldon,J. (2008b). Adult behavioral and pharmacological dysfunctions following disruption of the fetal brain balance between pro-inflammatory and IL-10-mediated anti-inflammatory signaling. Mol. Psychiatry *13*, 208-221.

Meyer,U., Nyffeler,M., Engler,A., Urwyler,A., Schedlowski,M., Knuesel,I., Yee,B.K., and Feldon,J. (2006b). The time of prenatal immune challenge determines the specificity of inflammation-mediated brain and behavioral pathology. J. Neurosci. *26*, 4752-4762.

Meyer,U., Nyffeler,M., Yee,B.K., Knuesel,I., and Feldon,J. (2008c). Adult brain and behavioral pathological markers of prenatal immune challenge during early/middle and late fetal development in mice. Brain Behav. Immun. *22*, 469-486.

Mikkola,H.K., Gekas,C., Orkin,S.H., and Dieterlen-Lievre,F. (2005). Placenta as a site for hematopoietic stem cell development. Exp. Hematol. *33*, 1048-1054.

Mittal,V.A., Ellman,L.M., and Cannon,T.D. (2008). Gene-environment interaction and covariation in schizophrenia: the role of obstetric complications. Schizophr. Bull. *34*, 1083-1094.

Mittal,V.A., Willhite,R., Daley,M., Bearden,C.E., Niendam,T., Ellman,L.M., and Cannon,T.D. (2009). Obstetric complications and risk for conversion to psychosis among individuals at high clinical risk. Early Interv. Psychiatry *3*, 226-230.

Muhle,R., Trentacoste,S.V., and Rapin,I. (2004). The genetics of autism. Pediatrics *113*, e472-e486.

Nagata,K., Takei,N., Nakajima,K., Saito,H., and Kohsaka,S. (1993). Microglial conditioned medium promotes survival and development of cultured mesencephalic neurons from embryonic rat brain. J. Neurosci. Res. *34*, 357-363.

Nan,X. and Bird,A. (2001). The biological functions of the methyl-CpG-binding protein MeCP2 and its implication in Rett syndrome. Brain Dev. *23 Suppl 1*, S32-S37.

Neumann,H. (2001). Control of glial immune function by neurons. Glia *36*, 191-199.

Ni,L., Acevedo,G., Muralidharan,B., Padala,N., To,J., and Jonakait,G.M. (2007). Toll-like receptor ligands and CD154 stimulate microglia to produce a factor(s) that promotes excess cholinergic differentiation in the developing rat basal forebrain: implications for neurodevelopmental disorders. Pediatr. Res. *61*, 15-20.

Nikodemova,M. and Watters,J.J. (2012). Efficient isolation of live microglia with preserved phenotypes from adult mouse brain. J. Neuroinflammation. *9*, 147.

Nimmerjahn,A., Kirchhoff,F., and Helmchen,F. (2005). Resting microglial cells are highly dynamic surveillants of brain parenchyma in vivo. Science *308*, 1314-1318.

Nyffeler,M., Meyer,U., Yee,B.K., Feldon,J., and Knuesel,I. (2006). Maternal immune activation during pregnancy increases limbic GABAA receptor immunoreactivity in the adult offspring: implications for schizophrenia. Neuroscience *143*, 51-62.

Odell,D., Maciulis,A., Cutler,A., Warren,L., McMahon,W.M., Coon,H., Stubbs,G., Henley,K., and Torres,A. (2005). Confirmation of the association of the C4B null allele in autism. Hum. Immunol. *66*, 140-145.

Old,E.A. and Malcangio,M. (2012). Chemokine mediated neuron-glia communication and aberrant signalling in neuropathic pain states. Curr. Opin. Pharmacol. *12*, 67-73.

Onore,C., Careaga,M., and Ashwood,P. (2012). The role of immune dysfunction in the pathophysiology of autism. Brain Behav. Immun. *26*, 383-392.

Pang,Y., Fan,L.W., Zheng,B., Cai,Z., and Rhodes,P.G. (2006). Role of interleukin-6 in lipopolysaccharide-induced brain injury and behavioral dysfunction in neonatal rats. Neuroscience *141*, 745-755.

Pappas,B.A. and Sherren,N. (2003). Neonatal 192 IgG-saporin lesion of forebrain cholinergic neurons: focus on the life span? Neurosci. Biobehav. Rev. *27*, 365-376.

Parker-Athill,E.C. and Tan,J. (2010). Maternal immune activation and autism spectrum disorder: interleukin-6 signaling as a key mechanistic pathway. Neurosignals. *18*, 113-128.

Patterson,P.H. (2011a). Infectious Behavior: Brain-Immune Connections in Autism, Schizophrenia and Depression. (Cambridge, Massachusetts: The MIT Press).

Patterson,P.H. (2011b). Maternal infection and immune involvement in autism. Trends Mol. Med. *17*, 389-394.

Perry,E.K., Lee,M.L., Martin-Ruiz,C.M., Court JA, Volsen,S.G., Merrit,J., Folly,E., Iversen,P.E., Bauman,M.L., Perry,R.H., and Wenk,G.L. (2001). Cholinergic activity in autism: abnormalities in the cerebral cortex and basal forebrain. Am. J. Psychiatry *158*, 1058-1066.

Pessah,I.N., Seegal,R.F., Lein,P.J., LaSalle,J., Yee,B.K., Van De,W.J., and Berman,R.F. (2008). Immunologic and neurodevelopmental susceptibilities of autism. Neurotoxicology *29*, 532-545.

Puma,C., Danik,M., Quirion,R., Ramon,F., and Williams,S. (2001). The chemokine interleukin-8 acutely reduces Ca(2+) currents in identified cholinergic septal neurons expressing CXCR1 and CXCR2 receptor mRNAs. J. Neurochem. *78*, 960-971.

Quintana,A., Molinero,A., Borup,R., Nielsen,F.C., Campbell,I.L., Penkowa,M., and Hidalgo,J. (2008). Effect of astrocyte-targeted production of IL-6 on traumatic brain injury and its impact on the cortical transcriptome. Dev. Neurobiol. *68*, 195-208.

Rezaie,P., Trillo-Pazos,G., Everall,I.P., and Male,D.K. (2002a). Expression of beta-chemokines and chemokine receptors in human fetal astrocyte and microglial co-cultures: potential role of chemokines in the developing CNS. Glia *37*, 64-75.

Rezaie,P., Trillo-Pazos,G., Greenwood,J., Everall,I.P., and Male,D.K. (2002b). Motility and ramification of human fetal microglia in culture: an investigation using time-lapse video microscopy and image analysis. Exp. Cell Res. *274*, 68-82.

Rhodes,K.E., Gekas,C., Wang,Y., Lux,C.T., Francis,C.S., Chan,D.N., Conway,S., Orkin,S.H., Yoder,M.C., and Mikkola,H.K. (2008). The emergence of hematopoietic stem cells is initiated in the placental vasculature in the absence of circulation. Cell Stem Cell *2*, 252-263.

Ricceri,L., Hohmann,C., and Berger-Sweeney,J. (2002). Early neonatal 192 IgG saporin induces learning impairments and disrupts cortical morphogenesis in rats. Brain Res. *954*, 160-172.

Riva,D., Bulgheroni,S., Aquino,D., Di Salle,F., Savoiardo,M., and Erbetta,A. (2011). Basal forebrain involvement in low-functioning autistic children: a voxel-based morphometry study. AJNR Am. J. Neuroradiol. *32*, 1430-1435.

Robertson,R.T., Gallardo,K.A., Claytor,K.J., Ha,D.H., Ku,K.H., Yu,B.P., Lauterborn,J.C., Wiley,R.G., Yu,J., Gall,C.M., and Leslie,F.M. (1998). Neonatal treatment with 192 IgG-saporin produces long-term forebrain cholinergic deficits and reduces dendritic branching and spine density of neocortical pyramidal neurons. Cereb. Cortex *8*, 142-155.

Roessmann,U. and Gambetti,P. (1986). Astrocytes in the developing human brain. An immunohistochemical study. Acta Neuropathol. *70*, 308-313.

Roumier,A., Pascual,O., Bechade,C., Wakselman,S., Poncer,J.C., Real,E., Triller,A., and Bessis,A. (2008). Prenatal activation of microglia induces delayed impairment of glutamatergic synaptic function. PLoS. One. *3*, e2595.

Samuelsson,A.M., Jennische,E., Hansson,H.A., and Holmang,A. (2006). Prenatal exposure to interleukin-6 results in inflammatory neurodegeneration in hippocampus with NMDA/GABA(A) dysregulation and impaired spatial learning. Am. J. Physiol Regul. Integr. Comp Physiol *290*, R1345-R1356.

Sanz,E., Hofer,M.J., Unzeta,M., and Campbell,I.L. (2008). Minimal role for STAT1 in interleukin-6 signaling and actions in the murine brain. Glia *56*, 190-199.

Sato,T.A., Gupta,D.K., Keelan,J.A., Marvin,K.W., and Mitchell,M.D. (2001). Expression of interleukin-1beta mRNA in murine uterine and gestational tissues: relationship with gestational age. Am. J. Reprod. Immunol. *46*, 413-419.

Sato,T.A., Keelan,J.A., and Mitchell,M.D. (2003). Critical paracrine interactions between TNF-alpha and IL-10 regulate lipopolysaccharide-stimulated human choriodecidual cytokine and prostaglandin E2 production. J. Immunol. *170*, 158-166.

Schadt,E.E. (2009). Molecular networks as sensors and drivers of common human diseases. Nature *461*, 218-223.

Schwarz,J.M., Hutchinson,M.R., and Bilbo,S.D. (2011). Early-life experience decreases drug-induced reinstatement of morphine CPP in adulthood via microglial-specific epigenetic programming of anti-inflammatory IL-10 expression. J. Neurosci. *31*, 17835-17847.

Seita,J., Asakawa,M., Ooehara,J., Takayanagi,S., Morita,Y., Watanabe,N., Fujita,K., Kudo,M., Mizuguchi,J., Ema,H., Nakauchi,H., and Yoshimoto,T. (2008). Interleukin-27 directly induces differentiation in hematopoietic stem cells. Blood *111*, 1903-1912.

Shafer,L.L., McNulty,J.A., and Young,M.R. (2002). Brain activation of monocyte-lineage cells: involvement of interleukin-6. Neuroimmunomodulation. *10*, 295-304.

Shen,Q., Li,Z.Q., Sun,Y., Wang,T., Wan,C.L., Li,X.W., Zhao,X.Z., Feng,G.Y., Li,S., St Clair,D., He,L., and Yu,L. (2008). The role of pro-inflammatory factors in mediating the effects on the fetus of prenatal undernutrition: implications for schizophrenia. Schizophr. Res. *99*, 48-55.

Shi,L., Fatemi,S.H., Sidwell,R.W., and Patterson,P.H. (2003). Maternal influenza infection causes marked behavioral and pharmacological changes in the offspring. J. Neurosci. *23*, 297-302.

Shi,L., Smith,S.E., Malkova,N., Tse,D., Su,Y., and Patterson,P.H. (2009). Activation of the maternal immune system alters cerebellar development in the offspring. Brain Behav. Immun. *23*, 116-123.

Shi,L., Tu,N., and Patterson,P.H. (2005). Maternal influenza infection is likely to alter fetal brain development indirectly: the virus is not detected in the fetus. Int. J. Dev. Neurosci. *23*, 299-305.

Shirts,B.H., Kim,J.J., Reich,S., Dickerson,F.B., Yolken,R.H., Devlin,B., and Nimgaonkar,V.L. (2007). Polymorphisms in MICB are associated with human herpes virus seropositivity and schizophrenia risk. Schizophr. Res. *94*, 342-353.

Smith,S.E., Li,J., Garbett,K., Mirnics,K., and Patterson,P.H. (2007). Maternal immune activation alters fetal brain development through interleukin-6. J. Neurosci. *27*, 10695-10702.

Spooren,A., Kolmus,K., Laureys,G., Clinckers,R., De Keyser,J., Haegeman,G., and Gerlo,S. (2011). Interleukin-6, a mental cytokine. Brain Res. Rev. *67*, 157-183.

Sredni-Kenigsbuch,D. (2002). TH1/TH2 cytokines in the central nervous system. Int. J. Neurosci. *112*, 665-703.

St Clair,D., Xu,M., Wang,P., Yu,Y., Fang,Y., Zhang,F., Zheng,X., Gu,N., Feng,G., Sham,P., and He,L. (2005). Rates of adult schizophrenia following prenatal exposure to the Chinese famine of 1959-1961. JAMA *294*, 557-562.

Steyaert,J.G. and De la,M.W. (2008). What's new in autism? Eur. J. Pediatr. *167*, 1091-1101.

Streit,W.J., Hurley,S.D., McGraw,T.S., and Semple-Rowland,S.L. (2000). Comparative evaluation of cytokine profiles and reactive gliosis supports a critical role for interleukin-6 in neuron-glia signaling during regeneration. J. Neurosci. Res. *61*, 10-20.

Taruscio,D., Carbone,P., Granata,O., Baldi,F., and Mantovani,A. (2011). Folic acid and primary prevention of birth defects. Biofactors *37*, 280-284.

Thomsen,M.S., Hay-Schmidt,A., Hansen,H.H., and Mikkelsen,J.D. (2010). Distinct neural pathways mediate alpha7 nicotinic acetylcholine receptor-dependent activation of the forebrain. Cereb. Cortex *20*, 2092-2102.

Thomsen,M.S., Mikkelsen,J.D., Timmermann,D.B., Peters,D., Hay-Schmidt,A., Martens,H., and Hansen,H.H. (2008). The selective alpha7 nicotinic acetylcholine receptor agonist A-582941 activates immediate early genes in limbic regions of the forebrain: Differential effects in the juvenile and adult rat. Neuroscience *154*, 741-753.

Tilgner,J., Volk,B., and Kaltschmidt,C. (2001). Continuous interleukin-6 application in vivo via macroencapsulation of interleukin-6-expressing COS-7 cells induces massive gliosis. Glia *35*, 234-245.

Tomson,T., Battino,D., Bonizzoni,E., Craig,J., Lindhout,D., Sabers,A., Perucca,E., and Vajda,F. (2011). Dose-dependent risk of malformations with antiepileptic drugs: an analysis of data from the EURAP epilepsy and pregnancy registry. Lancet Neurol. *10*, 609-617.

Torrey,E.F., Buka,S., Cannon,T.D., Goldstein,J.M., Seidman,L.J., Liu,T., Hadley,T., Rosso,I.M., Bearden,C., and Yolken,R.H. (2009). Paternal age as a risk factor for schizophrenia: how important is it? Schizophr. Res. *114*, 1-5.

Tran,P.B., Banisadr,G., Ren,D., Chenn,A., and Miller,R.J. (2007). Chemokine receptor expression by neural progenitor cells in neurogenic regions of mouse brain. J. Comp Neurol. *500*, 1007-1033.

Tran,P.B. and Miller,R.J. (2003a). Chemokine receptors in the brain: a developing story. J. Comp Neurol. *457*, 1-6.

Tran,P.B. and Miller,R.J. (2003b). Chemokine receptors: signposts to brain development and disease. Nat. Rev. Neurosci. *4*, 444-455.

Tran,P.B., Ren,D., Veldhouse,T.J., and Miller,R.J. (2004). Chemokine receptors are expressed widely by embryonic and adult neural progenitor cells. J. Neurosci. Res. *76*, 20-34.

Turbic,A., Leong,S.Y., and Turnley,A.M. (2011). Chemokines and inflammatory mediators interact to regulate adult murine neural precursor cell proliferation, survival and differentiation. PLoS. One. *6*, e25406.

Uchino,S. and Waga,C. (2012). SHANK3 as an autism spectrum disorder-associated gene. Brain Dev.

Urakubo,A., Jarskog,L.F., Lieberman,J.A., and Gilmore,J.H. (2001). Prenatal exposure to maternal infection alters cytokine expression in the placenta, amniotic fluid, and fetal brain. Schizophr. Res. *47*, 27-36.

Vargas,D.L., Nascimbene,C., Krishnan,C., Zimmerman,A.W., and Pardo,C.A. (2005). Neuroglial activation and neuroinflammation in the brain of patients with autism. Ann. Neurol. *57*, 67-81.

Walsh,C.A., Morrow,E.M., and Rubenstein,J.L. (2008). Autism and brain development. Cell *135*, 396-400.

Wang,H., Davila-Garcia,M.I., Yarl,W., and Gondre-Lewis,M.C. (2011). Gestational nicotine exposure regulates expression of AMPA and NMDA receptors and their signaling apparatus in developing and adult rat hippocampus. Neuroscience *188*, 168-181.

Warren,R.P., Burger,R.A., Odell,D., Torres,A.R., and Warren,W.L. (1994). Decreased plasma concentrations of the C4B complement protein in autism. Arch. Pediatr. Adolesc. Med. *148*, 180-183.

Weintraub,K. (2011). The prevalence puzzle: Autism counts. Nature *479*, 22-24.

Wenk,G.L. and Hauss-Wegrzyniak,B. (1999). Altered cholinergic function in the basal forebrain of girls with Rett syndrome. Neuropediatrics *30*, 125-129.

Williams,C.L., Meck,W.H., Heyer,D.D., and Loy,R. (1998). Hypertrophy of basal forebrain neurons and enhanced visuospatial memory in perinatally choline-supplemented rats. Brain Res. *794*, 225-238.

Xiang,Y., Li,Y., Zhang,Z., Cui,K., Wang,S., Yuan,X.B., Wu,C.P., Poo,M.M., and Duan,S. (2002). Nerve growth cone guidance mediated by G protein-coupled receptors. Nat. Neurosci. *5*, 843-848.

Young,A.M., Campbell,E., Lynch,S., Suckling,J., and Powis,S.J. (2011). Aberrant NF-kappaB expression in autism spectrum condition: a mechanism for neuroinflammation. Front Psychiatry *2*, 27.

Zaretsky,M.V., Alexander,J.M., Byrd,W., and Bawdon,R.E. (2004). Transfer of inflammatory cytokines across the placenta. Obstet. Gynecol. *103*, 546-550.

Zhang,P.L., Levy,A.M., Ben Simchon,L., Haggiag,S., Chebath,J., and Revel,M. (2007). Induction of neuronal and myelin-related gene expression by IL-6-receptor/IL-6: a study on embryonic dorsal root ganglia cells and isolated Schwann cells. Exp. Neurol. *208*, 285-296.

Zhong,C., Du,C., Hancock,M., Mertz,M., Talmage,D.A., and Role,L.W. (2008). Presynaptic type III neuregulin 1 is required for sustained enhancement of hippocampal transmission by nicotine and for axonal targeting of alpha7 nicotinic acetylcholine receptors. J. Neurosci. *28*, 9111-9116.

Zuckerman,L. and Weiner,I. (2003). Post-pubertal emergence of disrupted latent inhibition following prenatal immune activation. Psychopharmacology (Berl) *169*, 308-313.

VIII. Tables

Table 2. Comparison of maternal weight gain/loss following injection. Pregnant mice were injected at E12.5 with polyinosinic-polycitidylic acid (poly(I:C), 20 mg/kg) or with saline. Mice were weighed on the day of injection (E12.5) and the following day (E13.5). Saline-injected mice gained weight while poly(I:C)-injected mice lost weight. Values reported are the mean ± SEM. Weight gain/loss was compared for statistical significance using a student's t-test, p<0.001.

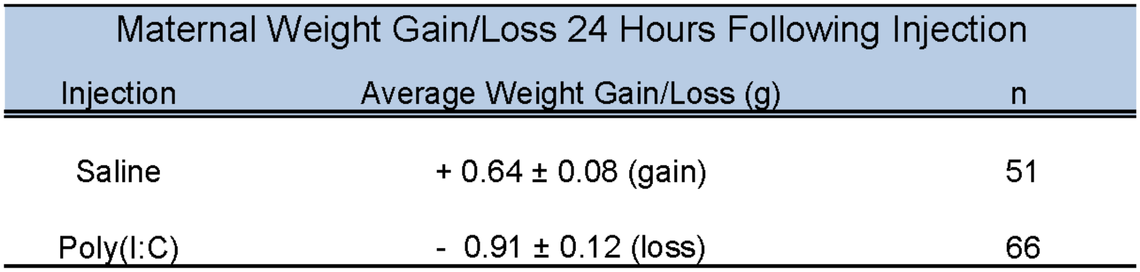

Maternal Weight Gain/Loss 24 Hours Following Injection

Injection	Average Weight Gain/Loss (g)	n
Saline	+ 0.64 ± 0.08 (gain)	51
Poly(I:C)	- 0.91 ± 0.12 (loss)	66

Table 3. Assessment of sickness behavior. At 4 hours and 24 hours following injection with poly(I:C) (20 mg/kg) or with saline mice were placed in a novel environment (new cage) for 2 min. Behavior in 5 categories was observed and ranked from 0 to 4 with 4 representing normal behavior and 0 being no normal behavior. Intermediate scores of 1 represented 1observed behavior in that category, 2 for 2-3 instances of that behavior and 3 for 4-5 observed instances. Values reported here are the mean ± SEM. Scores for the 2 groups were compared for statistical significance using a non-parametric Mann-Whitney test. At 4 hours $p< 0.0001$ for all 5 behavior categories and total score.

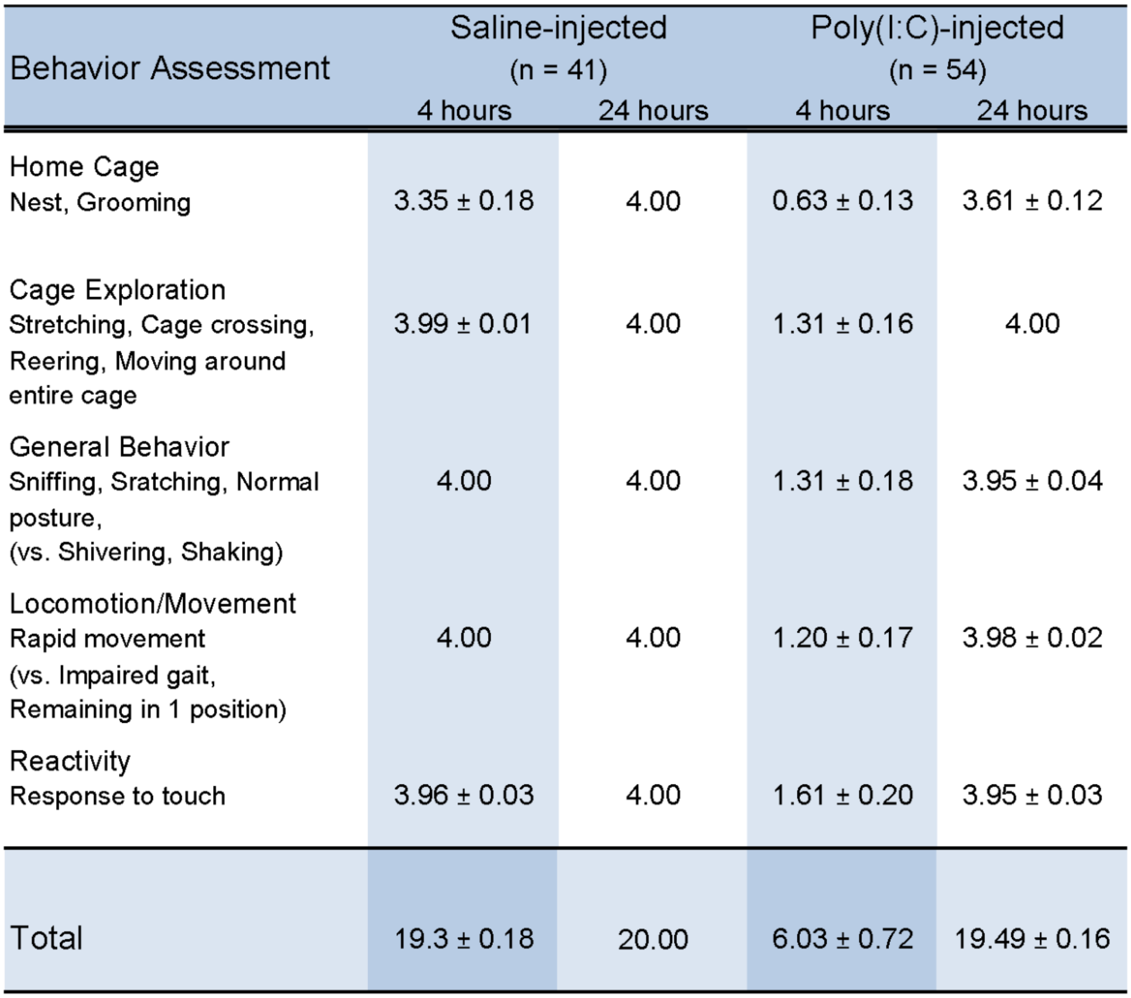

Behavior Assessment	Saline-injected (n = 41)		Poly(I:C)-injected (n = 54)	
	4 hours	24 hours	4 hours	24 hours
Home Cage Nest, Grooming	3.35 ± 0.18	4.00	0.63 ± 0.13	3.61 ± 0.12
Cage Exploration Stretching, Cage crossing, Reering, Moving around entire cage	3.99 ± 0.01	4.00	1.31 ± 0.16	4.00
General Behavior Sniffing, Sratching, Normal posture, (vs. Shivering, Shaking)	4.00	4.00	1.31 ± 0.18	3.95 ± 0.04
Locomotion/Movement Rapid movement (vs. Impaired gait, Remaining in 1 position)	4.00	4.00	1.20 ± 0.17	3.98 ± 0.02
Reactivity Response to touch	3.96 ± 0.03	4.00	1.61 ± 0.20	3.95 ± 0.03
Total	19.3 ± 0.18	20.00	6.03 ± 0.72	19.49 ± 0.16

Table 4. Crown to rump lengths. Embryos of both saline-injected (control) and poly(I:C)-injected mice were measured at the time of dissection. The average length was determined for each litter and the litter averages considered as an n of 1. The values reported here represent the average of litter averages ± SEM. Data were compared using a student's t-test. No significant difference in crown to rump lengths was found between embryos of poly(I:C)-treated females and controls at equivalent days of gestation.

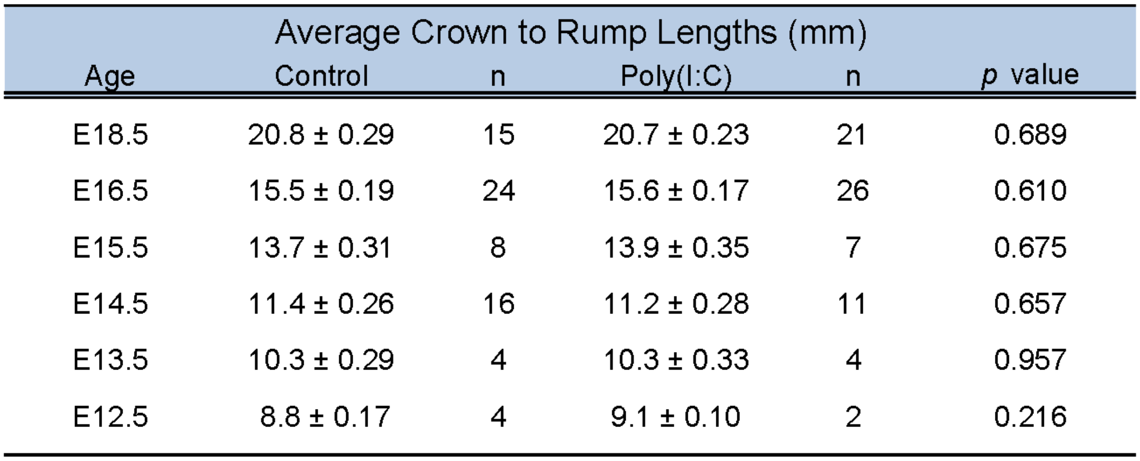

	Average Crown to Rump Lengths (mm)				
Age	Control	n	Poly(I:C)	n	*p* value
E18.5	20.8 ± 0.29	15	20.7 ± 0.23	21	0.689
E16.5	15.5 ± 0.19	24	15.6 ± 0.17	26	0.610
E15.5	13.7 ± 0.31	8	13.9 ± 0.35	7	0.675
E14.5	11.4 ± 0.26	16	11.2 ± 0.28	11	0.657
E13.5	10.3 ± 0.29	4	10.3 ± 0.33	4	0.957
E12.5	8.8 ± 0.17	4	9.1 ± 0.10	2	0.216

Tables 5A and 5B. Summary of cytokines and chemokines in E16.5 fetal brain CD11b$^+$ (microglial) and CD11b$^-$ fractions. Pregnant wild type and IL-6 KO mice were injected at E12.5 with poly(I:C) (20 mg/kg) or sterile saline (control). Fetal brains from an entire litter were collected at E16.5 and single cell suspensions were prepared using 0.05% trypsin and a Gentle MACS® dissociator. An enriched population of CD11b$^+$ (i.e., microglial) cells was obtained using magnetic beads and the autoMACS® cell sorter. CD11b- fractions were retained and assayed as well. Lysates were assayed for protein expression using a Luminex® 32-plex mouse cytokine/chemokine assay. Cells were separated on 3 different occasions from 12 separate litters (1 litter from each of the treatment groups for each assay). The Luminex® 32-plex assay was conducted 3 times. Samples were run in duplicate in each assay. Data was normalized to the amount of protein for each sample and raw data is expressed as pg/mg protein. For comparison across assays, these numbers were log transformed and the difference between logs was assessed using a single-sample one-tailed t-test. Raw data, log-transformed data, differences between logs and p values for all cytokines and chemokines are reported in Supplementary Tables 3A-10B in the Appendix. The panel of cytokines/chemokines included cytokines: Interleukin- 1α (IL-1α), IL-1β, IL-2, IL-3, IL-4, IL-5, IL-6, IL-7, IL-9, IL-10, IL-12 p40, IL-12 p70, IL-13, IL-15, IL-17, IFNγ, TNFα, LIF, G-CSF, GM-CSF, M-CSF, VEGF and chemokines: Eotaxin, IP-10, KC, LIX, MCP-1, MIG, MIP-1α, MIP-1β, MIP-2 and RANTES. Cytokines not listed in the tables were below detectable limits in all of the samples. Abbreviations for chemokines are found in the List of Abbreviations**.** nd = not detected, blank = not determined.

Table 5A. Wild type fetal microglia produce elevated pro-inflammatory cytokines and chemokines following maternal immune challenge.

Table 5B CD11b- fractions from control IL-6 KO fetal brains have increased levels of pro-inflammatory molecules as compared with WT controls.

Table 5A. Comparison of cytokine/chemokine levels in CD11b$^+$ control and poly(I:C) treatment groups from wild type and IL-6 KO mice.

CD11b$^+$ Enriched Microglial Fractions							
WT Control vs WT Poly(I:C)		IL-6 KO Control vs IL-6 KO Poly(I:C)		WT Control vs IL-6 KO Control		WT Poly(I:C) vs IL-6 KO Poly(I:C)	
Cytokine	*p* value	Cytokine	*p* value	Cytokine	*p* value	Cytokine	*p* value
↑ GM-CSF	0.030	↓ IL-10	0.034			↓ IL-15	0.038
↑ IL-1α	0.038						
↑ IL-4	0.040						
↑ IL-9	0.035						
↑ M-CSF	0.038						
Chemokine	*p* value	Chemokine	*p* value	Chemokine	*p* value	Chemokine	*p* value
↑ MIP-1β (CCL4)	0.004						
↑ RANTES (CCL5)	0.012						
↑ Eotaxin (CCL11)	0.044						
↑ LIX (CXCL5)	0.011						

Table 5B. Comparison of cytokine/chemokine levels in CD11b$^-$ control and treatment groups from wild type and IL-6 KO mice.

CD11b$^-$ Fractions							
WT Control vs WT Poly(I:C)		IL-6 KO Control vs IL-6 KO Poly(I:C)		WT Control vs IL-6 KO Control		WT Poly(I:C) vs IL-6 KO Poly(I:C)	
Cytokine	*p* value	Cytokine	*p* value	Cytokine	*p* value	Cytokine	*p* value
↓ IL-10	0.032			↑ IFNγ	0.043		
				↑ IL-9	0.016		
				↑ IL-10	0.033		
				↑ IL-12 p70	0.038		
				↑ IL-13	0.034		
Chemokine	*p* value	Chemokine	*p* value	Chemokine	*p* value	Chemokine	*p* value
↓ MCP-1 (CCL2)	0.003	↓ MIP-2 (CXCL2)	0.018	↑ MCP-1 (CCL2)	0.039		
				↑ MIP-1α (CCL3)	0.041		
				↑ MIG (CXCL9)	0.026		
				↑ RANTES (CCL5)	0.037		

IX. Figures

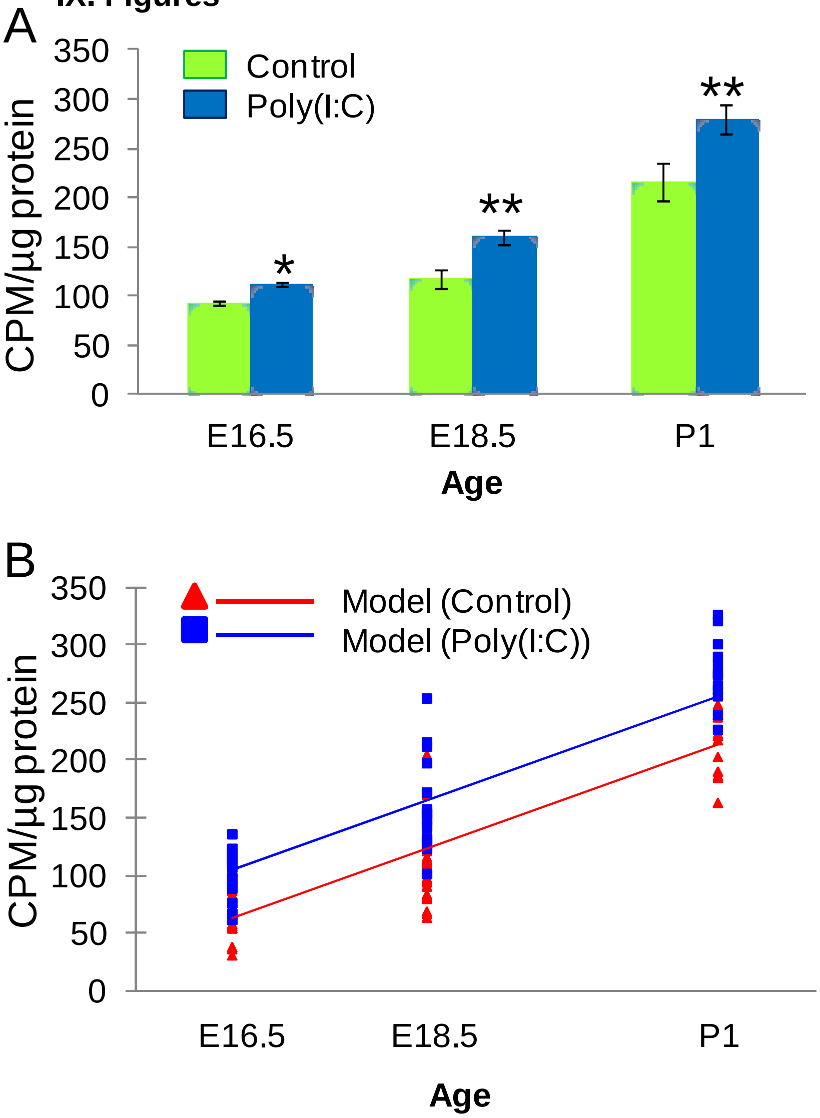

Figure 1. ChAT activity in the fetal basal forebrain increases following maternal poly(I:C) injection. Protein was extracted from E16.5, E18.5 and P1 basal forebrain (BF)s of offspring of saline-injected and poly(I:C)-injected mice, and the synthesis of ^{14}C-acetylcholine from ^{14}C-acetyl-CoA quantified. Counts were normalized to the amount of protein in each sample and data are expressed as CPM/µg protein. A) CPM/µg protein for all BFs from each litter were averaged and considered as an n of 1. Data were compared for significance using a two-way ANOVA with a post hoc Tukey test ($p < 0.001$, n=4; *p<0.05, **p<0.01). B) Individual BF samples were considered as an n of 1. An analysis of covariance (ANCOVA) with post hoc Tukey test was performed comparing ChAT activity between treatment groups while taking into account the effect due to time. The models indicate that poly(I:C) BF samples have significantly higher ChAT activity than controls over this time period ($p < 0.0001$, control: n=69, poly(I:C): n=61; $R^2 = 0.777$ for regression of CPM/µg protein by time).

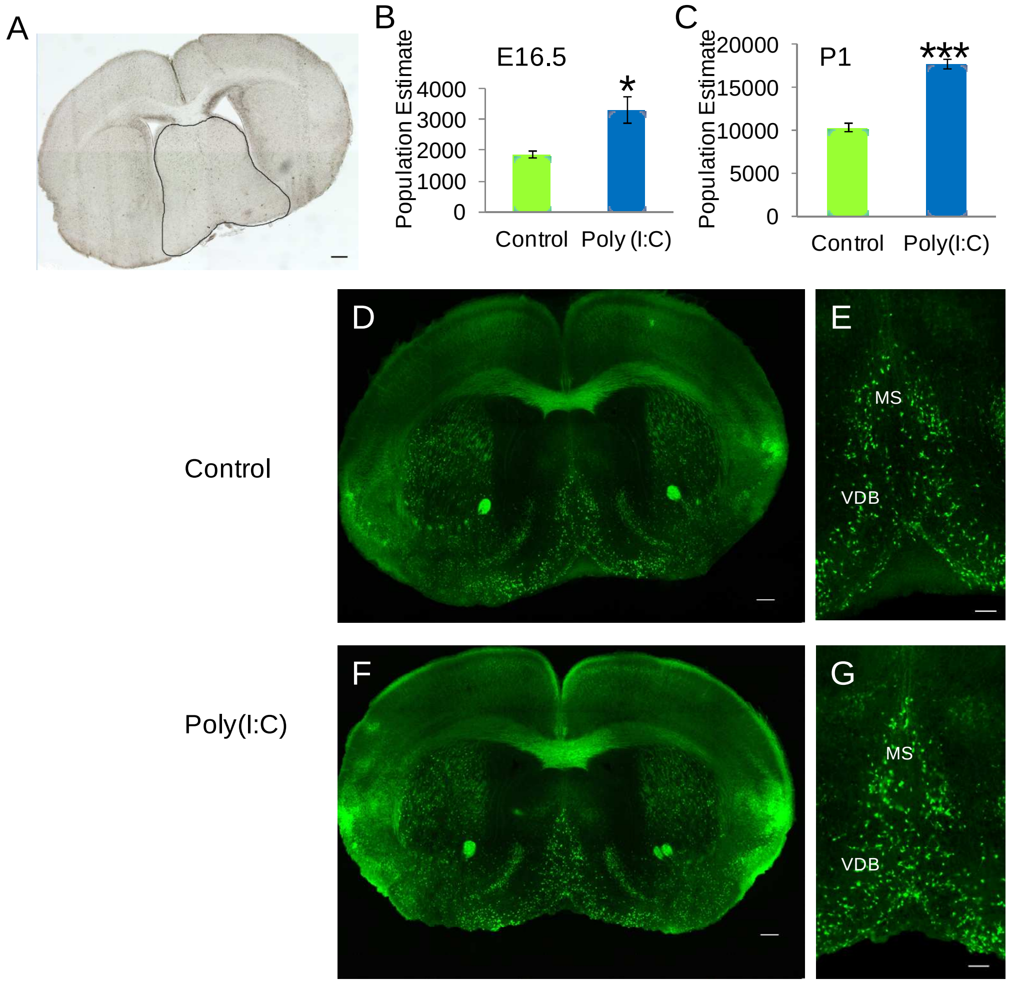
A
B
E16.5
Population Estimate
4000
3000
2000
1000
0
*
Control
Poly (I:C)
C
P1
Population Estimate
20000
15000
10000
5000
0
***
Control
Poly(I:C)
D
E
MS
VDB
Control
F
G
MS
VDB
Poly(I:C)

Figure 2. The number of cholinergic neurons in the fetal basal forebrain increases following maternal immune activation. Coronal sections (60 μm) of brains from the E16.5 and P1 offspring of saline-injected and poly(I:C)-injected transgenic ChAT-EGFP mice were prepared for fluorescence microscopy (see *Materials and Methods*). Stereo Investigator® software was used to randomly and systematically sample sections and estimate the cholinergic population size. (A) P1 coronal section with region outlined indicating the area in which ChAT+ cells were counted. Data in (B) and C) are expressed as a population estimate and compared using a Student's t-test. Estimates from brains of a single litter were averaged and considered as an n of 1. (B) Sections from a 600 μm portion of E16.5 BFs were sampled. Control average population estimate1,869 ± 111; E16.5 poly(I:C) estimate 3,336 ± 451 (**p*=0.034, n=3). (C) Sections from a 720 μm portion of P1 BFs were sampled. Control estimate 10,354 ± 497; poly(I:C) estimate 17,770 ± 616 (****p*< 0.001, n=4). (D-G) Micrographs showing ChAT-EGFP expression in Pl coronal sections (D, F) and in a portion of the basal forebrain (E, G). Micrographs are from control (D, E) and poly(I:C) (F,G) treatment groups. (A, D, F) scale bar=250 μm. (E,G) scale bar=100 μm. MS=medial septum, VDB=vertical diagonal band.

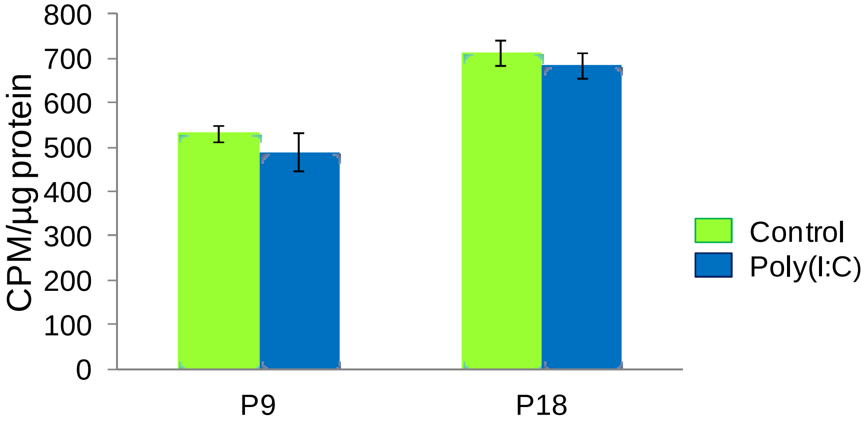

Figure 3. The effect of maternal immune activation on BF ChAT activity is transient. Protein was extracted from wild type P9 and P18 basal forebrains (BFs) of offspring of saline-injected (Control) and poly(I:C)-injected mice, and the synthesis of ^{14}C-acetylcholine from ^{14}C-acetyl-CoA quantified. Counts were normalized to the amount of protein in each sample and data were expressed as CPM/µg protein. BFs from each litter were averaged and considered an n of 1. Data were compared for significance using a two-way ANOVA (*p*=0.916 for difference due to treatment, n=4 for each treatment). Control P9: 532 ± 19; Poly(I:C) P9: 490 ± 45; Control P18: 713 ± 29; Poly(I:C) P18: 683 ± 28.

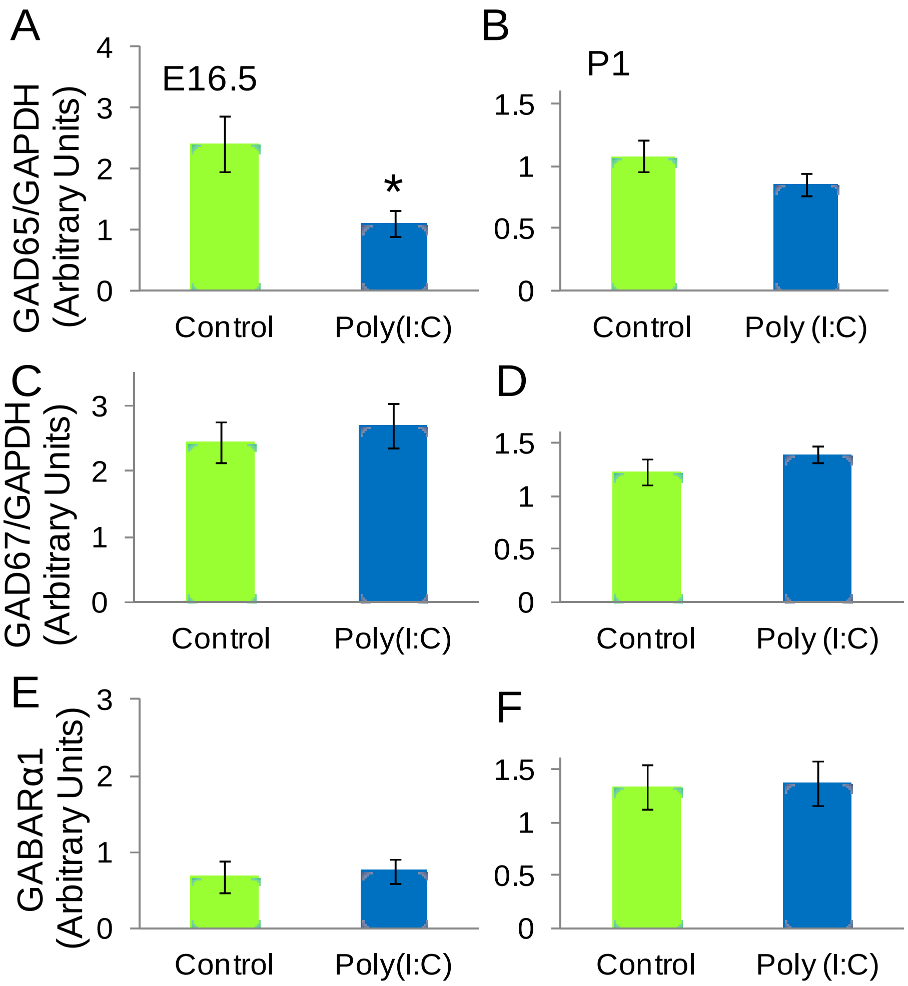

Figure 4. GAD65 mRNA decreases in the E16.5 fetal basal forebrain following poly(I:C) injection. RNA was extracted from the basal forebrains (BFs) of E16.5 (A,C,E) and P1 (B,D,F) offspring of saline and poly(I:C)-injected mice, reverse transcribed and real time PCR (RT-PCR) performed to quantify message levels of GAD65 (A,B), GAD67 (C,D) and the α-subunit 1 of the GABA receptor (GABARα1) (E,F). Expression levels of these molecules were normalized to GAPDH levels and ratios are expressed as arbitrary units. Data were compared using a Student's t-test. (A) Message levels for GAD65 were significantly lower in the E16.5 fetal BF following maternal poly(I:C) injection, *p=0.031, n=5 for each group. (C and E) n=5; (B,D,F) n=3. Average for each litter is considered as an n of 1. GAD=glutamic acid decarboxylase, GABA=gamma-aminobutyric acid.

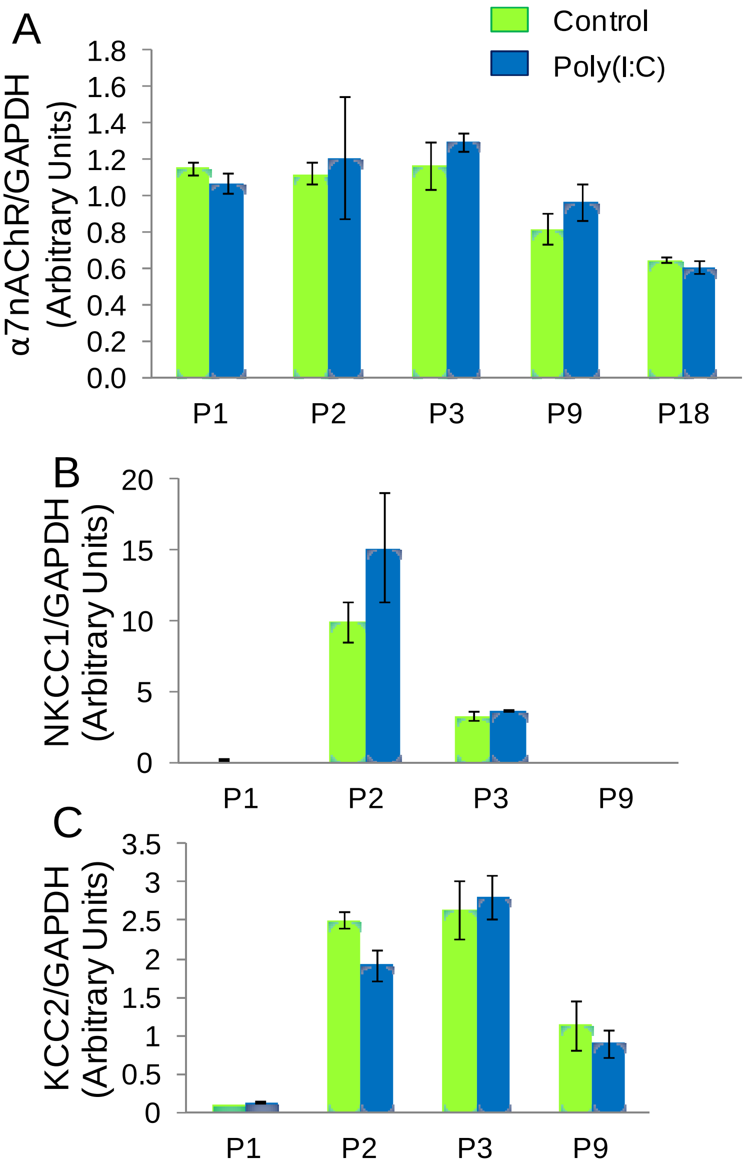

Figure 5. α7nAChR, NKCC1 and KCC2 mRNA levels in the postnatal hippocampus following maternal immune activation. RNA was extracted from hippocampi of P1, P2,P3 ,P9 and P18 pups born to saline- or poly(I:C)-injected mice. RT-PCR data was normalized to GAPDH levels and the ratio expressed as arbitrary units. Data were compared for significance with a two-way ANOVA. (A) α7n AChR is expressed in the perinatal hippocampus throughout early postnatal development and similarly in both groups (p = 0.544); NKCC1 (B) and KCC2 (C) are also present at similar levels in both groups. (B) NKCC1 (p=0.221) (C) KCC2 (p=0.167) (n=3 for P1, P2, P3; n=4 for P9 and P18). The average for each litter is considered as an n of 1. α7n AChR=α7 subunit nicotinic acetylcholine receptor; NKCC1= sodium-potassium chloride co-transporter; KCC2=potassium chloride co-transporter.

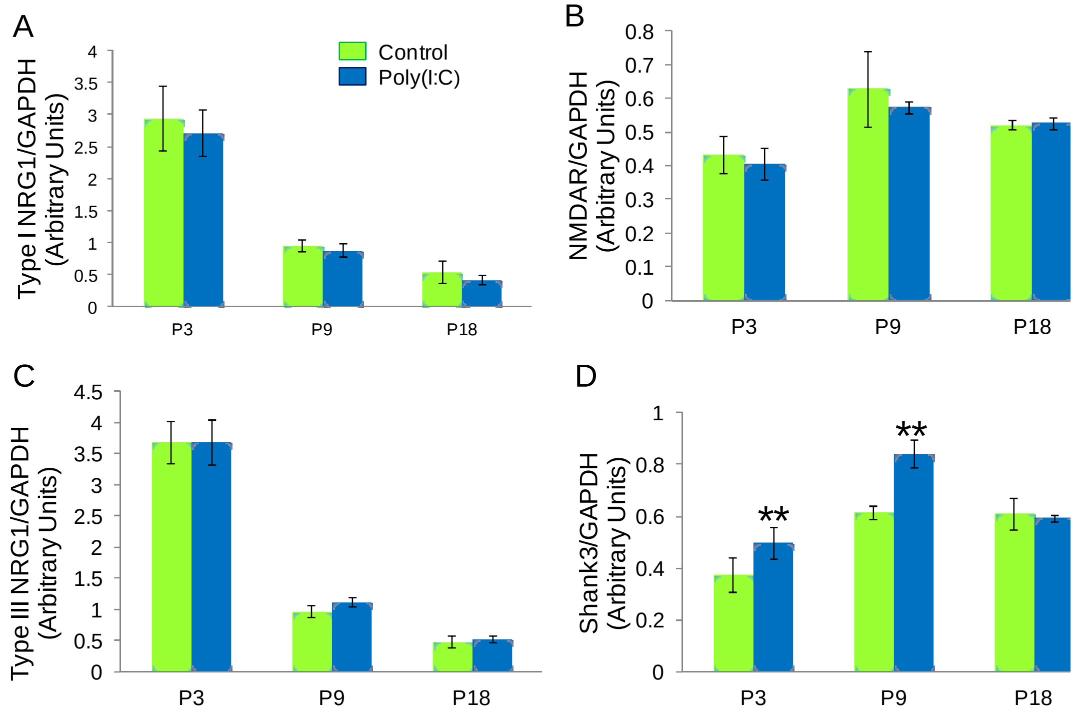

Figure 6. mRNA expression of NRG1, NMDAR and Shank 3 in the postnatal hippocampus following maternal poly(I:C) injection. RNA was extracted from hippocampi of P3, P9 and P18 pups born to saline- or poly(I:C)-injected mice. RT-PCR data was normalized to GAPDH levels and the ratio expressed as arbitrary units. Data are compared using a two-way ANOVA and post hoc Tukey test. No significant difference is found in mRNA expression between control and poly(I:C) groups for (A) type 1 NRG1 (*p*=0.508), (B) NMDAR (*p*=0.521) nor (C) type III NRG1 (*p*=0.627). N=4 for P9 and P18 poly(I:C) samples; n=3 for all others. The average for each litter is considered as an n of 1. (D) mRNA levels for Shank3 are higher in poly(I:C) samples than in controls at P3 (control: 0.374 ± 0.066; poly(I:C): 0.498 ± 0.061) and P9 (control: 0.615 ± 0.023; poly(I:C): 0.843 ± 0.053). N=4 for P9 and P18 poly(I:C) samples, n=3 for all others. ***p*< 0.01, indicates a difference between poly(I:C) and control. NRG1=neuregulin1; NMDAR=NR1 subunit of the NMDA receptor; Shank3=SH3 and multiple ANKyrin repeat domains 3.

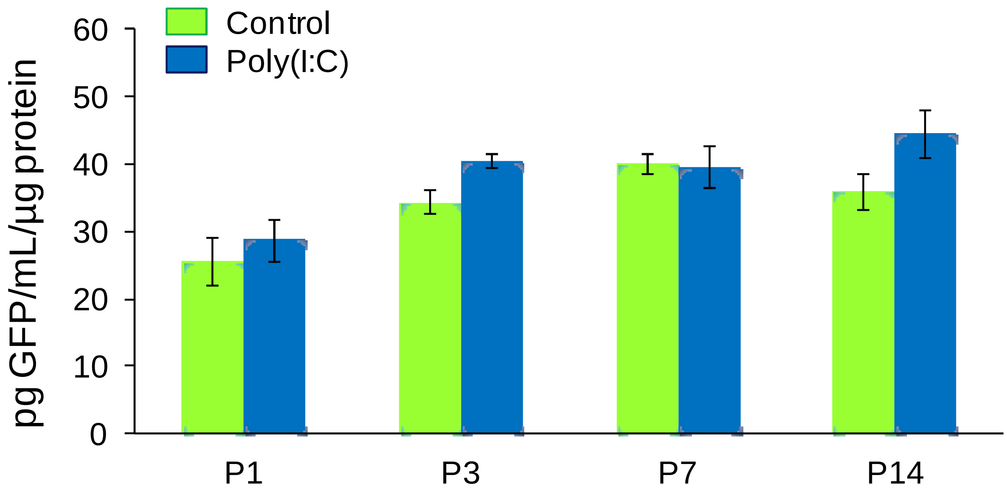

Figure 7. Postnatal ChAT protein expression in the hippocampus of offspring following maternal poly(I:C). Protein was extracted from the hippocampi of P1, P3, P7 and P14 pups of saline and poly(I:C)-injected ChAT-GFP transgenic mice. 70 µg protein was assayed using a GFP ELISA (see *Materials and Methods*) and the amount of GFP protein quantified as an indicator of ChAT protein quantity. Data are expressed as pg/ml GFP per µg protein. Data were analyzed using a two-way ANOVA. *p*=0.066 for treatment effect, n=3 per group. The average for each litter is considered as an n of 1.

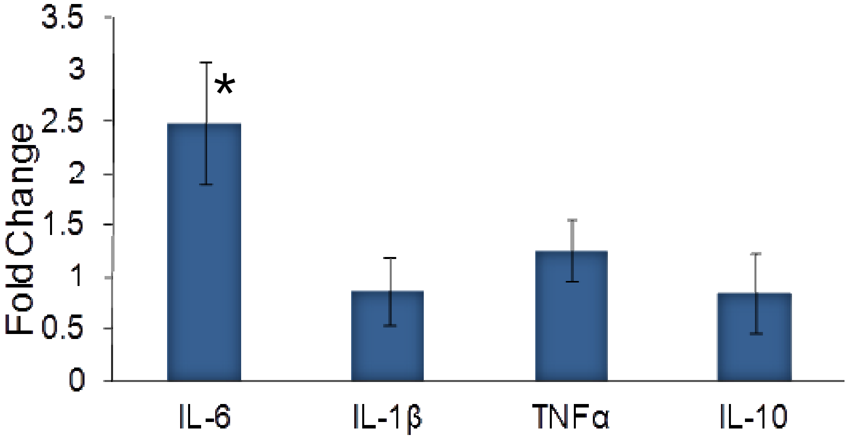

Figure 8. Fetal microglia produce increased levels of IL-6 mRNA following maternal immune challenge. Pregnant mice were injected at E12.5 with poly(I:C) (20 mg/kg) or sterile saline (control) and fetal brains from an entire litter were collected at E16.5. These were minced, trypsinized and dissociated using the Gentle MACS® cell dissociator. An enriched population of $CD11b^+$ (i.e., microglial) cells was obtained using magnetic beads and the autoMACS® cell sorter. RNA was extracted, reverse transcribed and real time PCR (RT-PCR) performed to determine message levels for cytokines. These levels were normalized to GAPDH levels and data are expressed as the fold change (poly[I:C]-treated over control) for each cytokine. Data for each cytokine were compared for significance using a single sample one-tailed t-test. Message levels for IL-6 were significantly higher in poly(I:C)-treated samples than in controls (**p*=0.044, n=4). Others showed no change over control levels. IL-1β fold change 0.86 (*p*=0.655, n= 6); TNFα fold change 1.25 (*p*=0.211, n=7); IL-10 fold change 0.85 (*p*=0.346, n=9).

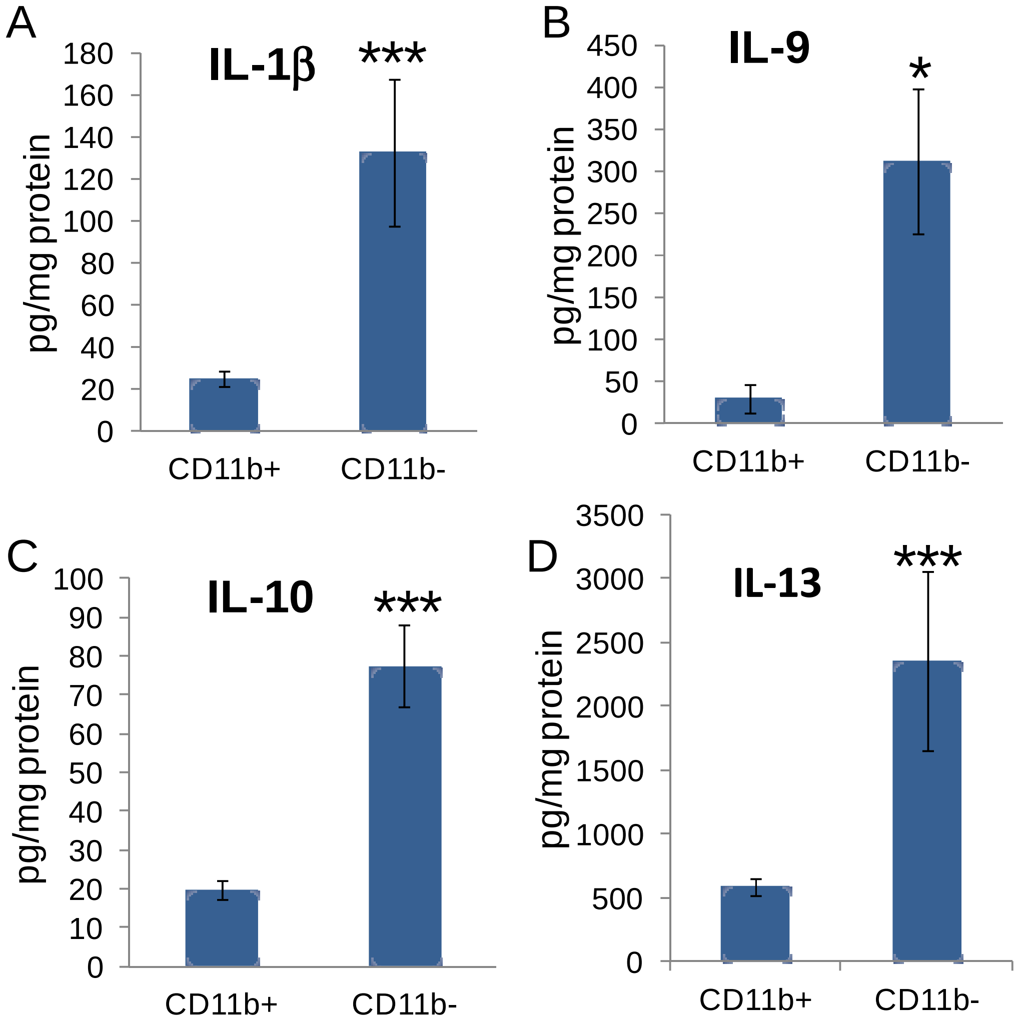

Figure 9. Non-microglial cells produce cytokines. Pregnant wild-type mice were injected at E12.5 with poly(I:C) (20 mg/kg) or sterile saline (CT) and fetal brains from an entire litter were collected at E16.5. After separation with αCD11b beads, protein was extracted from both the enriched population of CD11b$^+$ (i.e., microglial cells) and the CD11b$^-$ (i.e., all other fetal brain cells). Cells were isolated on 3 different occasions from 6 separate litters. The Luminex® 32-plex assay was conducted 3 times. Data here from microglial fractions and those from non-microglial fractions were pooled disregarding poly(I:C) or saline treatment. The data are expressed as pg/mg protein and were compared for significance using a Student's t-test. (A) IL-1β, ***p=0.001, n=6 per group; (B) IL-9, *p=0.047, n=6; (C) IL-10, ***p=0.0009, n=6; (D) IL-13, ***p=0.004, n=6.

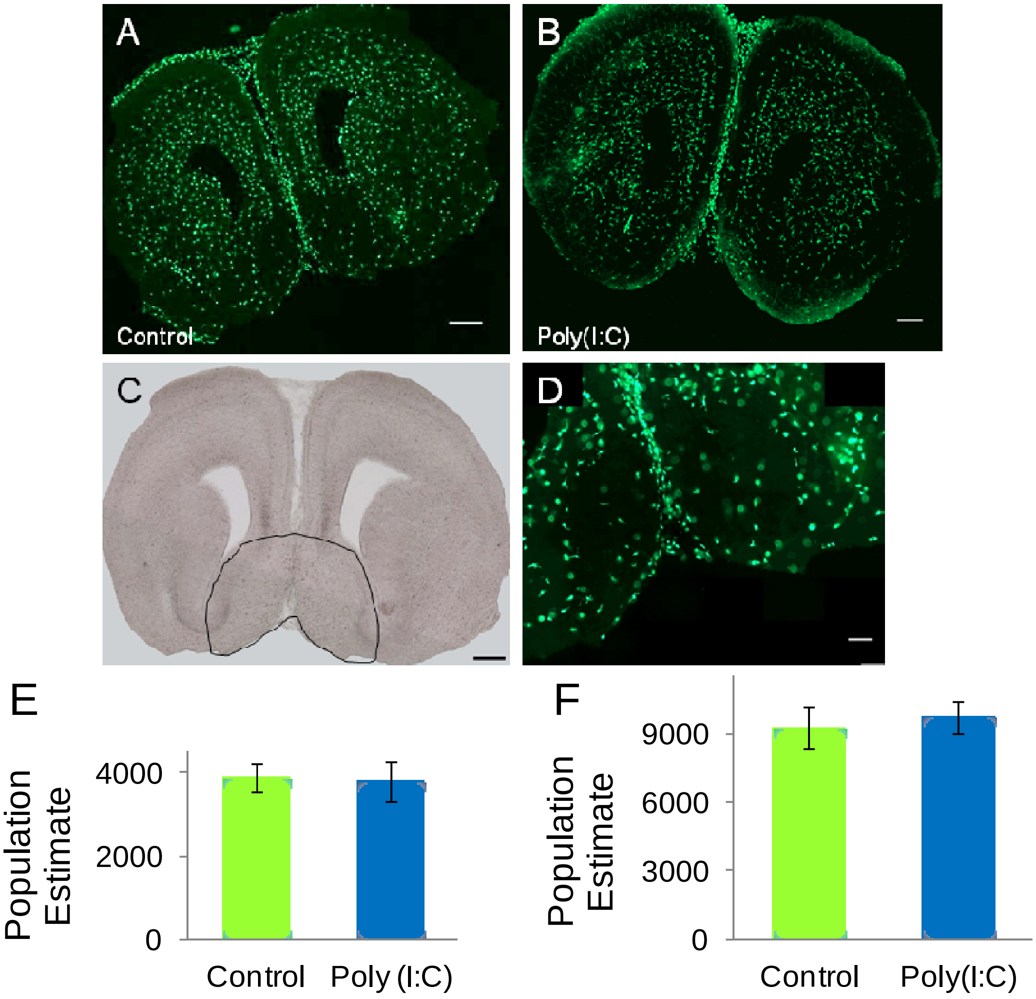

Figure 10. The number of microglia in the fetal basal forebrain does not change following maternal immune activation. Coronal sections (60 µm) of brains from the E16.5 and P1 offspring of saline-injected and poly(I:C)-injected transgenic CX3CR1-EGFP mice were prepared for fluorescence microscopy (see *Materials and Methods*). Stereo Investigator® software was used to randomly and systematically sample sections and estimate the microglial population size of a 600 µm portion of the E16.5 basal forebrain (BF) and a 720 µm portion of the P1 BF. (A and B) Micrographs showing microglia in E16.5 coronal brain sections from control (A) and poly(I:C) (B) embryos. (C) E16.5 coronal section with region outlined indicating the area in which microglia were counted. (D) Micrograph showing microglia in the BF of an E16.5 coronal section. (E and F) Stereological estimates of microglial population size in E16.5 (E) and P1 (F) BFs of control and poly(I:C)-treatment groups. Data are expressed as a population estimate and compared using a Student's t-test. Estimates from all brains of a single litter were averaged and considered as an n of 1. (E) E16.5 control population estimate: 3,888 ± 353; E16.5 poly(I:C) estimate: 3,800 ± 479 (p= 0.884, control n=5, poly(I:C) n= 4). (F) P1 control estimate 9,156 ± 933; P1 poly(I:C) estimate 9,381 ± 719 (p= 0.858, n=3). (A-C) scale bar = 250 µm. (D) scale bar = 100 µm.

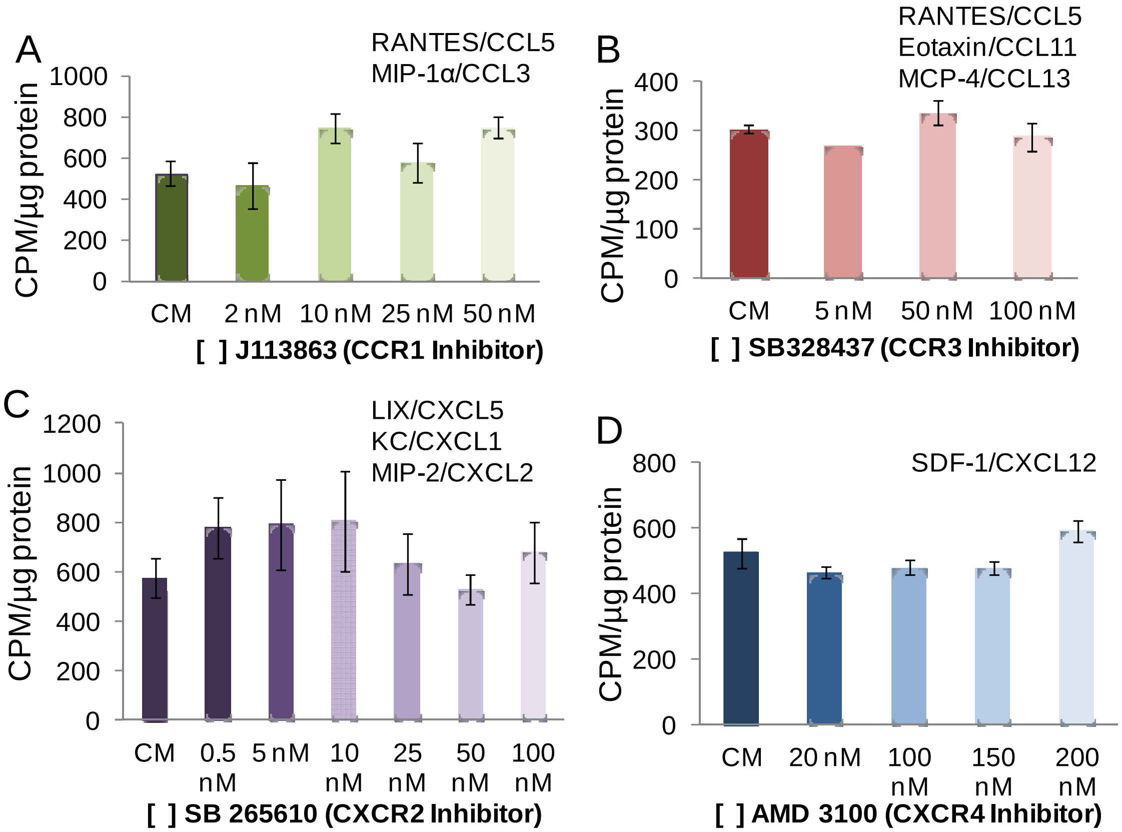

Figure 11. Inhibition of chemokine receptors CCR1, CCR3, CXCR2 and CXCR4 does not reduce ChAT activity in basal forebrain cultures. E15 rat BF cells were cultured in microglial conditioned medium with or without chemokine receptor inhibitor. After 5 days a ChAT assay was performed and the amount of ^{14}C produced was measured. Results are expressed as CPM/µg protein. Data were analyzed for significance with an ANOVA (A) CCR1 inhibitor, *p*=0.100, n=3 per treatment; (B) CCR3 inhibitor, *p*=0.260, n=3; (C) CXCR2 inhibitor, *p*=0.621, n=3; and (D) CXCR4 inhibitor, *p*=0.078, n=3. Ligands for receptors are indicated above each graph. RANTES=Regulated And Normal T cell Expressed and Secreted; MIP-1α=Macrophage inflammatory protein 1 alpha; Eotaxin=eosinophil chemoattractant cytokine; MCP-4=Monocyte Chemo-attractant Protein4; LIX=Epithelial-derived Neutrophil-Activating peptide 78 (ENA-78); KC=Keratinocyte-derived Chemokine; MIP-2=Macrophage Inflammatory Protein 2; SDF-1=Stromal-Derived Factor 1.

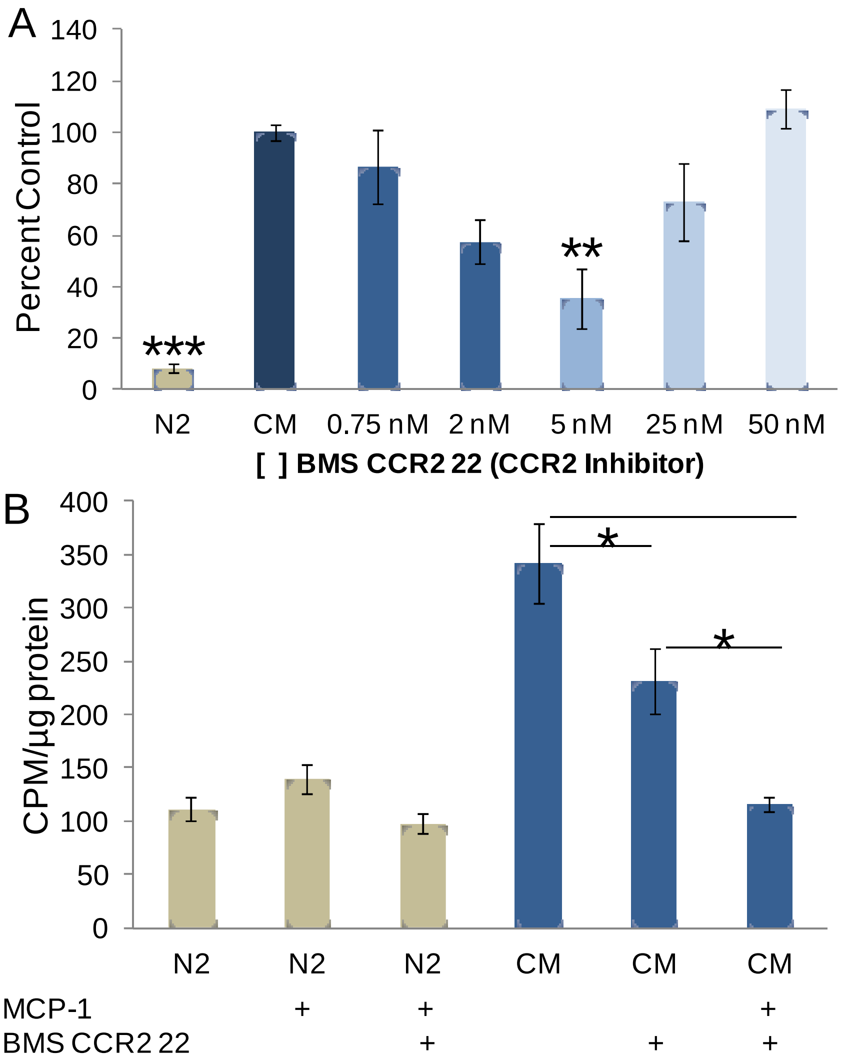

Figure 12. Inhibition of chemokine receptor CCR2 and addition of exogenous MCP-1. (A) E15 rat BF cells were cultured in microglial conditioned medium (CM) with or without the CCR2 inhibitor BMS CCR2 22 at increasing concentrations. After 5 days a ChAT assay was performed and the amount of ^{14}C produced was measured. Results are compiled from 2 independent experiments and the data in CPM/µg protein are expressed as percent control (percent of average CM). Data were analyzed for significance with an ANOVA and post-hoc Tukey test. n≥ 3 per treatment; **p< 0.01, ***p< 0.001 when compared to CM alone. (B) E15 rat BF cells were cultured in CM or N2 with or without BMS CCR2 22 (5 nM) MCP-1 (20 ng/ml) and assayed for ChAT activity after 3 days. Results are from one representative experiment of 2. Data are expressed as CPM/µg protein and were analyzed for significance with an ANOVA and post hoc Tukey test. n=3 per treatment. *p<0.05, ***p< 0.001. All N2 groups were significantly different from CM (p< 0.001). There was no significant difference between N2 groups with or without CCR2 inhibitor or MCP-1.

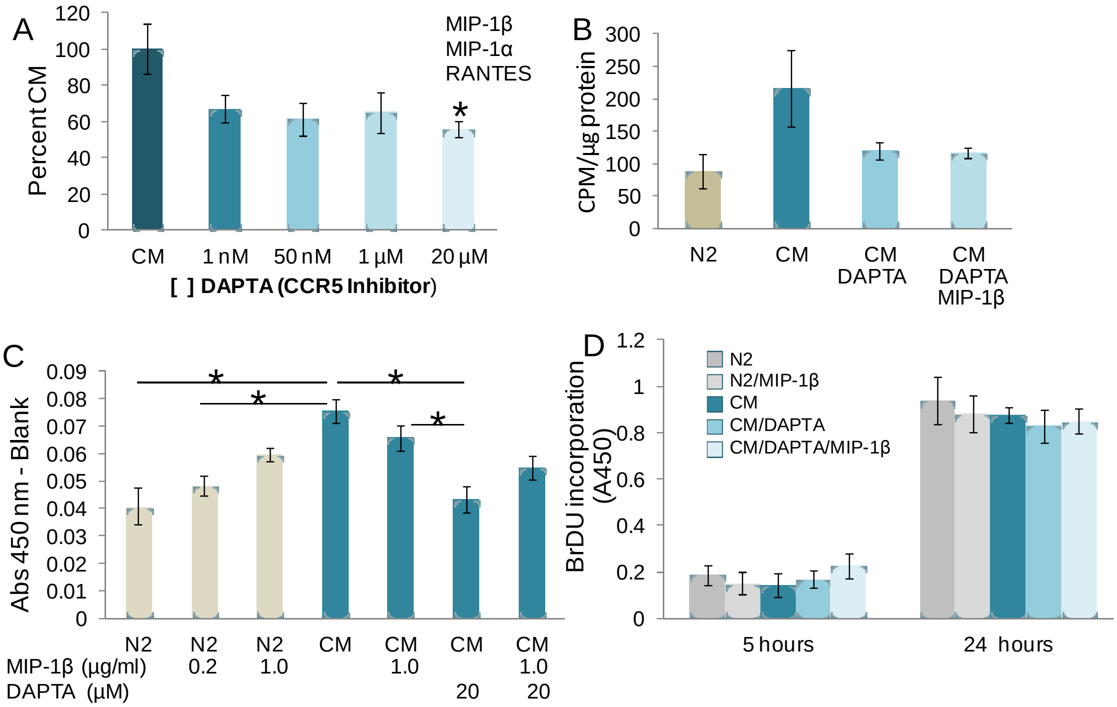

Figure 13. Inhibition of CCR5 results in decreased ChAT activity and reduction of cell number in E15 rat basal forebrain cultures. ChAT activity decreases with inhibition of CCR5. E15 rat BF cells were cultured in N2 or microglial conditioned medium (CM) with or without DAPTA (CCR5 inhibitor). After 3 days a ChAT assay was performed and the amount of ^{14}C produced was measured. (A) ChAT activity is reduced with 20 µM DAPTA. Data were compiled from 4 independent experiments and expressed as the percent of CM. Data were analyzed for significance with an ANOVA and post hoc Tukey test. P=0.02, compared to CM alone. CM, n=12; 1.0 nM n=9; 50 nM, n=5; 1.0 µM n=8; and 20 µM, n=11; *p<0.05. (B) MIP-1β (200 ng/ml) was added to BF cells along with DAPTA. MIP-1β does not reverse the decrease in ChAT activity due to DAPTA inhibition of CCR5. Data are expressed as CPM/µg protein and were compared using an ANOVA. P=0.112. (C) E15 rat BF cells were seeded at 25,000 cells per well in 96 well plates in N2 or CM with or without DAPTA (20 µM) and/or MIP-1β (200 ng/ml or 1 µg/ml). After 2 days 20 µl CellTiter96® Aqueous One Solution was added to each well. Living cells convert this MTS tetrazolium reagent to a colored formazan product. Quantification by absorbance at 450 nm is directly proportional to the number of living cells. Data are expressed as Absorbance at 450 nm – blank. Data were analyzed for significance with an ANOVA and post-hoc Tukey test. p<0.001, n≥ 3; *p< 0.05. (D) E15 rat BF cells were seeded in 96 well plates at 70,000 cells/well in N2 or CM with or without DAPTA (20 µM) and/or MIP-1β (1 µg/ml) and BrDU labeling medium. After 5 and 24 hours cells were washed, fixed and BrDU incorporation assessed using a colorimetric system with an HRP-linked αBrDU antibody and TMB substrate. Data are expressed in units of absorbance at 450 nm and are compared with an ANOVA. 5 hours: p=0.727, n=7; 24 hours: p=0.391, n=8. Abs=Absorbance.

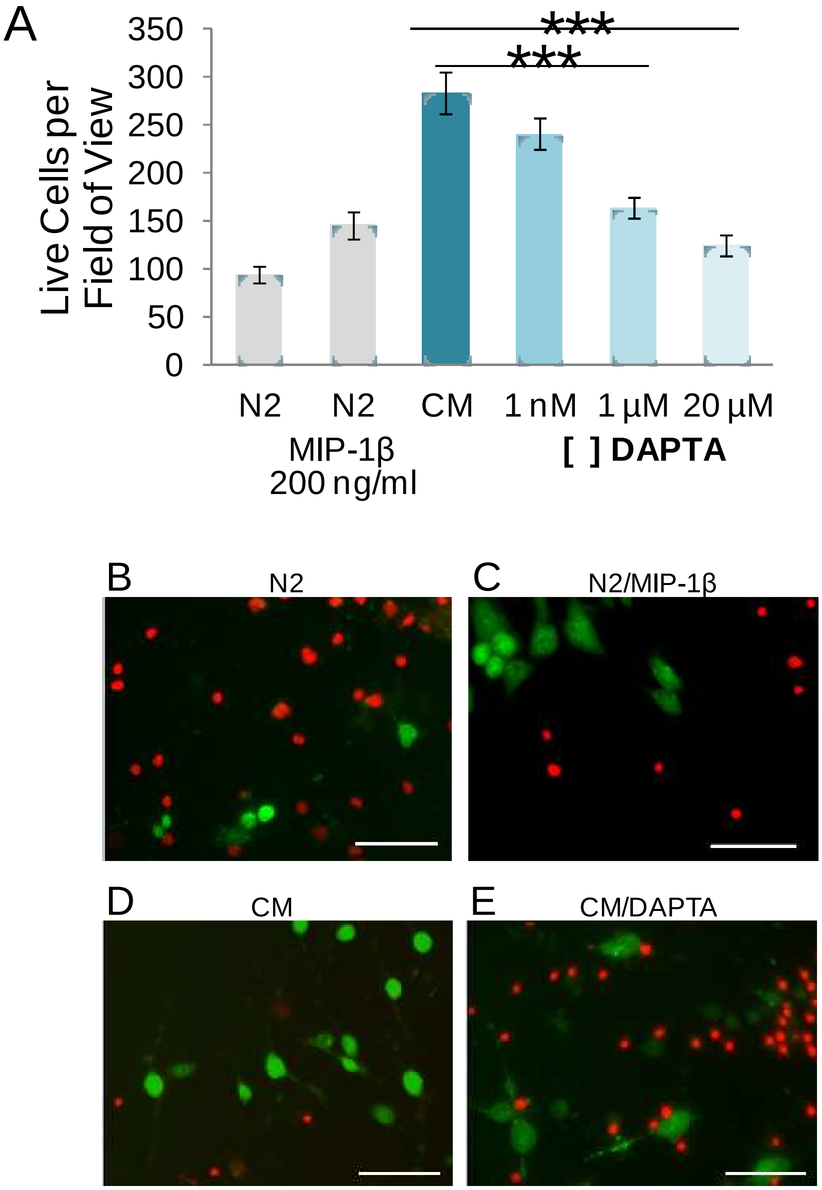

Figure 14. Inhibition of CCR5 reduces cell survival. (A) BF Cells were cultured on glass coverslips in 35mm petri dishes in N2 or conditioned medium (CM) with or without DAPTA or MIP-1β (200 ng/ml). After 2 days they were incubated with Live/Dead® assay reagents for 30 min. and mounted on slides. Ten fields of view at 20x were counted for each treatment using fluorescent microscopy. Data are reported as the number of live cells per field of view and analyzed with an ANOVA and post hoc Tukey test. ***p< 0.001. (B-E) Micrographs of cultured cells with Live/Dead® reagents in N2 (B), N2 with MIP-1β (200 ng/ml) (C), CM (D) and CM with DAPTA (1 µM) (E). scale bar=20 µm.

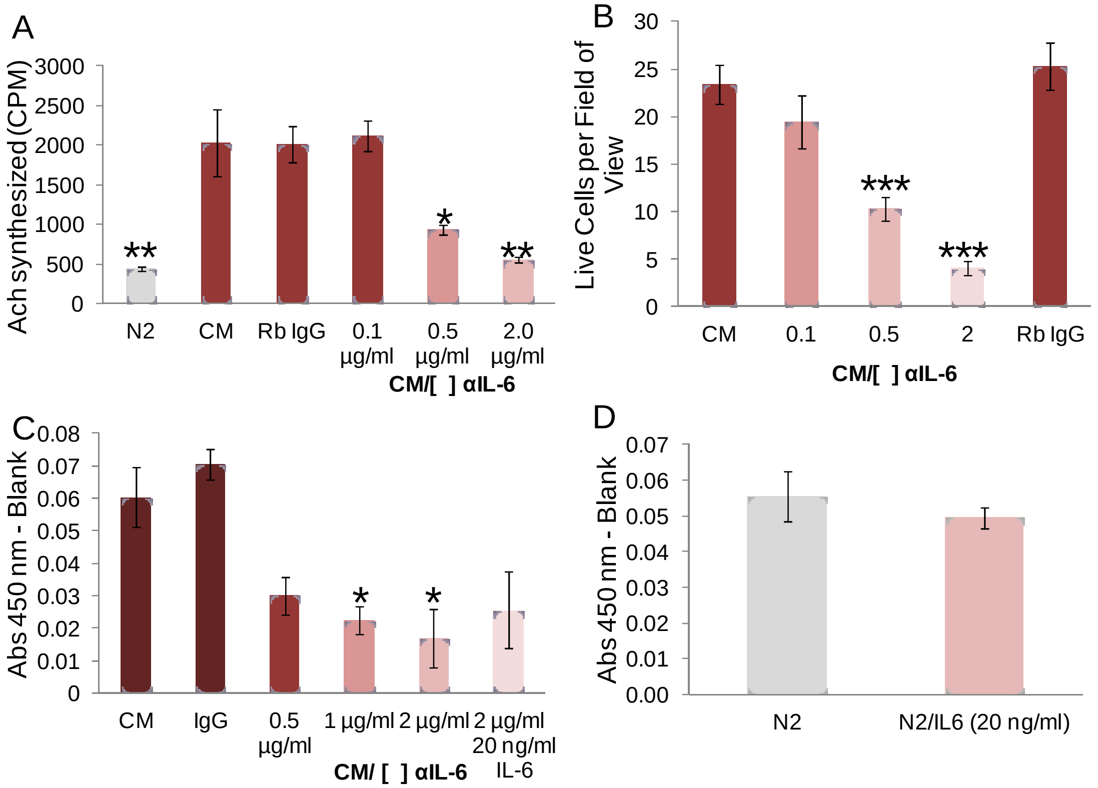

Figure 15. IL-6 is a survival factor for basal forebrain cells in culture. (A) E15 rat basal forebrain (BF) cells were cultured in N2 or conditioned medium (CM) ± with various concentrations of αIL-6 or rabbit IgG (2µg/ml). After 5 days, cultures were harvested and a ChAT assay performed to measure ^{14}C-acetylcholine synthesized. Results are from 1 representative experiment of 4. Data are expressed as CPM and compared using an ANOVA. p< 0.001, n = 3 for each treatment. (B) E15 rat BF cells were cultured in CM on coverslips in 35 mm petri dishes ± various concentrations of αIL-6 or Rb IgG (2µg/ml). After 2 days cells were washed and incubated with Live/Dead reagents® Ethidium homodimer-1 (4 µM) and calcein AM (2 µM) for 30 min. Mounted coverslips were viewed using fluoresence microscopy, and live cells were counted in 10 fields of view at 40x. Results are from 1 representative experiment of 3 and data were compared using an ANOVA. p<0.001, n = 3 for each treatment. (C and D) E15 rat BF cells were seeded at 25,000 cells/well in 96 well plates cultured in CM (C) or N2 (D) ± αIL-6 and/or recombinant rat IL-6 (20 ng/ml) or Rb IgG (2µg/ml). After 2 days CellTiter 96® Aqueous One Solution reagent was added and the cultures incubated for 4 hours at 37℃. The amount of colored formazan product produced was measured by absorbance at 450 nm using a plate reader. The quantity of product is directly proportional to the number of living cells. Data are expressed as the absorbance at 450 nm – Blank. (C) Data were compared using an ANOVA with a post-hoc Tukey test. p= 0.002, n=3 for each treatment. (D) Data were compared using a Student's t-test. *p*= 0.463, n=3. * p< 0.05, ** p<0.01 *** p< 0.001. CPM = counts per minute; Abs = absorbance.

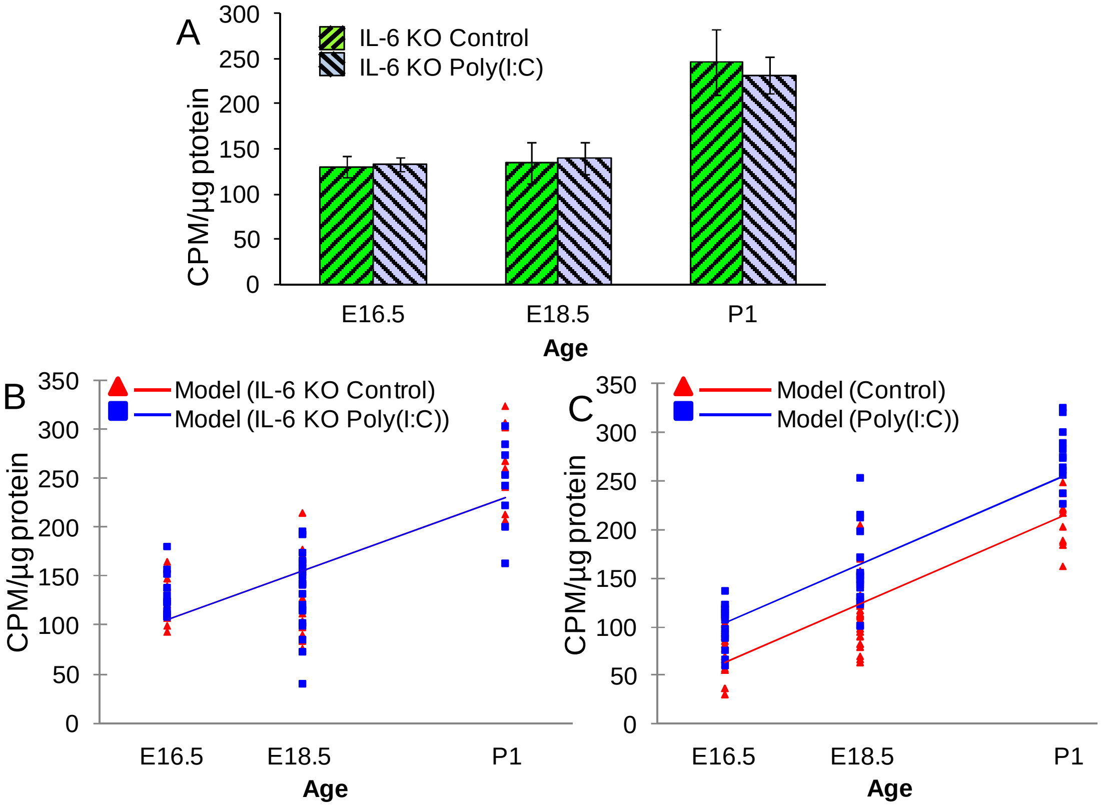

Figure 16. ChAT activity in the IL-6 KO fetal basal forebrain does not change following maternal poly(I:C) injection. Protein was extracted from E16.5, E18.5 and P1 basal forebrains (BFs) of offspring of saline-injected and poly(I:C)-injected IL-6 KO mice. The synthesis of ^{14}C-acetylcholine from ^{14}C-acetyl-CoA in these samples was quantified. Counts were normalized to the amount of protein in each sample and data expressed as CPM/µg protein. A) CPM/µg protein for all BFs from each litter were averaged and considered as an n of 1. Data were compared for significance using a two-way ANOVA and post hoc Tukey test (*p*=0.917, n=2 for each treatment group at E16.5 and P1, n=3 for control at E18.5 and n=4 for poly(I:C) at E18.5. B) Individual IL-6 KO BF samples were considered as an n of 1. An analysis of covariance (ANCOVA) with post hoc Tukey test was performed comparing ChAT activity between treatment groups while taking into account the effect due to time. The model indicates that there is no significant difference in ChAT activity between the poly(I:C) and control groups over this time period. The data from both groups can be represented by a single line (*p*=0.984, control: n=40, poly(I:C): n=43; R^2=0.509 for regression of CPM/µg protein by time). The IL-6 KO data contrasts with (C), the wild type ANCOVA, where the control and poly(I:C) treatment groups are represented by 2 separate lines and the model indicates that WT poly(I:C) BF samples have significantly higher ChAT activity than controls over the entire time period (see Figure 1).

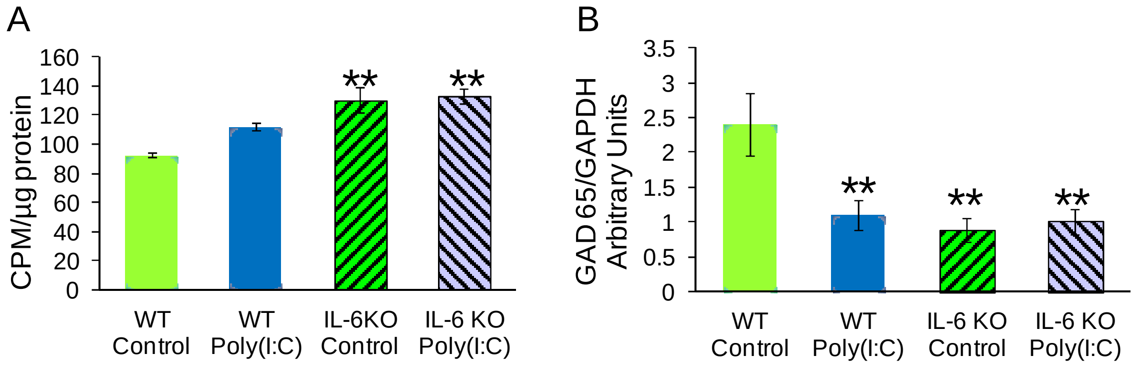

Figure 17. Higher ChAT activity and lower message levels of GAD65 in E16.5 IL-6 KO basal forebrains. (A) Protein was extracted from wild type and IL-6 KO E16.5 basal forebrains (BFs) of embryos of saline-injected and poly(I:C)-injected mice, and the synthesis of ^{14}C-acetylcholine from ^{14}C-acetyl-CoA quantified. Counts were normalized to the amount of protein in each sample and data expressed as CPM/µg protein. BFs from each litter were averaged and considered an n of 1. Data were compared using a two-way ANOVA with poly(I:C) and the absence of IL-6 as the 2 treatment factors. A post hoc Tukey test was used to determine significance. IL-6 KO BF samples produce significantly higher amounts of ^{14}C-acetylcholine than both WT control and WT poly(I:C) samples. There is no significant difference in the amount of ^{14}C-acetylcholine produced due to poly(I:C) treatment within the IL-6 KO group (WT poly(I:C)-treated samples produce significantly higher amounts of ^{14}C-acetylcholine than WT controls; $**p < 0.01$; n= 4 for control groups, n=2 for IL-6 KO groups). (B) RNA was extracted from BFs of E16.5 embryos of saline- or poly(I:C)-injected WT and IL-6 KO mice. RT-PCR data was normalized to GAPDH levels and the ratio expressed as arbitrary units. Data are compared using a two-way ANOVA and post hoc Tukey test. No significant difference is found in mRNA expression between control and poly(I:C) treatments within the IL-6 KO group. IL-6 KO GAD65 message levels are lower than WT controls and are not significantly different from WT poly(I:C) levels ($**p < 0.01$; n=5 for WT and IL-6 KO poly(I:C) samples, n= 3 for IL-6 KO control). Abbreviations: GAD = glutamic acid decarboxylase.

X. List of Abbreviations

AGM	Aorta-gonad-mesonephros region
ASD	Autism Spectrum Disorders
BDNF	Brain derived neurotrophic factor
BF	Basal forebrain
C4B	Complement factor 4B
CCR	C-C chemokine receptor
ChAT	Choline acetyltransferase
CNS	Central nervous system
CNTF	Ciliary neurotrophic factor
CNV	Copy number variation
CT-1	Cardiotrophin-1
CXCR	CXC chemokine receptor
DAP12	DNAX activating protein of 12 kDa
DISC-1	Disrupted in Schizophrenia-1
DRG	Dorsal root ganglia
EGFP	Enhanced green fluorescent protein
EGL	External granule layer
Eotaxin	Eosinophil chemoattractant cytokine (CCL11)
GABA	Gamma-aminobutyric acid
GAD	Glutamic acid decarboxylase
GM-CSF	Granulocyte macrophage-colony stimulating factor

GWA	Genome wide association
HSC	Hematopoietic stem cells
Iba-1	Ionized calcium binding adaptor molecule 1
IFNγ	Interferon gamma
IP-10	Interferon gamma-induced protein 10 (CXCL10)
JAK	Janus kinase
KC	Keratinocyte-derived chemokine (CXCL1, Gro-α)
KCC2	Potassium chloride co-transporter
LIF	Leukemia inhibitory factor
LIX	Epithelial-derived neutrophil-activating peptide 78 (ENA-78)
LPS	Lipopolysaccharide
Mash2	Mammalian achaete scute homolog 2
MCP-1	Monocyte chemotactic protein 1 (CCL2)
M-CSF	Macrophage colony-stimulating factor
MeCP2	Methyl-CpG binding protein
MHC	Major histocompatibility complex
MIA	Maternal immune activation
MIG	Monokine induced by gamma interferon (CXCL9)
MIP-1α	Macrophage inflammatory protein 1 alpha (CCL3)
MIP-1β	Macrophage inflammatory protein 1 beta (CCL4)
MIP-2	Macrophage inflammatory protein 2
nAChR	Nicotinic acetylcholine receptor
NFκB	Nuclear factor kappa B

NGF	Neurotrophic growth factor
NKCC1	Sodium potassium chloride co-transporter
NMDAR	N-methyl-D-aspartic acid receptor
NPN	Neuropoietin
NRG1	Neuregulin1
NRGN	Neugrin
NT-3	Neurotrophin-3
Nurr1	Nuclear receptor related 1
OPC	oligodendrocyte precursor cell
OSM	Oncostatin
PDGF	Platelet-derived growth factor
Pitx3	Pituitary homeobox 3
PNS	Peripheral nervous system
RANTES	Regulated and normal T cell expressed and secreted (CCL5)
SDF-1	Stromal cell-derived factor 1 (CXCL12)
Shank3	SH3 and multiple ankyrin repeat domains 3
Shh	Sonic hedgehog
SHP-2	SH2-domain-containing tyrosine phosphatase
SOCS	Suppressor of cytokine signaling
SOS	Son of sevenless
STAT	Signal transducer and activator of transcription
SZ	Schizophrenia
TCF4	Transcription factor 4

TH	Tyrosine hydroxylase
TNFα	Tumor necrosis factor α
TSC	Tuberous sclerosis

XI. Appendix A: Supplementary Tables

Supplementary Tables 1 and 2. NKCC and KCC2 Levels. RNA was extracted from hippocampi of P1, P2,P3 and P9 pups born to saline- or poly(I:C)-injected mice and RT-PCR was performed. Abbreviations: NKCC1= sodium-potassium chloride co-transporter; KCC2= potassium chloride co-transporter.

Supplementary Table 1. Raw cycle threshold (Ct) values for chloride transporters from P1 to P9 show that while message for NKCC1 decreases, message for KCC2 increases . Data for control and poly(I:C) samples at each time point were combined.

	Average Ct Values				
	NKCC1	SEM	KCC2	SEM	n
P1	30.4935	± 0.164	31.3106	± 0.157	6
P2	23.8102	± 0.120	26.2407	± 0.352	6
P3	24.7318	± 0.235	24.7318	± 0.267	6
P9	28.2849	± 0.324	21.0789	± 0.433	8

Supplementary Table 2. Similar message expression of chloride transporters between control and poly(I:C) groups at each time point. Raw cycle threshold (Ct) values do not indicate a premature switch to KCC2 transcription in the poly(I:C)-treated hippocampi samples.

		Average Ct Values					
	Transporter	Control	SEM	n	Poly(I:C)	SEM	n
P1	NKCC1	30.2598	± 0.269	3	30.7273	± 0.081	3
P1	KCC2	31.4329	± 0.308	3	31.1883	± 0.113	3
P2	NKCC1	23.6523	± 0.190	3	23.9681	± 0.103	3
P2	KCC2	25.6066	± 0.455	3	26.8748	± 0.107	3
P3	NKCC1	24.2078	± 0.041	3	24.5127	± 0.576	3
P3	KCC2	24.5442	± 0.107	3	24.9193	± 0.480	3
P9	NKCC1	27.9073	± 0.300	4	28.6625	± 0.552	4
P9	KCC2	20.5255	± 0.685	4	21.6323	± 0.449	4

Supplementary Tables 3A-10B. Comparisons of cytokine and chemokine levels in fetal brains of wild type and IL-6 KO mice from control (saline) and poly(I:C) treatment groups. Pregnant wild type and IL-6 KO mice were injected at E12.5 with poly(I:C) (20mg/kg) or sterile saline (control). Fetal brains from an entire litter were dissected and pooled at E16.5 and single cell suspensions were prepared using 0.05% trypsin and a Gentle MACS® dissociator. An enriched population of CD11b$^+$ (i.e., microglial) cells was obtained using magnetic beads and an autoMACS® cell sorter. CD11b- fractions were retained and assayed as well. Lysates were assayed for protein expression using a Luminex® 32-plex mouse cytokine/chemokine assay. Cells were separated on 3 different occasions from 12 separate litters (1 litter from each of the treatment groups for each assay). The Luminex® 32-plex assay was conducted 3 times. Samples were run in duplicate in each assay. Data was normalized to the amount of protein for each sample and raw data is expressed as pg/mg protein. For comparison across assays, these numbers were log transformed and the difference between logs was assessed using a single-sample one-tailed t-test. Raw data, log-transformed data, differences between logs and p values are reported here for all cytokines (Supplementary Tables 3A-10A) and chemokines (Supplementary Tables 3B-10B). Statistically significant differences in levels of cytokines or chemokines between groups are highlighted.

The panel of cytokines/chemokines included cytokines: Interleukin- 1α (IL-1α), IL-1β, IL-2, IL-3, IL-4, IL-5, IL-6, IL-7, IL-9, IL-10, IL-12 p40, IL-12 p70, IL-13, IL-15, IL-17, IFNγ, TNFα, LIF, G-CSF, GM-CSF, M-CSF, VEGF and chemokines: Eotaxin, IP-10, KC, LIX, MCP-1, MIG, MIP-1α, MIP-1β, MIP-2 and RANTES. Cytokines not listed in the tables were below detectable limits in all of the samples. Abbreviations for chemokines are found in the List of Abbreviations**.**

nd = not detected, blank = not determined.

Supplementary Table 3A. CD11b$^+$ (Microglial) Cytokines: Wild Type Control (Saline) vs. Wild Type Poly(I:C) Treatments.

CD11b$^+$ Cytokines: WT Control vs. WT Poly(I:C) Treatments

Cytokine	Wild Type Control	Log 1	Wild Type Poly(I:C)	Log 2	Δ Logs	Avg	SEM	*p* value
G-CSF	6.48	0.812	8.93	0.951	0.139	0.191	0.175	0.194
	6.39	0.806	20.98	1.322	0.516			
	0.93	-0.033	0.77	-0.116	-0.083			
GM-CSF	5.53	0.743	9.63	0.984	0.241	0.276	0.071	0.030
	12.31	1.090	18.38	1.264	0.174			
	1.28	0.107	3.31	0.520	0.413			
IFN-ϒ	4.07	0.610	7.73	0.888	0.279	0.615	0.404	0.134
	19.26	1.285	27.00	1.431	0.147			
	0.13	-0.886	3.41	0.533	1.419			
IL-1α	93.43	1.970	277.03	2.443	0.472	0.298	0.087	0.038
	65.99	1.819	109.99	2.041	0.222			
	4.03	0.605	6.38	0.805	0.200			
IL-1β	22.03	1.343	27.56	1.440	0.097	-0.009	0.152	0.521
	26.63	1.425	40.71	1.610	0.184			
	28.51	1.455	13.99	1.146	-0.309			
IL-4	1.07	0.029	1.97	0.294	0.264	0.352	0.107	0.040
	12.93	1.112	21.81	1.339	0.227			
	1.36	0.133	4.97	0.697	0.564			
IL-6	2.99	0.476	7.74	0.889	0.413	0.438	0.189	0.073
	6.61	0.820	8.78	0.943	0.123			
	0.95	-0.022	5.68	0.754	0.777			
IL-9	844.3	2.926	1845.65	3.266	0.340	0.283	0.079	0.035
	7.12	0.852	17.17	1.235	0.382			
	0.84	-0.077	1.12	0.050	0.127			
IL-10	8.66	0.938	9.52	0.979	0.041	-0.001	0.165	0.497
	10.09	1.004	18.39	1.265	0.261			
	37.71	1.576	18.63	1.270	-0.306			
IL-12 p40	15.99	1.204	24.57	1.390	0.187	0.615	0.351	0.111
	20.06	1.302	44.57	1.649	0.347			
	0.087	-1.060	1.78	0.250	1.311			
IL-12 p70	42.11	1.624	47.29	1.675	0.050	0.153	0.130	0.180
	57.99	1.763	149.03	2.173	0.410			
	13.49	1.130	13.42	1.128	-0.002			
IL-13	402.68	2.605	781.52	2.893	0.288	-0.261	0.625	0.642
	286.48	2.457	784.43	2.895	0.437			
	36.15	1.558	1.12	0.050	-1.508			
IL-15	42.48	1.628	87.96	1.944	0.316	0.185	0.067	0.054
	31.24	1.495	43.23	1.636	0.141			
	7.59	0.880	9.52	0.979	0.098			
M-CSF	54.96	1.740	123.7	2.092	0.352	0.275	0.080	0.038
	86.43	1.937	112.62	2.052	0.115			
	5.11	0.708	11.64	1.066	0.358			
TNFα	2.34	0.369	7.94	0.900	0.531	0.281	0.231	0.174
	10.01	1.000	6.6	0.820	-0.181			
	1.82	0.260	5.66	0.753	0.493			

Supplementary Table 3B. CD11b$^+$ (Microglial) Chemokines: Wild Type Control (Saline) vs. Wild Type Poly(I:C) Treatments.

CD11b$^+$ Chemokines: WT Control vs. WT Poly(I:C) Treatments

Chemokine	Wild Type Control	Log 1	Wild Type Poly(I:C)	Log 2	Δ Logs	Avg	SEM	*p* value
MCP-1	89.16	1.950	243.88	2.387	0.437			
(CCL2)	118.66	2.074	144.94	2.161	0.087	0.264	0.101	0.060
	30.72	1.487	56.90	1.755	0.268			
MIP-1α	275.98	2.441	504.20	2.703	0.262			
(CCL3)	386.15	2.587	378.20	2.578	-0.009	0.176	0.092	0.099
	74.64	1.873	140.43	2.147	0.274			
MIP-1β	71.58	1.855	114.99	2.061	0.206			
(CCL4)	44.74	1.651	81.38	1.911	0.260	0.249	0.022	0.004
	19.15	1.282	36.61	1.564	0.281			
RANTES	22.42	1.351	35.81	1.554	0.203			
(CCL5)	16.48	1.217	21.49	1.332	0.115	0.164	0.026	0.012
	1.76	0.246	2.63	0.420	0.174			
Eotaxin	23.6	1.373	43.55	1.639	0.266			
(CCL11)	9.11	0.960	14.21	1.153	0.193	0.334	0.107	0.044
	8.89	0.949	31.06	1.492	0.543			
KC	17.17	1.235	59.51	1.775	0.540			
(CXCL1)	43.32	1.637	46.86	1.671	0.034	0.303	0.147	0.088
	11.16	1.048	24.11	1.382	0.335			
MIP2	109.11	2.038	452.39	2.656	0.618			
(CXCL2)	973.94	2.989	619.32	2.792	-0.197	0.236	0.236	0.212
	129.06	2.111	250.23	2.398	0.288			
LIX	95.93	1.982	232.30	2.366	0.384			
(CXCL5)	99.70	1.999	227.32	2.357	0.358	0.322	0.049	0.011
	104.01	2.017	174.79	2.243	0.225			
MIG	nd		2.18	0.338	0.338			
(CXCL9)	12.86	1.109	12.12	1.084	-0.026	0.334	0.207	0.124
	3.07	0.487	15.04	1.177	0.690			
IP-10	31.54	1.499	137.24	2.137	0.639			
(CXCL10)	550.28	2.741	201.04	2.303	-0.437	0.178	0.320	0.317
	29.16	1.465	62.66	1.797	0.332			

Supplementary Table 4A. CD11b$^-$ Cytokines: Wild Type Control (Saline) vs. Wild Type Poly(I:C) Treatments.

CD11b$^-$ Cytokines: WT Control vs. WT Poly(I:C) Treatments

Cytokine	Wild Type Control	Log 1	Wild Type Poly(I:C)	Log 2	Δ LOGS	Avg.	SEM	*p* value
G-CSF	2.86	0.456	5.54	0.744	0.287			
	2.43	0.386	1.60	0.204	-0.181	-0.094	0.200	0.658
	2.30	0.362	0.94	-0.027	-0.389			
GM-CSF	4.48	0.651	7.17	0.856	0.204			
	2.11	0.324	0.80	-0.097	-0.421	-0.252	0.231	0.806
	1.35	0.130	0.39	-0.409	-0.539			
IFN-γ	6.08	0.784	12.66	1.102	0.319			
	0.53	-0.277	1.52	0.182	0.459	0.227	0.167	0.154
	1.04	0.017	0.83	-0.081	-0.098			
IL-1α	48.39	1.685	44.35	1.647	-0.038			
	0.96	-0.018	6.75	0.829	0.847	0.323	0.268	0.176
	2.97	0.473	4.28	0.631	0.159			
IL-1β	149.28	2.174	166.73	2.222	0.048			
	75.33	1.877	46.70	1.669	-0.208	-0.110	0.080	0.849
	63.59	1.803	42.82	1.632	-0.172			
IL-4	3.74	0.573	4.75	0.677	0.104			
	4.36	0.640	1.03	0.014	-0.626	-0.162	0.233	0.720
	0.54	-0.271	0.58	-0.234	0.037			
IL-6	1.64	0.215	2.42	0.384	0.169			
	nd		0.95	-0.022	-0.022	0.073		
	nd		nd					
IL-9	293.20	2.467	209.49	2.321	-0.146			
	144.69	2.160						
	78.50	1.895						
IL-10	42.17	1.625	38.42	1.585	-0.040			
	87.42	1.942	80.47	1.906	-0.036	-0.052	0.014	0.032
	83.02	1.919	69.17	1.840	-0.079			
IL-12 p40	11.89	1.075	12.24	1.088	0.013			
	1.25	0.097	8.04	0.905	0.808	0.145	0.351	0.360
	16.09	1.207	6.60	0.820	-0.387			
IL-12 p70	16.00	1.204	41.02	1.613	0.409			
	6.16	0.790	6.68	0.825	0.035	0.131	0.141	0.225
	5.25	0.720	4.67	0.669	-0.051			
IL-13	1465.04	3.166	858.04	2.934	-0.232			
	287.59	2.459	46.46	1.667	-0.792	-0.407	0.192	0.916
	81.33	1.910	51.59	1.713	-0.198			
IL-15	5.51	0.741	9.92	0.997	0.255			
	1.30	0.114	1.74	0.241	0.127	-0.087	0.280	0.607
	2.46	0.391	0.56	-0.252	-0.643			
M-CSF	5.28	0.723	7.18	0.856	0.133			
	0.76	-0.120	0.72	-0.144	-0.025	-0.035	0.100	0.620
	0.74	-0.130	0.45	-0.344	-0.214			
TNFα	nd		nd					
	0.41	-0.390	0.68	-0.168	0.222	0.306		
	0.41	-0.391	nd		0.391			

Supplementary Table 4B. CD11b$^-$ Chemokines: Wild Type Control (Saline) vs. Wild Type Poly(I:C) Treatments.

CD11b$^-$ Chemokines: WT Control vs. WT Poly(I:C) Treatments

Chemokine	Wild Type Control	Log 1	Wild Type Poly(I:C)	Log 2	Δ LOGS	Avg	SEM	*p* value
MCP-1	68.93	1.838	41.57	1.619	-0.220			
(CCL2)	41.33	1.616	21.29	1.328	-0.288	-0.253	0.020	0.003
	30.95	1.491	17.39	1.240	-0.250			
MIP-1α	41.31	1.616	44.57	1.649	0.033			
(CCL3)	25.53	1.407	10.74	1.031	-0.376	-0.183	0.119	0.868
	11.44	1.058	7.13	0.853	-0.205			
MIP-1β	12.98	1.113	21.09	1.324	0.211			
(CCL4)	12.62	1.101	12.49	1.097	-0.004	-0.058	0.173	0.615
	14.93	1.174	6.22	0.794	-0.380			
RANTES	12.06	1.081	11.82	1.073	-0.009			
(CCL5)	1.53	0.185	1.38	0.140	-0.045	-0.092	0.066	0.851
	1.55	0.190	0.93	-0.032	-0.222			
Eotaxin	2.83	0.452	4.23	0.626	0.175			
(CCL11)	6.91	0.839	4.68	0.670	-0.169	0.009	0.099	0.468
	4.10	0.613	4.31	0.634	0.022			
KC	3.18	0.502	4.98	0.697	0.195			
(CXCL1)	2.51	0.400	3.57	0.553	0.153	-0.121	0.295	0.639
	2.88	0.459	0.56	-0.252	-0.712			
MIP2	19.60	1.292	156.17	2.194	0.901			
(CXCL2)	14.32	1.156	24.45	1.388	0.232	0.159	0.451	0.379
	13.29	1.124	2.94	0.468	-0.656			
LIX	nd		nd					
(CXCL5)	33.67	1.527	52.81	1.723	0.195			
	nd		nd					
MIG	3.70	0.568	6.85	0.836	0.267			
(CXCL9)	4.39	0.642	5.90	0.771	0.128	0.046	0.157	0.398
	5.70	0.756	3.15	0.498	-0.258			
IP-10	60.67	1.783	51.21	1.709	-0.074			
(CXCL10)	21.06	1.323	24.29	1.385	0.062	-0.108	0.109	0.786
	30.63	1.486	14.93	1.174	-0.312			

Supplementary Table 5A. CD11b$^+$ (Microglial) Cytokines: IL-6 KO Control (Saline) vs. IL-6 KO Poly(I:C) Treatments.

CD11b$^+$ Cytokines: IL-6 KO Control vs. IL-6 KO Poly(I:C) Treatments								
Cytokine	IL-6 KO Control	Log 1	IL-6 KO Poly(I:C)	Log 2	Δ Logs	Avg	SEM	*p* value
G-CSF	nd		4.97	0.696	0.696	0.264	0.224	0.180
	19.64	1.293	17.22	1.236	-0.057			
	3.36	0.526	4.79	0.680	0.154			
GM-CSF	20.89	1.320	11.51	1.061	-0.259	0.326		
	nd		8.14	0.911	0.911			
	nd		nd					
IFN-ϒ	1.01	0.004	3.89	0.590	0.586	0.300	0.157	0.098
	22.68	1.356	25.22	1.402	0.046			
	0.93	-0.031	1.72	0.236	0.267			
IL-1α	191.83	2.283	262.44	2.419	0.136	0.009	0.064	0.452
	162.41	2.211	143.22	2.156	-0.055			
	1.50	0.176	1.32	0.121	-0.056			
IL-1β	22.94	1.361	20.47	1.311	-0.049	-0.056	0.051	0.807
	48.51	1.686	51.81	1.714	0.029			
	9.40	0.973	6.71	0.827	-0.146			
IL-4	28.75	1.459	21.12	1.325	-0.134	-0.074	0.041	0.893
	0.69	-0.162	0.56	-0.254	-0.093			
	1.75	0.243	1.77	0.248	0.005			
IL-6	nd		nd					
	nd		nd					
	nd		nd					
IL-9	953.88	2.979				0.420		
	13.59	1.133	82.59	1.917	0.784			
	1.09	0.038	1.24	0.095	0.057			
IL-10	20.08	1.303	12.66	1.102	-0.200	-0.129	0.036	0.034
	23.00	1.362	18.35	1.264	-0.098			
	27.12	1.433	22.05	1.343	-0.090			
IL-12 p40	4.35	0.638	nd			0.002		
	36.55	1.563	36.70	1.565	0.002			
	nd		nd					
IL-12 p70	116.66	2.067	111.73	2.048	-0.019	0.011	0.019	0.309
	18.25	1.261	18.48	1.267	0.005			
	14.33	1.156	15.97	1.203	0.047			
IL-13	408.80	2.612	800.87	2.904	0.292	0.222	0.085	0.061
	591.27	2.772	665.93	2.823	0.052			
	9.15	0.961	19.16	1.282	0.321			
IL-15	56.69	1.754	34.56	1.539	-0.215	-0.037	0.089	0.643
	3.20	0.505	3.55	0.550	0.045			
	2.18	0.338	2.49	0.396	0.058			
M-CSF	31.62	1.500	72.49	1.860	0.360	0.048	0.157	0.394
	128.72	2.110	106.12	2.026	-0.084			
	5.91	0.772	4.36	0.639	-0.132			
TNFα	4.64	0.667	11.15	1.047	0.381	-0.013	0.198	0.523
	24.05	1.381	13.67	1.136	-0.246			
	1.25	0.098	0.84	-0.076	-0.174			

Supplementary Table 5B. CD11b$^+$ (Microglial) Chemokines: IL-6 KO Control (Saline) vs. IL-6 KO Poly(I:C) Treatments.

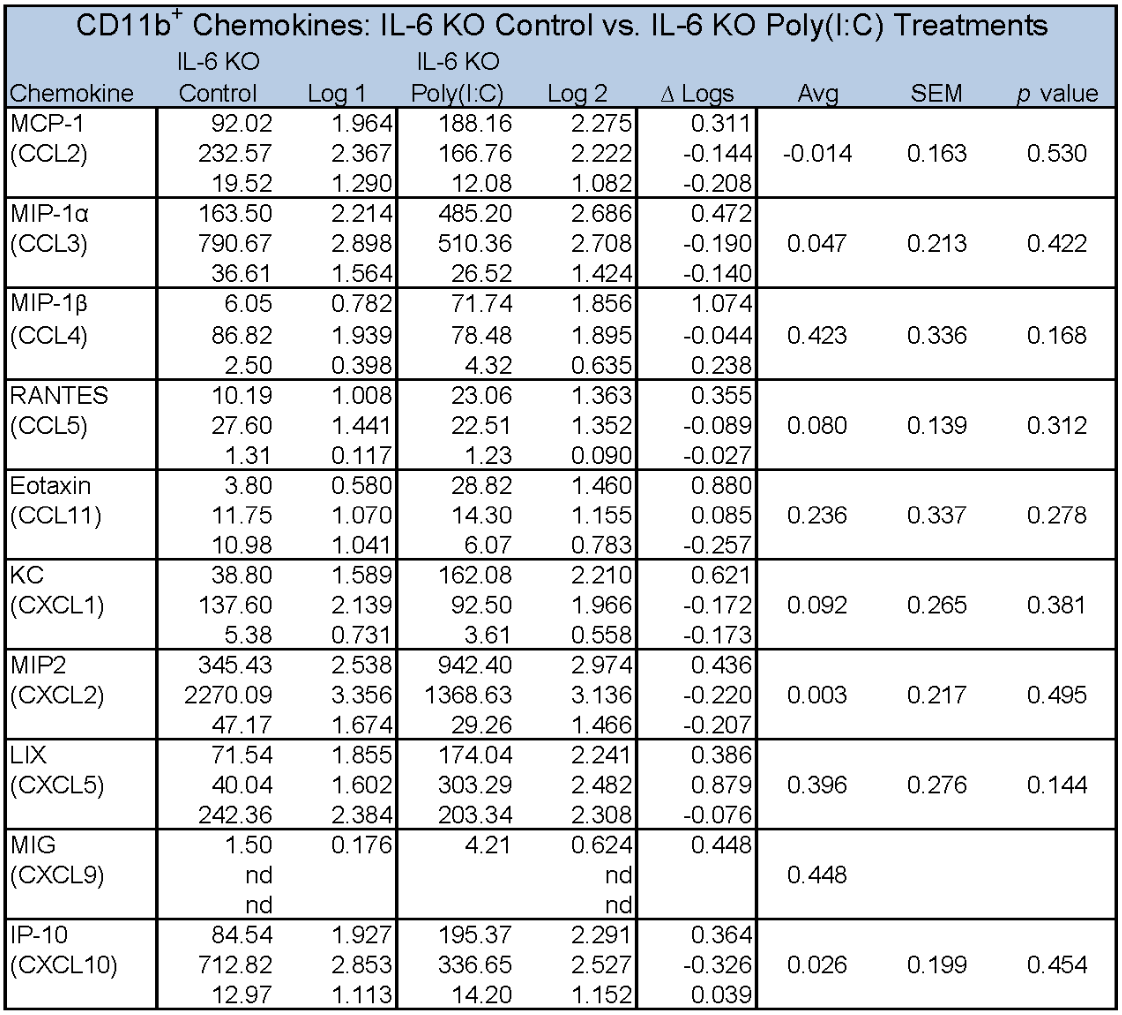

CD11b$^+$ Chemokines: IL-6 KO Control vs. IL-6 KO Poly(I:C) Treatments

Chemokine	IL-6 KO Control	Log 1	IL-6 KO Poly(I:C)	Log 2	Δ Logs	Avg	SEM	*p* value
MCP-1	92.02	1.964	188.16	2.275	0.311	-0.014	0.163	0.530
(CCL2)	232.57	2.367	166.76	2.222	-0.144			
	19.52	1.290	12.08	1.082	-0.208			
MIP-1α	163.50	2.214	485.20	2.686	0.472	0.047	0.213	0.422
(CCL3)	790.67	2.898	510.36	2.708	-0.190			
	36.61	1.564	26.52	1.424	-0.140			
MIP-1β	6.05	0.782	71.74	1.856	1.074	0.423	0.336	0.168
(CCL4)	86.82	1.939	78.48	1.895	-0.044			
	2.50	0.398	4.32	0.635	0.238			
RANTES	10.19	1.008	23.06	1.363	0.355	0.080	0.139	0.312
(CCL5)	27.60	1.441	22.51	1.352	-0.089			
	1.31	0.117	1.23	0.090	-0.027			
Eotaxin	3.80	0.580	28.82	1.460	0.880	0.236	0.337	0.278
(CCL11)	11.75	1.070	14.30	1.155	0.085			
	10.98	1.041	6.07	0.783	-0.257			
KC	38.80	1.589	162.08	2.210	0.621	0.092	0.265	0.381
(CXCL1)	137.60	2.139	92.50	1.966	-0.172			
	5.38	0.731	3.61	0.558	-0.173			
MIP2	345.43	2.538	942.40	2.974	0.436	0.003	0.217	0.495
(CXCL2)	2270.09	3.356	1368.63	3.136	-0.220			
	47.17	1.674	29.26	1.466	-0.207			
LIX	71.54	1.855	174.04	2.241	0.386	0.396	0.276	0.144
(CXCL5)	40.04	1.602	303.29	2.482	0.879			
	242.36	2.384	203.34	2.308	-0.076			
MIG	1.50	0.176	4.21	0.624	0.448	0.448		
(CXCL9)	nd			nd				
	nd			nd				
IP-10	84.54	1.927	195.37	2.291	0.364	0.026	0.199	0.454
(CXCL10)	712.82	2.853	336.65	2.527	-0.326			
	12.97	1.113	14.20	1.152	0.039			

Supplementary Table 6A. CD11b$^-$ Cytokines: IL-6 KO Control (Saline) vs. IL-6 KO Poly(I:C) Treatments.

CD11b$^-$ Cytokines: IL-6 KO Control vs. IL-6 KO Poly(I:C) Treatments

Cytokine	IL-6 KO Control	Log 1	IL-6 KO Poly(I:C)	Log 2	Δ Logs	Avg	SEM	*p* value
G-CSF	5.30	0.724	5.69	0.755	0.031			
	2.02	0.305	0.69	-0.161	-0.467	-0.307	0.169	0.895
	1.92	0.283	0.63	-0.201	-0.484			
GM-CSF	7.90	0.898	8.63	0.936	0.038			
	2.25	0.352	2.38	0.377	0.025	-0.160	0.192	0.754
	1.78	0.250	0.51	-0.292	-0.543			
IFN-ϒ	9.69	0.986	19.51	1.290	0.304			
	1.77	0.248	1.64	0.215	-0.033	-0.035	0.196	0.562
	1.83	0.261	0.77	-0.114	-0.375			
IL-1α	75.21	1.876	63.71	1.804	-0.072			
	3.57	0.553	1.25	0.097	-0.456	-0.123	0.179	0.719
	3.91	0.592	5.62	0.750	0.158			
IL-1β	372.22	2.571	378.22	2.578	0.007			
	109.48	2.039	91.00	1.959	-0.080	-0.194	0.159	0.826
	73.50	1.866	22.82	1.358	-0.508			
IL-4	7.48	0.874	3.99	0.601	-0.273			
	1.65	0.217	1.62	0.209	-0.007	-0.315	0.191	0.121
	1.00	0.000	0.22	-0.666	-0.666			
IL-6	nd		nd					
	nd		nd					
	nd		nd					
IL-9	597.23	2.776	761.59	2.882	0.106			
	275.54	2.440	139.02	2.143	-0.297	-0.096		
	nd		nd					
IL-10	67.33	1.828	48.59	1.687	-0.142			
	132.79	2.123	150.50	2.178	0.054	-0.185	0.152	0.174
	97.77	1.990	33.25	1.522	-0.468			
IL-12 p40	17.08	1.232	18.08	1.257	0.025			
	3.66	0.563	4.55	0.658	0.095	-0.090	0.151	0.694
	11.21	1.050	4.58	0.661	-0.389			
IL-12 p70	31.20	1.494	33.66	1.527	0.033			
	7.66	0.884	8.68	0.939	0.054	-0.091	0.135	0.716
	8.24	0.916	3.59	0.555	-0.361			
IL-13	3625.82	3.559	3478.26	3.541	-0.018			
	601.86	2.779	396.40	2.598	-0.181	-0.451	0.355	0.166
	110.81	2.045	7.77	0.890	-1.154			
IL-15	7.88	0.897	8.43	0.926	0.029			
	1.85	0.267	1.59	0.201	-0.066	-0.117	0.102	0.814
	1.36	0.134	0.66	-0.180	-0.314			
M-CSF	8.20	0.914	7.51	0.876	-0.038			
	0.79	-0.104	0.92	-0.034	0.070	-0.096	0.116	0.753
	0.88	-0.054	0.42	-0.375	-0.321			
TNFα	nd		nd					
	0.59	-0.226	0.54	-0.271	-0.045	-0.045		
	nd		nd					

Supplementary Table 6B. CD11b$^-$ Chemokines: IL-6 KO Control (Saline) vs. IL-6 KO Poly(I:C) Treatments.

CD11b$^-$ Chemokines: IL-6 KO Control vs. IL-6 KO Poly(I:C) Treatments

Chemokine	IL-6 KO Control	Log 1	IL-6 KO Poly(I:C)	Log 2	Δ Logs	Avg	SEM	*p* value
MCP-1	148.10	2.171	139.51	2.145	-0.026	-0.284	0.225	0.166
(CCL2)	89.57	1.952	71.89	1.857	-0.095			
	39.40	1.595	7.31	0.864	-0.732			
MIP-1α	121.51	2.085	141.42	2.151	0.066	-0.193	0.158	0.827
(CCL3)	53.47	1.728	36.54	1.563	-0.165			
	15.83	1.199	5.24	0.719	-0.480			
MIP-1β	24.47	1.389	22.71	1.356	-0.032	-0.343	0.292	0.180
(CCL4)	6.27	0.797	5.32	0.726	-0.071			
	6.49	0.812	0.77	-0.114	-0.926			
RANTES	19.42	1.288	27.93	1.446	0.158	-0.101	0.167	0.696
(CCL5)	2.13	0.328	1.91	0.281	-0.047			
	1.81	0.258	0.70	-0.155	-0.413			
Eotaxin	4.79	0.680	5.02	0.701	0.020	-0.012	0.124	0.534
(CCL11)	7.36	0.867	11.25	1.051	0.184			
	6.43	0.808	3.70	0.568	-0.240			
KC	9.09	0.959	8.60	0.934	-0.024	0.009	0.153	0.479
(CXCL1)	1.13	0.053	2.20	0.342	0.289			
	1.71	0.233	0.99	-0.004	-0.237			
MIP2	77.04	1.887	57.51	1.760	-0.127	-0.148	0.029	0.018
(CXCL2)	9.67	0.985	6.02	0.780	-0.206			
	8.74	0.942	6.75	0.829	-0.112			
LIX	nd		nd			-0.023		
(CXCL5)	72.29	1.859	68.54	1.836	-0.023			
	nd		nd					
MIG	5.54	0.744	35.36	1.549	0.805	0.097	0.385	0.412
(CXCL9)	7.15	0.854	7.24	0.860	0.005			
	6.95	0.842	2.10	0.322	-0.520			
IP-10	114.64	2.059	111.68	2.048	-0.011	-0.264	0.221	0.177
(CXCL10)	34.55	1.538	28.99	1.462	-0.076			
	32.62	1.513	6.46	0.810	-0.703			

Supplementary Table 7A. CD11b$^+$ (Microglial) Cytokines: Wild Type Control (Saline) vs. IL-6 KO Control (Saline)Treatments.

CD11b$^+$ Cytokines: WT Control vs. IL-6 KO Control Treatments								
	Wild Type		IL-6 KO					
Cytokine	Control	Log 1	Control	Log 2	Δ LOGS	Avg	SEM	*p* value
G-CSF	6.48	0.812	nd					
	6.39	0.806	19.64	1.293	0.488	0.523		
	0.93	-0.033	3.36	0.526	0.559			
GM-CSF	5.53	0.743	20.89	1.320	0.577			
	12.31	1.090	nd			0.577		
	1.28	0.107	nd					
IFN-Ƴ	4.07	0.610	1.01	0.004	-0.605			
	19.26	1.285	22.68	1.356	0.071	0.107	0.422	0.412
	0.13	-0.886	0.93	-0.031	0.855			
IL-1α	93.43	1.970	191.83	2.283	0.312			
	65.99	1.819	162.41	2.211	0.391	0.091	0.261	0.607
	4.03	0.605	1.50	0.176	-0.429			
IL-1β	22.03	1.343	22.94	1.361	0.018			
	26.63	1.425	48.51	1.686	0.260	-0.068	0.219	0.460
	28.51	1.455	9.40	0.973	-0.482			
IL-4	1.07	0.029	28.75	1.459	1.429			
	12.93	1.112	0.69	-0.162	-1.273	0.089	0.780	0.460
	1.36	0.133	1.75	0.243	0.110			
IL-6	2.99	0.476	nd					
	6.61	0.820	nd					
	0.95	-0.022	nd					
IL-9	844.30	2.926	953.88	2.979	0.053			
	7.12	0.852	13.59	1.133	0.281	0.150	0.068	0.079
	0.84	-0.077	1.09	0.038	0.115			
IL-10	8.66	0.938	20.08	1.303	0.365			
	10.09	1.004	23.00	1.362	0.358	0.193	0.168	0.815
	37.71	1.576	27.12	1.433	-0.143			
IL-12 p40	15.99	1.204	4.35	0.638	-0.565			
	20.06	1.302	36.55	1.563	0.261	-0.152		
	0.09	-1.060	nd					
IL-12 p70	42.11	1.624	116.66	2.067	0.443			
	57.99	1.763	18.25	1.261	-0.502	-0.011	0.273	0.514
	13.49	1.130	14.33	1.156	0.026			
IL-13	402.68	2.605	408.80	2.612	0.007			
	286.48	2.457	591.27	2.772	0.315	-0.092	0.268	0.618
	36.15	1.558	9.15	0.961	-0.597			
IL-15	42.48	1.628	56.69	1.754	0.125			
	31.24	1.495	3.20	0.505	-0.990	-0.469	0.324	0.858
	7.59	0.880	2.18	0.338	-0.542			
M-CSF	54.96	1.740	31.62	1.500	-0.240			
	86.43	1.937	128.72	2.110	0.173	-0.001	0.124	0.504
	5.11	0.708	5.91	0.772	0.063			
TNFα	2.34	0.369	4.64	0.667	0.297			
	10.01	1.000	24.05	1.381	0.381	0.172	0.169	0.207
	1.82	0.260	1.25	0.098	-0.162			

Supplementary Table 7B. CD11b$^+$ (Microglial) Chemokines: Wild Type Control (Saline) vs. IL-6 KO Control (Saline)Treatments.

CD11b$^+$ Chemokines: WT Control vs. IL-6 KO Control Treatments

Chemokine	Wild Type Control	Log 1	IL-6 KO Control	Log 2	Δ LOGS	Avg	SEM	*p* value
MCP-1	89.16	1.950	92.02	1.964	0.014			
(CCL2)	118.66	2.074	232.57	2.367	0.292	0.036	0.142	0.822
	30.72	1.487	19.52	1.290	-0.197			
MIP-1α	275.98	2.441	163.50	2.214	-0.227			
(CCL3)	386.15	2.587	790.67	2.898	0.311	-0.075	0.195	0.632
	74.64	1.873	36.61	1.564	-0.309			
MIP-1β	71.58	1.855	6.05	0.782	-1.073			
(CCL4)	44.74	1.651	86.82	1.939	0.288	-0.556	0.426	0.839
	19.15	1.282	2.50	0.398	-0.884			
RANTES	22.42	1.351	10.19	1.008	-0.342			
(CCL5)	16.48	1.217	27.60	1.441	0.224	-0.082	0.165	0.666
	1.76	0.246	1.31	0.117	-0.128			
Eotaxin	23.60	1.373	3.80	0.580	-0.793			
(CCL11)	9.11	0.960	11.75	1.070	0.111	-0.197	0.298	0.712
	8.89	0.949	10.98	1.041	0.092			
KC	17.17	1.235	38.80	1.589	0.354			
(CXCL1)	43.32	1.637	137.60	2.139	0.502	0.180	0.252	0.275
	11.16	1.048	5.38	0.731	-0.317			
MIP2	109.11	2.038	345.43	2.538	0.500			
(CXCL2)	973.94	2.989	2270.09	3.356	0.368	0.144	0.293	0.336
	129.06	2.111	47.17	1.674	-0.437			
LIX	95.93	1.982	71.54	1.855	-0.127			
(CXCL5)	99.70	1.999	40.04	1.602	-0.396	-0.052	0.224	0.581
	104.01	2.017	242.36	2.384	0.367			
MIG	nd		1.50	0.176	0.176			
(CXCL9)	12.86	1.109	nd					
	3.07	0.487	nd					
IP-10	31.54	1.499	84.54	1.927	0.428			
(CXCL10)	550.28	2.741	712.82	2.853	0.112	0.063	0.227	0.404
	29.16	1.465	12.97	1.113	-0.352			

Supplementary Table 8A. CD11b$^-$ Cytokines: Wild Type Control (Saline) vs. IL-6 KO Control (Saline) Treatments.

CD11b$^-$ Cytokines: WT Control vs. IL-6 KO Control Treatments

Cytokine	Wild Type Control	Log 1	IL-6 KO Control	Log 2	Δ Logs	Avg	SEM	*p* value
G-CSF	2.86	0.456	5.30	0.724	0.268	0.036	0.116	0.391
	2.43	0.386	2.02	0.305	-0.080			
	2.30	0.362	1.92	0.283	-0.078			
GM-CSF	4.48	0.651	7.90	0.898	0.246	0.131	0.063	0.087
	2.11	0.324	2.25	0.352	0.028			
	1.35	0.130	1.78	0.250	0.120			
IFN-γ	6.08	0.784	9.69	0.986	0.202	0.324	0.101	0.043
	0.53	-0.277	1.77	0.248	0.525			
	1.04	0.017	1.83	0.261	0.244			
IL-1α	48.39	1.685	75.21	1.876	0.192	0.294	0.140	0.085
	0.96	-0.018	3.57	0.553	0.570			
	2.97	0.473	3.91	0.592	0.119			
IL-1β	149.28	2.174	372.22	2.571	0.397	0.207	0.099	0.086
	75.33	1.877	109.48	2.039	0.162			
	63.59	1.803	73.50	1.866	0.063			
IL-4	3.74	0.573	7.48	0.874	0.301	0.050	0.236	0.427
	4.36	0.640	1.65	0.217	-0.423			
	0.54	-0.271	1.00	0.000	0.271			
IL-6	1.64	0.215	nd		-0.215			
	nd		nd					
	nd		nd					
IL-9	293.20	2.467	597.23	2.776	0.309	0.294	0.012	0.016
	144.69	2.160	275.54	2.440	0.280			
	78.50	1.895						
IL-10	42.17	1.625	67.33	1.828	0.203	0.152	0.041	0.033
	87.42	1.942	132.79	2.123	0.182			
	83.02	1.919	97.77	1.990	0.071			
IL-12 p40	11.89	1.075	17.08	1.232	0.157	0.156	0.180	0.239
	1.25	0.097	3.66	0.563	0.467			
	16.09	1.207	11.21	1.050	-0.157			
IL-12 p70	16.00	1.204	31.20	1.494	0.290	0.193	0.056	0.038
	6.16	0.790	7.66	0.884	0.095			
	5.25	0.720	8.24	0.916	0.196			
IL-13	1465.04	3.166	3625.82	3.559	0.394	0.283	0.077	0.034
	287.59	2.459	601.86	2.779	0.321			
	81.33	1.910	110.81	2.045	0.134			
IL-15	5.51	0.741	7.88	0.897	0.155	0.017	0.137	0.456
	1.30	0.114	1.85	0.267	0.153			
	2.46	0.391	1.36	0.134	-0.257			
M-CSF	5.28	0.723	8.20	0.914	0.191	0.094	0.052	0.104
	0.76	-0.120	0.79	-0.104	0.015			
	0.74	-0.130	0.88	-0.054	0.076			
TNFα	nd		nd			0.278		
	0.41	-0.390	0.59	-0.226	0.165			
	0.41	-0.391	nd		0.391			

Supplementary Table 8B. CD11b$^-$ Chemokines: Wild Type Control (Saline) vs. IL-6 KO Control (Saline) Treatments.

CD11b$^-$ Chemokines: WT Control vs. IL-6 KO Control Treatments

Chemokine	Wild Type Control	Log 1	IL-6 KO Control	Log 2	Δ Logs	Avg	SEM	*p* value
MCP-1	68.93	1.838	148.10	2.171	0.332			
(CCL2)	41.33	1.616	89.57	1.952	0.336	0.258	0.076	0.039
	30.95	1.491	39.40	1.595	0.105			
MIP-1α	41.31	1.616	121.51	2.085	0.469			
(CCL3)	25.53	1.407	53.47	1.728	0.321	0.310	0.095	0.041
	11.44	1.058	15.83	1.199	0.141			
MIP-1β	12.98	1.113	24.47	1.389	0.275			
(CCL4)	12.62	1.101	6.27	0.797	-0.304	-0.130	0.203	0.706
	14.93	1.174	6.49	0.812	-0.362			
RANTES	12.06	1.081	19.42	1.288	0.207			
(CCL5)	1.53	0.185	2.13	0.328	0.144	0.139	0.040	0.037
	1.55	0.190	1.81	0.258	0.067			
Eotaxin	2.83	0.452	4.79	0.680	0.229			
(CCL11)	6.91	0.839	7.36	0.867	0.027	0.150	0.062	0.068
	4.10	0.613	6.43	0.808	0.195			
KC	3.18	0.502	9.09	0.959	0.456			
(CXCL1)	2.51	0.400	1.13	0.053	-0.347	-0.039	0.250	0.555
	2.88	0.459	1.71	0.233	-0.226			
MIP2	19.60	1.292	77.04	1.887	0.594			
(CXCL2)	14.32	1.156	9.67	0.985	-0.171	0.081	0.257	0.392
	13.29	1.124	8.74	0.942	-0.182			
LIX	nd		nd					
(CXCL5)	33.67	1.527	72.29	1.859	0.332	0.332		
	nd		nd					
MIG	3.70	0.568	5.54	0.744	0.175			
(CXCL9)	4.39	0.642	7.15	0.854	0.212	0.158	0.037	0.026
	5.70	0.756	6.95	0.842	0.086			
IP-10	60.67	1.783	114.64	2.059	0.276			
(CXCL10)	21.06	1.323	34.55	1.538	0.215	0.173	0.075	0.074
	30.63	1.486	32.62	1.513	0.027			

Supplementary Table 9A. CD11b$^+$ (Microglial) Cytokines: Wild Type Poly(I:C) vs. IL-6 KO Poly(I:C) Treatments.

CD11b$^+$ Cytokines: WT Poly(I:C) vs. IL-6 KO Poly(I:C) Treatments

Cytokine	Wild Type Poly(I:C)	Log 1	IL-6 KO Poly(I:C)	Log 2	Δ Logs	Avg	SEM	*p* value
G-CSF	8.93	0.951	4.97	0.696	-0.254	0.152	0.326	0.657
	20.98	1.322	17.22	1.236	-0.086			
	0.77	-0.116	4.79	0.680	0.796			
GM-CSF	9.63	0.984	11.51	1.061	0.077	-0.138		
	18.38	1.264	8.14	0.911	-0.354			
	3.31	0.520	nd					
IFN-ϒ	7.73	0.888	3.89	0.590	-0.298	-0.208	0.089	0.072
	27.00	1.431	25.22	1.402	-0.030			
	3.41	0.533	1.72	0.236	-0.297			
IL-1α	277.03	2.443	262.44	2.419	-0.023	-0.198	0.247	0.253
	109.99	2.041	143.22	2.156	0.115			
	6.38	0.805	1.32	0.121	-0.684			
IL-1β	27.56	1.440	20.47	1.311	-0.129	-0.115	0.123	0.224
	40.71	1.610	51.81	1.714	0.105			
	13.99	1.146	6.71	0.827	-0.319			
IL-4	1.97	0.294	21.12	1.325	1.031	-0.337	0.760	0.350
	21.81	1.339	0.56	-0.254	-1.593			
	4.97	0.697	1.77	0.248	-0.448			
IL-6	7.74	0.889	nd					
	8.78	0.943	nd					
	5.68	0.754	nd					
IL-9	1845.65	3.266				0.363		
	17.17	1.235	82.59	1.917	0.682			
	1.12	0.050	1.24	0.095	0.045			
IL-10	9.52	0.979	12.66	1.102	0.124	0.065	0.036	0.107
	18.39	1.265	18.35	1.264	-0.001			
	18.63	1.270	22.05	1.343	0.073			
IL-12 p40	24.57	1.390	nd			-0.084		
	44.57	1.649	36.70	1.565	-0.084			
	1.78	0.250	nd					
IL-12 p70	47.29	1.675	111.73	2.048	0.373	-0.153	0.387	0.366
	149.03	2.173	18.48	1.267	-0.907			
	13.42	1.128	15.97	1.203	0.076			
IL-13	781.52	2.893	800.87	2.904	0.011	0.391	0.422	0.744
	784.43	2.895	665.93	2.823	-0.071			
	1.12	0.050	19.16	1.282	1.232			
IL-15	87.96	1.944	34.56	1.539	-0.406	-0.691	0.204	0.038
	43.23	1.636	3.55	0.550	-1.086			
	9.52	0.979	2.49	0.396	-0.582			
M-CSF	123.70	2.092	72.49	1.860	-0.232	-0.228	0.116	0.094
	112.62	2.052	106.12	2.026	-0.026			
	11.64	1.066	4.36	0.639	-0.426			
TNFα	7.94	0.900	11.15	1.047	0.147	-0.122	0.357	0.383
	6.60	0.820	13.67	1.136	0.316			
	5.66	0.753	0.84	-0.076	-0.829			

Supplementary Table 9B. CD11b$^+$ (Microglial) Chemokines: Wild Type Poly(I:C) vs. IL-6 KO Poly(I:C) Treatments.

CD11b$^+$ Chemokines: WT Poly(I:C) vs. IL-6 KO Poly(I:C) Treatments

Chemokine	Wild Type Poly(I:C)	Log 1	IL-6 KO Poly(I:C)	Log 2	Δ Logs	Avg	SEM	*p* value
MCP-1 (CCL2)	243.88	2.387	188.16	2.275	-0.113	-0.242	0.221	0.195
	144.94	2.161	166.76	2.222	0.061			
	56.90	1.755	12.08	1.082	-0.673			
MIP-1α (CCL3)	504.20	2.703	485.20	2.686	-0.017	-0.203	0.264	0.260
	378.20	2.578	510.36	2.708	0.130			
	140.43	2.147	26.52	1.424	-0.724			
MIP-1β (CCL4)	114.99	2.061	71.74	1.856	-0.205	-0.383	0.278	0.151
	81.38	1.911	78.48	1.895	-0.016			
	36.61	1.564	4.32	0.635	-0.928			
RANTES (CCL5)	35.81	1.554	23.06	1.363	-0.191	-0.167	0.102	0.121
	21.49	1.332	22.51	1.352	0.020			
	2.63	0.420	1.23	0.090	-0.330			
Eotaxin (CCL11)	43.55	1.639	28.82	1.460	-0.179	-0.295	0.213	0.150
	14.21	1.153	14.30	1.155	0.003			
	31.06	1.492	6.07	0.783	-0.709			
KC (CXCL1)	59.51	1.775	162.08	2.210	0.435	-0.031	0.399	0.472
	46.86	1.671	92.50	1.966	0.295			
	24.11	1.382	3.61	0.558	-0.825			
MIP2 (CXCL2)	452.39	2.656	942.40	2.974	0.319	-0.090	0.421	0.426
	619.32	2.792	1368.63	3.136	0.344			
	250.23	2.398	29.26	1.466	-0.932			
LIX (CXCL5)	232.30	2.366	174.04	2.241	-0.125	0.022	0.076	0.600
	227.32	2.357	303.29	2.482	0.125			
	174.79	2.243	203.34	2.308	0.066			
MIG (CXCL9)	2.18	0.338	4.21	0.624	0.286			
	12.12	1.084	nd					
	15.04	1.177	nd					
IP-10 (CXCL10)	137.24	2.137	195.37	2.291	0.153	-0.089	0.279	0.390
	201.04	2.303	336.65	2.527	0.224			
	62.66	1.797	14.20	1.152	-0.645			

Supplementary Table 10A. CD11b$^-$ Cytokines: Wild Type Poly(I:C) vs. IL-6 KO Poly(I:C) Treatments.

CD11b$^-$ Cytokines: WT Poly(I:C) vs. IL-6 KO Poly(I:C) Treatments

Cytokine	Wild Type Poly(I:C)	Log 1	IL-6 KO Poly(I:C)	Log 2	Δ Logs	Avg	SEM	*p* value
G-CSF	5.54	0.744	5.69	0.755	0.012	-0.176	0.109	0.124
	1.60	0.204	0.69	-0.161	-0.365			
	0.94	-0.027	0.63	-0.201	-0.174			
GM-CSF	7.17	0.856	8.63	0.936	0.080	0.224	0.126	0.892
	0.80	-0.097	2.38	0.377	0.474			
	0.39	-0.409	0.51	-0.292	0.117			
IFN-γ	12.66	1.102	19.51	1.290	0.188	0.063	0.065	0.781
	1.52	0.182	1.64	0.215	0.033			
	0.83	-0.081	0.77	-0.114	-0.033			
IL-1α	44.35	1.647	63.71	1.804	0.157	-0.152	0.290	0.326
	6.75	0.829	1.25	0.097	-0.732			
	4.28	0.631	5.62	0.750	0.118			
IL-1β	166.73	2.222	378.22	2.578	0.356	0.124	0.200	0.701
	46.70	1.669	91.00	1.959	0.290			
	42.82	1.632	22.82	1.358	-0.273			
IL-4	4.75	0.677	3.99	0.601	-0.076	-0.104	0.182	0.312
	1.03	0.014	1.62	0.209	0.195			
	0.58	-0.234	0.22	-0.666	-0.432			
IL-6	2.42	0.384	nd					
	0.95	-0.022	nd					
	nd		nd					
IL-9	209.49	2.321	761.59	2.882	0.561	1.352		
			139.02	2.143	2.143			
IL-10	38.42	1.585	48.59	1.687	0.102	0.019	0.175	0.463
	80.47	1.906	150.50	2.178	0.272			
	69.17	1.840	33.25	1.522	-0.318			
IL-12 p40	12.24	1.088	18.08	1.257	0.169	-0.079	0.127	0.299
	8.04	0.905	4.55	0.658	-0.247			
	6.60	0.820	4.58	0.661	-0.159			
IL-12 p70	41.02	1.613	33.66	1.527	-0.086	-0.029	0.072	0.364
	6.68	0.825	8.68	0.939	0.114			
	4.67	0.669	3.59	0.555	-0.114			
IL-13	858.04	2.934	3478.26	3.541	0.608	0.239	0.539	0.650
	46.46	1.667	396.40	2.598	0.931			
	51.59	1.713	7.77	0.890	-0.822			
IL-15	9.92	0.997	8.43	0.926	-0.071	-0.013	0.043	0.397
	1.74	0.241	1.59	0.201	-0.039			
	0.56	-0.252	0.66	-0.180	0.071			
M-CSF	7.18	0.856	7.51	0.876	0.020	0.033	0.041	0.746
	0.72	-0.144	0.92	-0.034	0.110			
	0.45	-0.344	0.42	-0.375	-0.031			
TNFα	nd		nd			-0.103		
	0.68	-0.168	0.54	-0.271	-0.103			
	nd		nd					

Supplementary Table 10B. CD11b$^-$ Chemokines: Wild Type Poly(I:C) vs. IL-6 KO Poly(I:C) Treatments.

CD11b$^-$ Chemokines: WT Poly(I:C) vs. IL-6 KO Poly(I:C) Treatments

Chemokine	Wild Type Poly(I:C)	Log 1	IL-6 KO Poly(I:C)	Log 2	Δ Logs	Avg	SEM	*p* value
MCP-1	41.57	1.619	139.51	2.145	0.526	0.226	0.301	0.734
(CCL2)	21.29	1.328	71.89	1.857	0.528			
	17.39	1.240	7.31	0.864	-0.376			
MIP-1α	44.57	1.649	141.42	2.151	0.501	0.300	0.217	0.849
(CCL3)	10.74	1.031	36.54	1.563	0.532			
	7.13	0.853	5.24	0.719	-0.134			
MIP-1β	21.09	1.324	22.71	1.356	0.032	-0.415	0.272	0.133
(CCL4)	12.49	1.097	5.32	0.726	-0.371			
	6.22	0.794	0.77	-0.114	-0.907			
RANTES	11.82	1.073	27.93	1.446	0.373	0.130	0.144	0.770
(CCL5)	1.38	0.140	1.91	0.281	0.141			
	0.93	-0.032	0.70	-0.155	-0.123			
Eotaxin	4.23	0.626	5.02	0.701	0.074	0.130	0.132	0.785
(CCL11)	4.68	0.670	11.25	1.051	0.381			
	4.31	0.634	3.70	0.568	-0.066			
KC	4.98	0.697	8.60	0.934	0.237	0.092	0.151	0.697
(CXCL1)	3.57	0.553	2.20	0.342	-0.210			
	0.56	-0.252	0.99	-0.004	0.248			
MIP2	156.17	2.194	57.51	1.760	-0.434	-0.227	0.298	0.263
(CXCL2)	24.45	1.388	6.02	0.780	-0.609			
	2.94	0.468	6.75	0.829	0.361			
LIX	nd		nd			0.113		
(CXCL5)	52.81	1.723	68.54	1.836	0.113			
	nd		nd					
MIG	6.85	0.836	35.36	1.549	0.713	0.209	0.263	0.744
(CXCL9)	5.90	0.771	7.24	0.860	0.089			
	3.15	0.498	2.10	0.322	-0.176			
IP-10	51.21	1.709	111.68	2.048	0.339	0.017	0.205	0.530
(CXCL10)	24.29	1.385	28.99	1.462	0.077			
	14.93	1.174	6.46	0.810	-0.364			

XI. Appendix B: Supplementary Figure

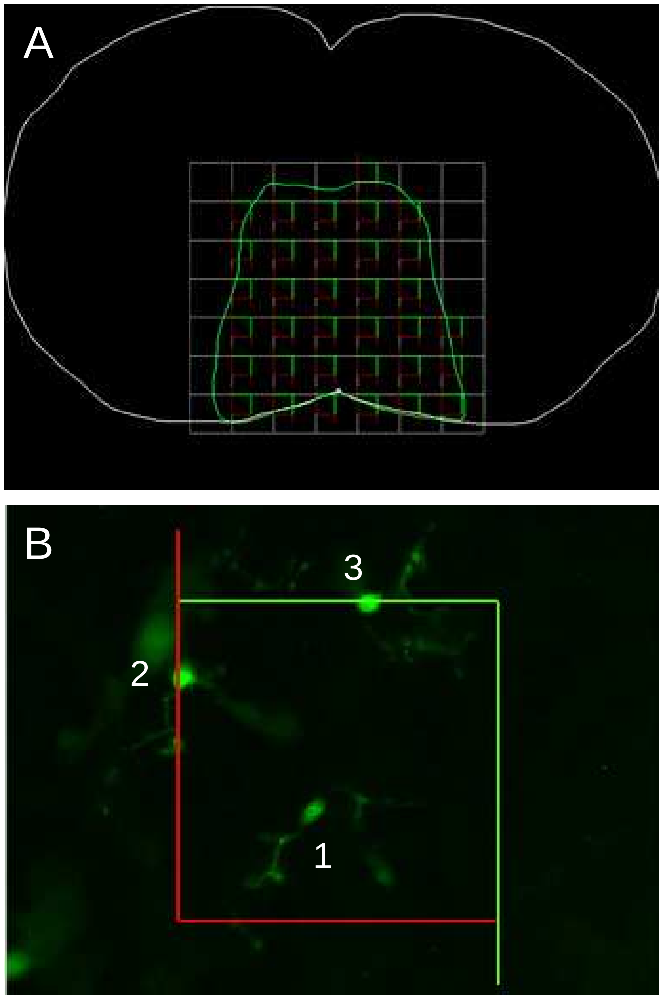

Supplementary Figure 1. Systematic random sampling: Grid and counting frame. After the sections and the regions of interest are outlined, a grid determines the distance between counting frames in the XY plane (A). The grid allows for counting frames to cover a fraction of the area of the region of interest and be evenly distributed throughout the region. The counting frame (B) size is set so that it fits into a single field of view at the magnification being used to count cells and so that it is large enough to contain 1 to 8 cells per counting frame. Counting rules are followed to ensure unbiased counting. Cells are only counted if the top of the soma comes into focus while focusing down from the top through the counting frame. Cells that come into focus above or below the frame are not counted. (The frame lines appear yellow in the guard zones above and below the counting frame.) All cells with the top of the soma entirely within the counting frame are counted (cell #1, B). Cells with the top of the soma touching an exclusion line (red lines) are not counted (cell #2, B). Cells with the top of the soma touching an inclusion line (green lines) are counted (cell #3, B).

XII. Curriculum Vitae

Lorelei Pratt
Born on May 8, 1953, New York City, NY

Education

Ph.D. in Cell and Molecular Biology **01/2013**
Rutgers, The State University of New Jersey-Newark
M.S. in Biology **10/2007**
Rutgers, The State University of New Jersey-Newark
NJ State Elementary School Teacher Certificate **05/1977**
Graduate Program, William Paterson University, Wayne, NJ
B.S. Bible Christian Education **05/1975**
Cairn University, Langhorne, PA
Dumont High School **06/1971**

Professional Experience

Graduate Research Assistant **06/2007-09/2012**
Department of Biological Sciences, Rutgers University, Newark, NJ

- Investigated the effects on the fetal cholinergic basal forebrain following maternal immune activation *in vivo*. This included an evaluation of the cytokine/chemokine phenotype of fetal microglia.

Instructor **07/2009-08/2009**
Department of Biological Sciences, Rutgers University, Newark, NJ

- 21:120:242 Anatomy & Physiology 2

Teaching Assistant **06/2002-05/2009**
Department of Biological Sciences, Rutgers University, Newark, NJ

- 120:241,242 Anatomy & Physiology Lab 1 and 2
- 120:343 Developmental Biology Lab
- 120:101,102 General Biology I and II Discussion and Lab
- 160:113,114 General Chemistry Lab I and II

Awards

2006 Graduate Merit Award
Executive Women of New Jersey Scholarship Program

Publications

1. Pratt, L., Ni, L., Ponzio, NM, Jonakait, GM. Maternal immune activation promotes fetal microglial activation and increases choline acetyltransferase activity and cholinergic cell number in the fetal basal forebrain: implications for autism. (2013) *Pediatr Res,* (submitted).
2. Jonakait, GM, Pratt L, Acevedo, G, Ni, L. Microglial regulation of cholinergic differentiation in the basal forebrain. (2012) *Dev Neurobio,* 72:857-64.

Poster Presentations

1. Pratt, L., Ni, L., Jonakait, GM. Maternal Inflammation and the Fetal Basal Forebrain. November 2011 Cell Symposium, *Autism,* Arlington, VA
2. Pratt, L., Ponzio, NM., Ni, L., Sheng, I., Jonakait, GM. Fetal Microglia Become Activated Following Maternal Immune Challenge. May 2010 IMFAR, Phila, PA